Non-linear buckling analysis for ultimate limit strength calculations of doubler plate repair on a damaged ship structure

by

MATHIAS SØRBY HAUGEN

THESIS

for the degree of

MASTER OF SCIENCE

(Master i Anvendt matematikk og mekanikk)

Faculty of Mathematics and Natural Sciences
University of Oslo

November 2012

Det matematisk- naturvitenskapelige fakultet
Universitetet i Oslo

Non-linear buckling analysis for ultimate limit strength calculations of doubler plate repair on a damaged ship structure

by

MATHIAS SØRBY HAUGEN

THESIS

for the degree of

MASTER OF SCIENCE

(Master i Anvendt matematikk og mekanikk)

Faculty of Mathematics and Natural Sciences
University of Oslo

November 2012

Det matematisk- naturvitenskapelige fakultet
Universitetet i Oslo

Preface

This thesis has been written to complete the Master of Science degree at the University of Oslo, Faculty of Mathematics and Natural Sciences, Department of Mathematics, Mechanics Division.

In the completion of the thesis I have been so fortunate to have been able to write and preform the whole thesis in collaboration with Ship Structures and Concepts department (TNTNO367) in the Maritime Advisory Division at Det Norske Veritas at Høvik.

I would like to express my greatest gratitude to my head supervisor, Dr. Lars Brubak at TNTNO367 for his guidance and much needed help throughout the whole period. His knowledge in this field has been inestimable. I would also like to thank my co-supervisor Professor Jostein Hellesland at the University of Oslo, Faculty of Mathematics and Natural Sciences, Department of Mathematics, Mechanics Division, for his advice and guidance. Thanks also to Ole J. Hareide and Henning Levanger former master students at the University of Oslo and now employees at Ship Structure and Concepts Division at Det Norske Veritas for great assistance and inspiration to preform this work. Last I would like to thank my dad, Øystein Haugen, for proofreading the thesis and with motivation throughout my work with this thesis.

Oslo, November 2012.

Mathias Sørby Haugen

Abstract

Repair of a damaged ship hull is time and cost consuming in shipping industry. A damage is something that often sets the ship operation out of business and every part that has an interest, are looking for ways to minimize the stay in a repair yard. Double plates are often used to repair damages on a ship hull, like buckling, corrosion, wastage and cracks of plates. Current standards rate repair with doublers as a temporary approach to fix the structure, which means that within a certain time the ship must once again seek a shipyard to fulfil the repair with a more, both time and cost consuming repair. The permanent method today is by replacing the the damaged section with a new one. Many shipyards though consider a doubler to be sufficient as a permanent repair, but lack of documentation and experimental material data result in temporary repairs.

This thesis contributes to broaden the extent of experimental material by a thorough finite element analysis, with use of the computerized program Abaqus, of various kinds of thickness ratios, imperfections and load conditions. All have been done with regard of the current standards [1] and guidelines [2]. The results of the analysis consists of both eigenvalue/buckling loads and ultimate capacity. The effect of the doubler, contributes to make the structure to be almost as strong as an intact plate and all systems consider damage on a stiffened panel. The result complies the thoughts of the shipyards, that a doubler can safely be used as a permanent repair.

In addition, it has been tried to develop a semi-analytical tool that could simplify and decrease in great extent the rate of the calculation time. A semi-analytical method creates possibilities to calculate the eigenvalue/buckling loads for a conservative estimation in the design of the structure much faster then in a finite element program. A procedure of this kind already exists for intact single plate with or without stiffeners and are implemented in a programme named PULS. The model created for doubler in this thesis will be able to conduct calculations for rather stiff systems. We have selected some limitations in the way of boundary conditions and chosen displacement field. The semi-analytical model has been implemented into a Matlab script.

Content

List of notations

$\boldsymbol{\epsilon}$	Vector with strain components
$\boldsymbol{\sigma}$	Vector with stress components
$\delta\mathbf{u}$	Virtual displacement
δ_{ij}	Kronecker‘s delta
ϵ	Normal strain
γ	Shear strain
λ_p	Load factor
$\mathbf{a_e}$	Topology matrix
$\mathbf{a}$	Eigenvector
$\mathbf{B}$	Unit displacement-strain matrix
$\mathbf{E}$	Material matrix
$\mathbf{F}$	Actual force
$\mathbf{f}$	Body force per unit volume
$\mathbf{K^G}$	Geometric stiffness matrix
$\mathbf{K^M}$	Material stiffness matrix
$\mathbf{k_e}$	Element stiffness matrix
$\mathbf{r_e}$	Element load vector
$\mathbf{T}$	Surface traction per unit area
ν	Poisson‘s ratio
Π	Total potential energy

σ	Normal stress
σ_e	von Mises stress
τ	Shear stress
a_i	Amplitude
D	Flexural rigidity for a isotropic plate
E	Young‘s modulus
f	Assumed shape function
$F(x, y)$	Airy‘s stress function
f_y	Yield stress
G	Shear module
H	Load potential
L	Length of the plate
M_x	Moment acting about the x-axis
M_y	Moment acting about the y-axis
N_x	In-plane normal force in x-direction
N_y	In-plane normal force in y-direction
N_{xy}	In-plane shear force
Q_x	Out-of-plane force in x-direction
Q_y	Out-of-plane force in y-direction
s	Width of the plate
S_σ	Area of the surface where the surface tractions are valid
S_x	Normal stress acting on the plate in x-direction
S_y	Normal stress acting on the plate in y-direction
S_{xy}	Shear stress acting on the plate
t	Thickness of the plate
U	Strain energy

u	Displacement in x-direction
U_0	Strain energy density
v	Displacement in y-direction
W	Definition of work
w	Displacement in z-direction
W_E	External work
W_I	Internal work

Chapter 1

Introduction

In marine structures such as ships and offshore floating equipment it is important that the strength is sufficient to bear extreme loading. Modern ship construction is vital in form of the ships load capacity, sailing characteristic and especially the financial part. The current ships have an endless variety of shapes and with different operability. Ships come in all varieties like cargo ships, offshore suppliers, passenger carriers, cruise ships and many more. Even if all these factors play a part, the different ships must fulfil the same rules and regulations, in form of safety and capability, and in addition be as economic as possible. This leads to an extreme amount of work for the constructors and designers. With the entry of computers the ship industry changed, present ships are designed and calculated by using computer software. This has increased the accuracy, but can often be quite time-consuming and require skills from the operators. Semi-analytical models are therefore a good remedy to decrease the computation process. PULS is one example of this, developed by Det Norske Veritas.

When it comes to the aspect of maintenance and repair of a ship structure, it is important to have a good inspection programme that serves the different kind of ships in the best way possible. An optimal programme drives the ship and the company to keep the operation going continuously. When damage on a ship occurs, the ship must often abort its operation and it can take some time before it is operational again. Quick temporary solutions are often used to keep the ships in business until the next scheduled inspection and maintenance. Double plates are used as this kind of fix and are only accepted as a temporary solution. This is an easy way to repair a structure, but when the ship is in dry dock the double plate must be removed and the original damage plate must be repaired. The reason why double plates are seen as a temporary fix is the lack of documentation and guidelines. The performance to a doubler plate is yet not accepted in the ship industry, but is often used. A double plate repair can only be seen as a permanent

fix when a specific problem is investigated separately and calculations are done for that precise problem and it cannot be transferred to other problems.

1.1 Problem formulation

In this thesis we will look at the possibility for double plate repair to be a permanent fix. The plate problem we will investigate is a section with plates and stiffeners. The section can typically be addressed to deck, sides or bottom of ship hulls. The plates are rectangular and are divided by stiffeners and transverse girders, as Fig. 1.1 shows. The transverse girders are assumed to have enough strength to be able to carry the rest, and they are being held completely fixed. We assume the stiffeners to have an open T-profile, which is quite common in ship constructions and can be seen in Fig. 1.2. The double plate we set to have the same dimensions as the original plate, but we will investigate how the thickness of the doubler will affect the system. The doubler will be divided into the same regions and welded in the same way as the original plates. A normal assumption for boundary conditions is to arrange simply supported edges, but because of the representation of neighbouring plates, like in a complete ship hull, the edges will remain straight and withstand rotation.

The loads acting on the section comes in the form of in-plane forces, compression and tension, which arrives from the hulls bending moment and shear forces. The lateral pressure from cargo or waves is being neglected in this thesis. In a normal fabrication of plates is it unusual or more precise impossible to fabricate a perfect plate. Plates have some imperfection regardless the fabrication process. This causes internal stress in the plate and the welding process makes stress even higher. The problem has of this some geometrical non-linearity from the start and we must model the problem with those. The material that the plate consist of is set to be steel, which can be seen as a stocky material and causes local buckling/deformation to occur in a greater extent than global. For this reason we will here focus on local deformations. From this our goal for this thesis is to investigate the effect of double plates. We will look at how doubler plates will strengthen an intact structure and a damage structure. In addition to this we will try to derive a semi-analytical model for calculation of critical loads in problems regarding double plates.

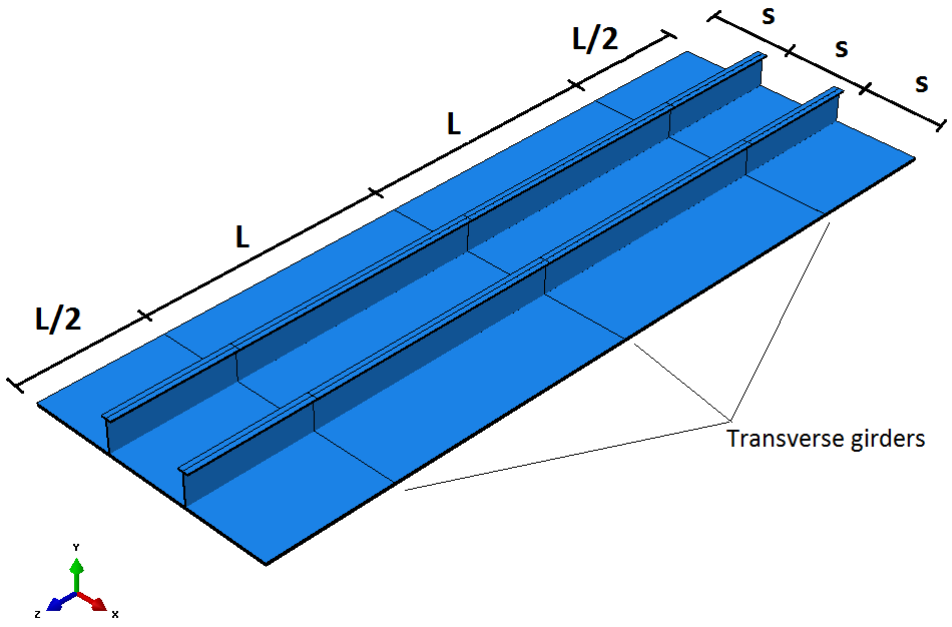

Figure 1.1: Definition of the plate problem with double plate.

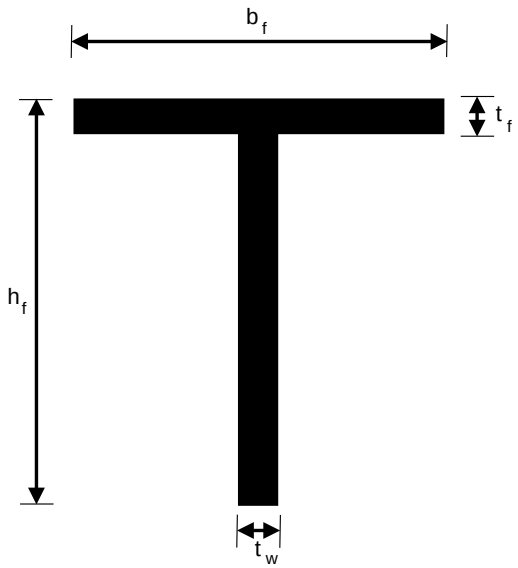

Figure 1.2: Sketch of a typical T-profile.

1.2 Double plates

Double plating as a repair is widely used in the shipping industry. It is used for repairing buckled plates, corroded plating, cracked plates and defected welds. The way the repair takes place is by covering the damage area by an extra (double) plate and welding around the double plate edge. A ship hull consists of whole sections put together or by rolled shapes. When these sections are damaged they are not able to carry any more additional load and the strength is controlled by local buckling in the plate elements. There are many factors implicated in the capacity of a plate:

- Kind of material in both plates.
- Positioning of the double plate.
- The end condition for the original plate.
- The extent of corrosion and cracking.
- Kind of weld used to assemble the two plates.

If double plates shall be used as permanent repair the problems about corrosion, buckling strength, fatigue and fracture must be solved. The International Association of Classification Societies (IACS) is a technically-based organization consisting of thirteen classification companies, among them DNV. They have made a recommendation with guidance for use of double plates as a temporary repair, [1], but they state that double plates can be used permanently if it is used as original compensation for openings, within the main hull structure. When it is used as a temporary repair it depends on the marine superintendent on the site to decide the location, measure, size, thickness, material properties and welds of the double plate.

In current design and standards, use of double plates as a permanent repair must undergo a full review and conduct a separate analysis of that special subject or case. These results will then only be acceptable for that particular problem and cannot be used on another case. This is time consuming and is rarely performed. Instead the shipyards use the simpler temporary approach. If or when a design based recommendation with guidance for doubler plates as a permanent repair emerges, both the time and cost for shipyard repair will reduce dramatically. Present the repair must be redone properly after some time, and then the doubler and the original plate is removed and a new plate is mounted in the spot to the original plate. The shipyard is then almost doing the work twice for one damage. Temporary repair is a quite wide expression. In some cases the ship can operate as long as a year before something permanent is done.

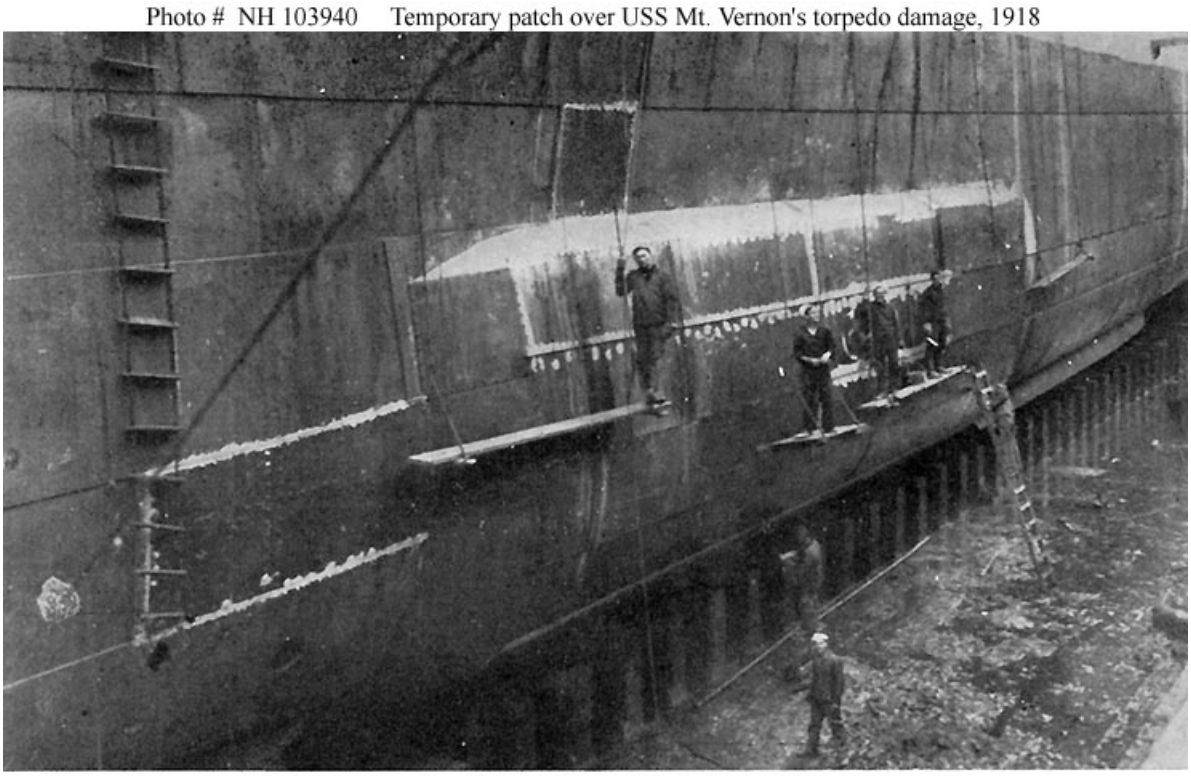

Figure 1.3: Double plate repair has been used in many years. Courtesy of U.S. Naval History and Heritage Command Photograph.

In a report done by the American Ship Structure Committee (ASSC) [2], the use of doubler plates in shipyards and the present regulations handled by classification societies was investigated, and a quick recall of the result is shown here:

Type of damage: Mostly used on buckling, corrosion, wastage and cracks.

Placing: Can be placed almost anywhere, except on fuel tanks. Some classification societies will not conduct this kind of repair under the water line.

Lifetime: More than half of the asked yards use it as an permanent repair. The others consider it temporary repair until the ship is dry docked.

Size and thickness: The thickness is usually a little bit smaller than the original plate. The size can vary, it depends on the damage.

Corner radius: Every society use rounded corners to avoid stress concentration. Usual measure is 3 inches in radius.

Welding: For wide and long plates it should be used filled welds around the whole edge and slot welds. For some slender plates it is sufficient to use filled welds.

Recommendation: Almost all societies would like to see more of double plate repairs and it should be used as a permanent repair. If the repair is conducted well, it will not cause trouble later on. It is far the best way to conduct a repair.

The answers from the shipyards are quite satisfying in comparison of the standard from IACS. And it can be used safely as ground rules for double plating. In correlation with what the American Ship Structure Committee investigated above, about the usage of double plates, some other general rules are essential. The repair is to be carried out according to the rules of the Classification Society and shall be supervised by the surveyor from the Society. The shipyard, repair yard, which is conducting the repair, must be a yard that can perform the task with the quality in accordance to the Society's requirements and standards. Welding of a hull structure is demanding when it comes to all aspects of shipbuilding or repairs. It must be carried out by qualified welders and at a place where the work can be done acceptably regarding whether conditions.

The material requirements in repair are basically the same as for a new construction. The quality of the material must be similar to the original construction, in form of heat treatment, chemical composition, mechanical properties and tolerances.

To perform a buckling analysis for doubler plates an eigenvalue analysis is conducted to estimate the critical buckling load and a non-linear analysis to check the ultimate strength. The effect of the doubler can of this be seen.

1.3 Previous work

Buckling of plates and shells is a topic that for hundreds of years has been of huge interest for scientist and engineers. It is well documented in literature and can be found back as early as 1759, when Euler worked with buckling of columns [3]. His contribution in buckling is highly regarded as one of the most important contributions to this field and is still a key factor in current theory. Euler was also probably the first to look at a plate problem, when he in 1776 preformed a vibration analysis on a plate problem. Bernoulli came up with what we today call Euler-Bernoulli bending theory for beams [4]. This was on bases on earlier work done by Euler and by the German physicist Chladni.

The plate equation occurred in 1813, when the French mathematician Germain developed the differential equation for a plate [5]. This equation was without the warping term, but was later added by Lagrange [6]. Poisson expanded the plate equation in 1829 to a solution for a plate under static loading [7]. Poisson was also the first to introduce three boundary conditions. When Navier looked into the plate thickness as a function of the rigidity D, he also implemented an exact method to transform the differential equation into an algebraic expression by using Fourier series [8]. Kirchhoff's hypotheses were implemented in 1850 and were a vital contribution to the theory for thin plates [9]. Kirchhoff contributed with this to simplify the energy functional of three dimensional elasticity theory for bent plates. In the transition between the 19th and 20th century the shipbuilding industry changed drastically, with the change of material, from wood to steel.

Galerkin developed a new integration method of the differential equation of elasticity, proposed by Bubnov and implemented it to the plate bending analysis [10]. One which had a large impact on the development of the theory of plates is Timoshenko [11, 12]. Some of his work is for instance the solution of circular plates with large deflections and the formulation of elastic stability problems. Timoshenko was also looking at buckling behaviour of rectangular plates under different compressive loadings, together with Gere and Bubnov [13]. Hencky worked with the theory of large deflection and the general theory of elastic stability for thin plates [14]. The differential equation we know today was developed by von Karman [15], he also in addition looked into post-buckling behaviour of plates. For plates with initial imperfection Marguerre used von Karman's equation to make it also apply for this [16]. The equation for thin plates for a compressive load was first developed by Navier. The phenomenon for simply supported plates exposed to loads in different directions was solved by using energy methods by Bryan. Ritz used free vibration of a rectangular plate with free edges to demonstrate his famous method for extending the Rayleigh principle [17].

Later, in the mid-1950's, the work with computerized solution of plate theories and the birth of Finite Element Method started, with use of numerical methods. This was done by Turner, Clough, Martin and Topp [18]. In the recent years there have been published an enormous amount of reports, articles and books about buckling of plates. Among those Det Norske Veritas have implemented new buckling code, Panel Ultimate Strength or also called PULS, which is based on a semi-analytical approach [19, 20]. When it comes to the subject of repair with double plating there are some research done by classification societies and most can be seen in Shipbuilding and Repair Quality Standard made by IACS [1]. Finally a review of how the different societies and shipyards present handles double plates [2].

1.4 Chapter presentation

In Chapter 1 we start with a brief introduction of marine structures, their operability, construction opportunities and some repair possibilities. Some history involving plate buckling and the development over the resent years is also included. In addition the scope of the thesis and a presentation of the chapters can be found here.

In Chapter 2 we can find some general theory regarding general plates and plate buckling. With a quick review of classical theory of common calculation methods for plates included.

In Chapter 3 the semi-analytical model is derived, with use of the variational method, Rayleigh Ritz.

In Chapter 4 we can find the basics for the finite element method and how it is been used in the thesis by the finite element software, Abaqus. Here are both the modelling procedure and problems encountered during the development of the complete model described.

In Chapter 5 the verification of the semi-analytical model developed during this thesis is presented. The verification process contains both some comments of the chosen displacement field and the verification itself against a finite element model.

In Chapter 6 the results of an intact plate will be presented. Here the impact of a double plated structure will be seen in respect to a single plate, with the single plate we have also the comparison between our Abaqus model and PULS.

In Chapter 7 we will look at how a double plate repair will strengthen a damaged single plate structure. And we will also see how different kind of thickness of the double plate will influence the result.

In Chapter 8 we discuss the results and draw up a conclusion of the work that has been preformed and finally some suggestion for further work are presented.

Chapter 2

General Theory

This chapter will give an overview of the theory and assumptions that are made in this thesis for development of the semi-analytical buckling model for double plates. For developing of the semi-analytical model the energy approach has been chosen, with use of Rayleigh-Ritz method as the variational method. In the first section we look at the general plate buckling theory, where the buckling phenomenon principles are undergoing a theoretical study and the yield criterion used in the thesis is thereby explained. Then we switch our focus on to the classical thin plate theory, with material properties, assumptions, boundary conditions, kinematics and more, to develop the differential equation for the plate. Next a more thoroughly understanding of the energy principles is carried out, for understanding of virtual work and potential energy. Before the variational method of choice, Rayleigh-Ritz, sum up the theoretical background we need. The theories presented in this chapter is based on well-known principles and are obtained from textbooks, articles and technical reports, Cook [21], Brubak [22], Bažant [23], Hellesland [24], IACS [1], ASSC [2], Bergan & Syvertsen [25], Byklum [20], Hareide [26], Brush & Almroth [27], Brunch [28] and Hals [29].

2.1 Plate buckling theory

The idea of buckling is in mathematical terms coupled against the stability of a structure. When a structure is loaded with such big in-plane load that it becomes unstable the construction will buckle. At this point the system reaches its critical load and the load-displacement curve will change its path. Buckling is in other words seen as structural instability, sudden failure.

2.1.1 Introduction

The load-displacement curve can be divided into two stages, one pre-bifurcation point and the other post-bifurcation point, see Fig.2.1, where the bifurcation point represents the point where buckling load is reached.

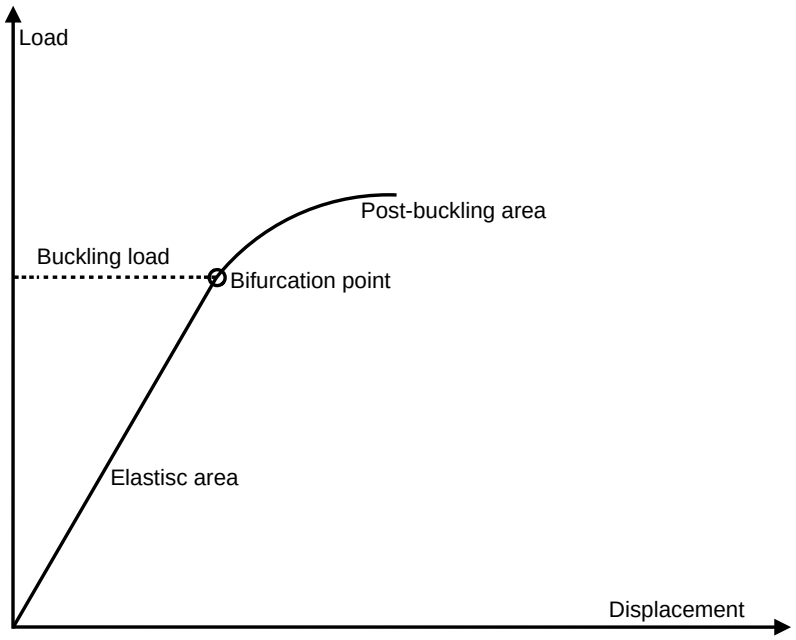

Figure 2.1: Description of bifurcation point.

When the load level is lower than the bifurcation point the system acts totally elastic. After this point the post-buckling area is reached and the bifurcation point must be determined to see if the response of the linear elastic buckling load is stable or not. This to see if the structure is able to carry more external loads without failing, post-buckling strength. By a stable response the ultimate capacity of a plate can be found in the post-buckling area. In contrast to columns, which loose its load carrying capacity when buckled, plates can continue to carry more load, especially for slender plates the post-buckling strength can be particularly higher than the buckling strength.

In compressive loading the limit of the load carrying capacity is known as the squash yield. Long slender plates will fail at a lower load by elastic buckling. But the most common plates have slenderness between these two extremes and will fail by a combination of buckling and yielding. It is therefore important in a buckling analysis to first calculate the critical/bifurcation load and then to decide the ultimate limit load level. In calculation of the bifurcation load, classical elasticity

theory is useful in connection with the differential equation for plates or by using energy methods. Buckling of a plate can appear either in global and local forms or in a combination of them. In this thesis we will focus on local buckling. From this the out-of-plane deflection is limited at the edges, which comes from girders and sliders alignment of the section analysed.

2.1.2 Critical load

The critical load is also referred to as the eigenvalue. Eigenvalue is calculated by not having any initial imperfections, no deformations in the plate before the critical load is reached, in other words a perfect plate. The eigenvalue calculation does not take any concern to yielding of the material, leading from stress. From this the critical buckling load is often taken as a conservative result for designing plates. The result of instability in a system is from a theoretical view caused by bifurcation in the solution of the equilibrium. The equilibrium equation has to be established for a deformed body to get the effects of membrane contribution in the deformation, which can be seen in Section 2.2.3. The theory is therefore called the second order theory. Bifurcation buckling is often called Euler buckling although the structure is not even near to be like an Euler column. This is because of the way the system handles the load, it moves slightly out of position, deforms, with increasing load and does not reach a point where it suddenly collapses.

2.1.3 Post-buckling

The critical load is often just the point at which buckling begins. The capacity for plates is not been fully used when critical load is reached and an elastic plate is able to carry even more external loads. This additional strength is vital in shipbuilding industry. When the critical load is reached, the plate buckles out and most of the load is carried by the material near the edges. If we take the material yielding into account we get a better and more accurate estimate of the real strength. To do this we must perform a calculation where initial imperfection of the plate is included. It is common to specify the imperfection from the first elastic buckling shape, eigenmode, which provides the critical load, eigenvalue. This mode is used by its properties as the least-favourable imperfection, since actual or real imperfections not are known.

When the external load exceeds the buckling load will the deformation after a while be so great that yielding of the material encounters and this leads to failure/collapse of the construction. If the limit for elastic deformation is exceeded by the increasing stress, plastic deformation takes over. The stress curve deflects

and we get a large displacement/deformation which is characteristic for most of the common metals. In the transformation between elastic and plastic conditions we find the yield point, Figure 2.2. The ability of elastic deformations maintain in the plastic area. This yields that with unloading of the system the strain will bounce a little bit back, referring to stippled line in Figure 2.2, but retains most of the deformation and we have permanent deformation in the system.

A system will collapse as described by structural instability, but in addition yielding of the material can also cause collapse. Yield strength is most common to define as the stress that gives permanent extension that equals 2%. To conduct an estimation of the capacity, the loading of the system ends when the material begins to yield in a point in the middle of the plate. From this the capacity is defined from the maximum load and by doing this we avoid having non-linear behaviour of the material. To determine when plastic deformations will occur we must have a yield criterion and one common criterion is the von Mises yield criterion.

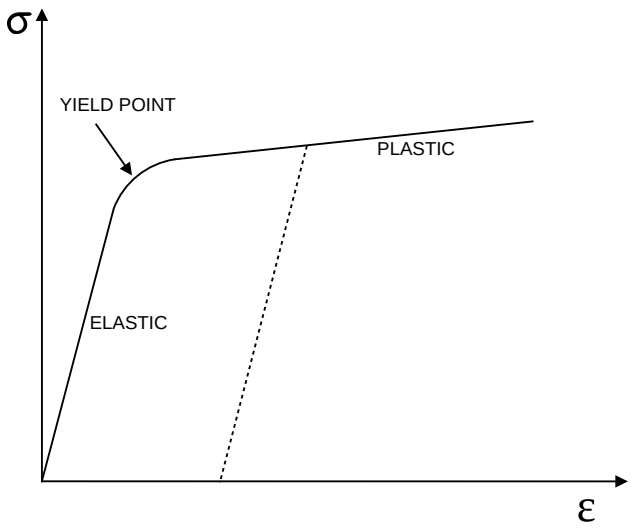

Figure 2.2: Transition between elastic and plastic behaviour.

To analyse the post-buckling behaviour, a non-linear approach with large displacement is used. It can, in mathematical terms, be quite difficult to obtain an exact solution and numerical methods are generally used. Of this it is normal to decide the capacity of a plate from the ultimate load level rather than the critical.

2.1.4 von Mises yield criterion

The von Mises yield criterion, or theory, is related to plasticity, as its ability to describe plastic behaviour of common metals. A material is stated to start yielding when the von Mises stress or often called "effective" stress, σ_e, reaches the critical value, known as yielding strength. The criterion is also referred to as the Maxwell-Huber-Hencky-von Mises theory, since Maxwell formulated it in 1865, Huber was the first to propose a criterion for shear energy, Hencky was a specialist in plasticity, but von Mises formulated what we now know as the yield criterion.

The von Mises criterion is defined as:

$$\sigma_e = \frac{1}{\sqrt{2}} \left[(\sigma_x - \sigma_y)^2 + (\sigma_y - \sigma_z)^2 + (\sigma_z - \sigma_x)^2 + 6 \left(\tau_{xy}^2 + \tau_{yz}^2 + \tau_{xz}^2 \right) \right]^{1/2} \quad (2.1.1)$$

With the assumption for plane stress taken into account, the criterion can be simplified into:

$$\sigma_e = \sqrt{\sigma_x^2 + \sigma_y^2 - \sigma_x \sigma_y + 3\tau_{xy}^2} \quad (2.1.2)$$

In principal it will be the membrane strain which causes the material to yield and then we end up with the expression for effective stress:

$$\sigma_e = \sqrt{(\sigma_x^m)^2 + (\sigma_y^m)^2 - \sigma_x^m \sigma_y^m + 3(\tau_{xy}^m)^2} \quad (2.1.3)$$

2.2 Thin plate theory

It is common to divide plate theory between thin and thick plates. Thin plates apply when the thickness is small with respect to the other dimensions. Typical the thickness is said to have maximum 0.1 ratio to the width. For thin plates we say that the neutral plan is in the xy-plan. There are two much known theories that are widely accepted, Love-Kirchhoff [9] and Mindlin-Reissner [30]. The first is called the classical plate theory and the second is called the first-order shear plate theory. In this thesis the focus is on the first one, classical plate theory.

2.2.1 Love-Kirchhoff plate theory

This is a two-dimensional mathematical model and is used to determine deformations and stresses in plates subjected to forces and torques. This is an expansion of Euler-Bernoulli beam theory [4]. It was developed by Love in 1888 and was based on the assumptions of Kirchhoff. The theory assumes that a mid-plan can be used to represent a three-dimensional plate in two-dimensional form. The kinematic assumptions made in this theory are (Kirchhoff's hypotheses), [22]:

- Straight lines that are normal to the mid-surface remain straight after deformation.
- Straight lines that are normal to the mid-surface remain normal to the mid-surface after deformation.
- The thickness of the plate does not change during a deformation.

This causes the vertical shear strain γ_{xz} and γ_{yz} to be negligible and ϵ_z, normal strain can also be neglected. Other fundamental assumptions are:

- The material is elastic, homogeneous and isotropic.
- In relation to the length and width of the plate the thickness is much smaller.
- Small deflections.
- The stress normal to the mid-surface, σ_z, is small with respect to the other stress components and can be neglected.

A material with these properties can be described by only two elasticity constants. Young's modules, E, and shear modules, G.

2.2.2 Material law

A three dimension infinitesimal element has the edges dx, dy, dz. With isotropic property, it has equal elastic properties in all directions. All edges have effect of normal stress and shear stress. With an assumption made by Kirchhoff, we neglect the effect of dz, see Fig 2.3. With this two dimensional problem, there are two types of approaches, plane stress and plane strain.

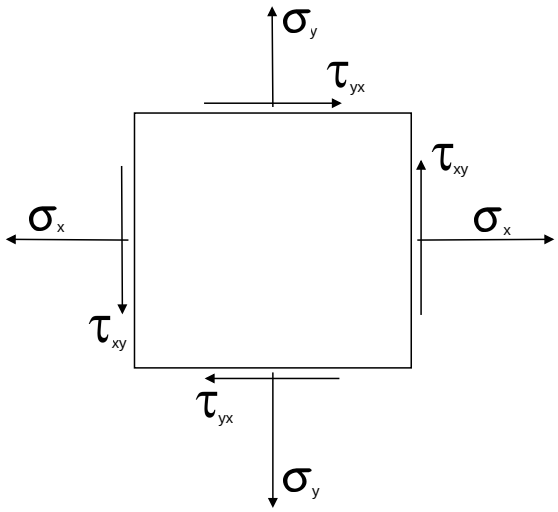

Figure 2.3: Illustration of a two-dimensional element state of stress.

Plane stress

For thin plates it is normal to assume plane stress and that is what we will concentrate on.

Plane stress is defined to be a state of stress where the normal stress, σ_z , and the shear stress, τ_{xz} and τ_{yz}, perpendicular to the xy-plan are assumed to be zero,[28].

From the assumptions above and with Hook's law for isotropic material we get:

$$\boldsymbol{\sigma} = \mathbf{E} \cdot \boldsymbol{\epsilon} \tag{2.2.1}$$

$$\begin{Bmatrix} \sigma_x \\ \sigma_y \\ \tau_{xy} \end{Bmatrix} = \frac{E}{(1-\nu^2)} \begin{bmatrix} 1 & \nu & 0 \\ \nu & 1 & 0 \\ 0 & 0 & \frac{1-\nu}{2} \end{bmatrix} \begin{Bmatrix} \epsilon_x \\ \epsilon_y \\ \gamma_{xy} \end{Bmatrix} \tag{2.2.2}$$

This leads to

$$\sigma_x = \frac{E}{1-\nu^2}\left(\epsilon_x + \nu\epsilon_y\right) \tag{2.2.3}$$

$$\sigma_y = \frac{E}{1-\nu^2}\left(\epsilon_y + \nu\epsilon_x\right) \tag{2.2.4}$$

$$\tau_{xy} = \frac{E}{2\left(1+\nu\right)}\gamma_{xy} = G\gamma_{xy} \tag{2.2.5}$$

Where G is the shear module and ν is the Poisson ratio.

2.2.3 Kinematic

Displacement

In consideration of an infinitesimal element, like Fig 2.3, it can be shown that the displacement, how the body deforms, have contribution both from displacement in the neutral plan and due to bending, see Fig 2.4. These are given superscript m for displacement to the mid-surface (neutral) and b for bending.

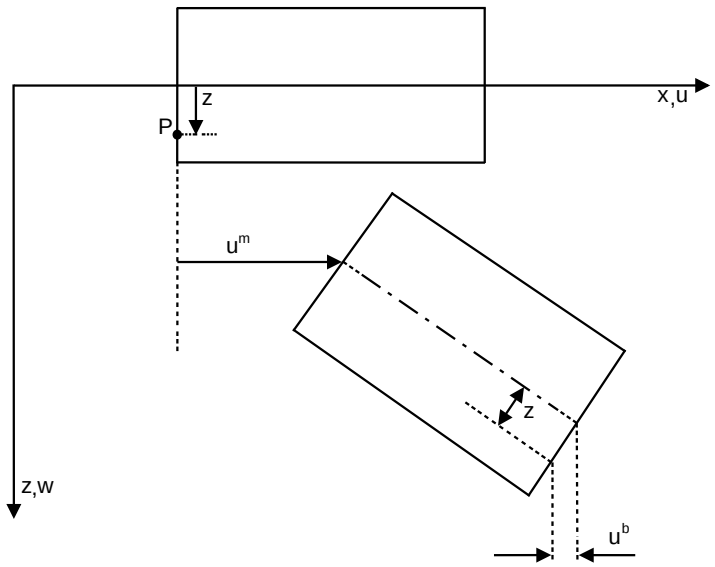

Figure 2.4: Displacement of an infinitesimal element.

$$\begin{aligned} u &= u^m + u^b \\ v &= v^m + v^b \end{aligned} \tag{2.2.6}$$

Bending strain

From the assumptions given, Kirchhoff's hypotheses, a point on the mid-surface will bend with the displacements u^b, v^b and w. This used in the same way as in regular plate bending theory.

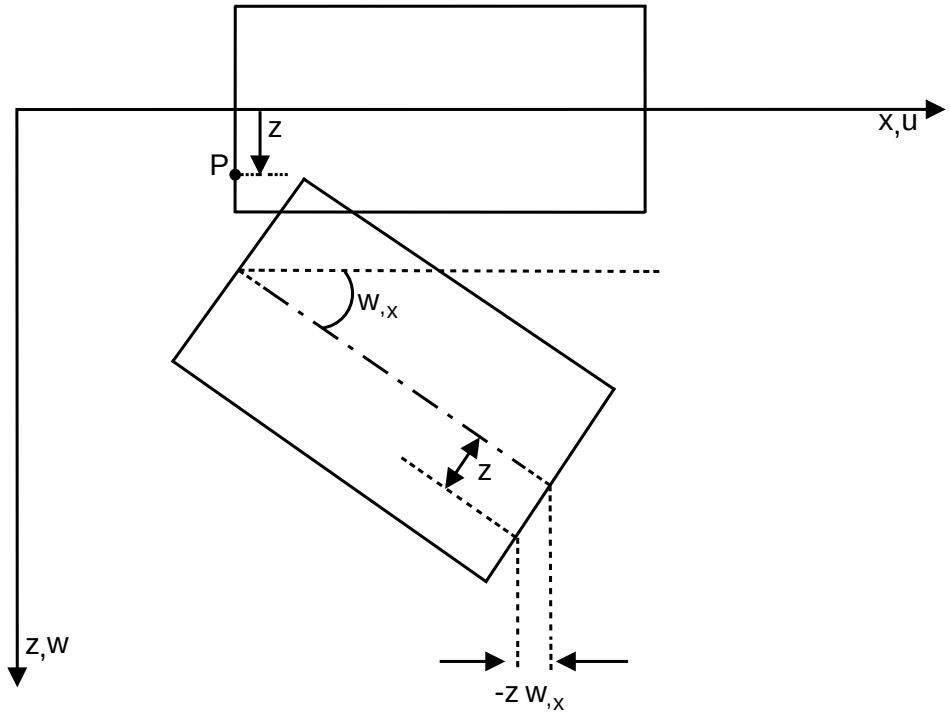

Figure 2.5: Infinitesimal element with contribution of bending deformation.

$$u^b = -z\frac{\partial w}{\partial x} = -zw_{,x} \tag{2.2.7}$$

$$v^b = -z\frac{\partial w}{\partial y} = -zw_{,y} \tag{2.2.8}$$

Bending strain is given with respect to obtain continuity between strains and displacements.

$$\epsilon_x^b = u_{,x}^b = -zw_{,xx} \tag{2.2.9}$$

$$\epsilon_y^b = v_{,y}^b = -zw_{,yy} \tag{2.2.10}$$

$$\gamma_{xy}^b = u_{,y}^b + v_{,x}^b = -2zw_{,xy} \tag{2.2.11}$$

w is displacement in transverse direction. The deflection is relative to the imperfection and therefore the bending strain will not be affected by this.

Membrane strain

Membrane strain is in large deflection theory given by Green strains, but here small deflection is assumed, hence axial force remains constant. We consider a plate without imperfection and derive the normal strains in x- and y-direction, see Fig. 2.6.

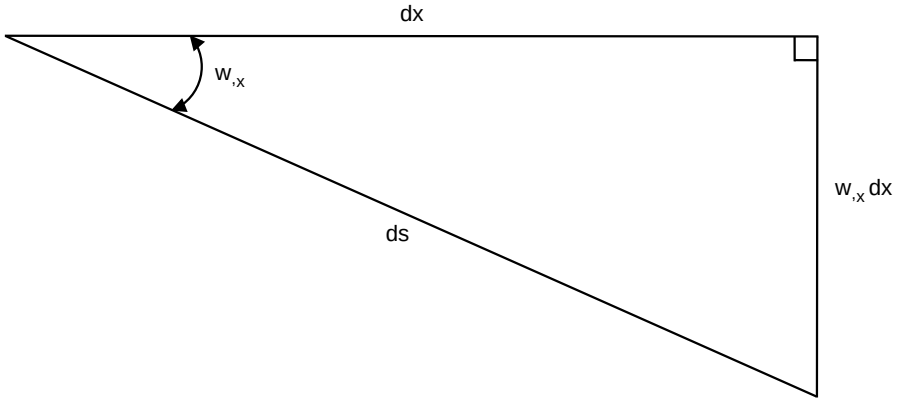

Figure 2.6: Definition of relative length for membrane strain.

The strain is then calculated with aspect to the change relative in length, [21].

$$\epsilon^m = \frac{ds - dx}{dx} = \frac{ds}{dx} - 1 \tag{2.2.12}$$

Where ds is the length after deflection.

$$ds = \sqrt{1 + w_{,x}^2}dx \tag{2.2.13}$$

This expression can be simplified to:

$$ds \approx \left(1 + \frac{1}{2}w_{,x}^2\right)dx \tag{2.2.14}$$

The simplification can be used because the expression is based on the two first terms of binomial expansion and is valid for $\mid w_{,x} \mid << 1$, [21]. Strain in x-direction then becomes:

$$\epsilon_x^m = \frac{\left(1 + \frac{1}{2}w_{,x}^2\right)dx - dx}{dx} = \frac{\left(1 + \frac{1}{2}w_{,x}^2\right)dx}{dx} - 1 = u_{,x}^m + \frac{1}{2}w_{,x}^2 \tag{2.2.15}$$

Equal for y-direction:

$$\epsilon_y^m = \frac{\left(1 + \frac{1}{2}w_{,x}^2\right)dy - dy}{dy} = \frac{\left(1 + \frac{1}{2}w_{,y}^2\right)dy}{dy} - 1 = u_{,y}^m + \frac{1}{2}w_{,y}^2 \tag{2.2.16}$$

The shear strain, γ_{xy}, is given by Bažant and Cedolin and is based on von Karman's kinematic relations for a plate, [23].

$$\gamma_{xy}^m = u_{,y}^m + v_{,x}^m + w_{,x}^m w_{,y}^m \tag{2.2.17}$$

Total strain

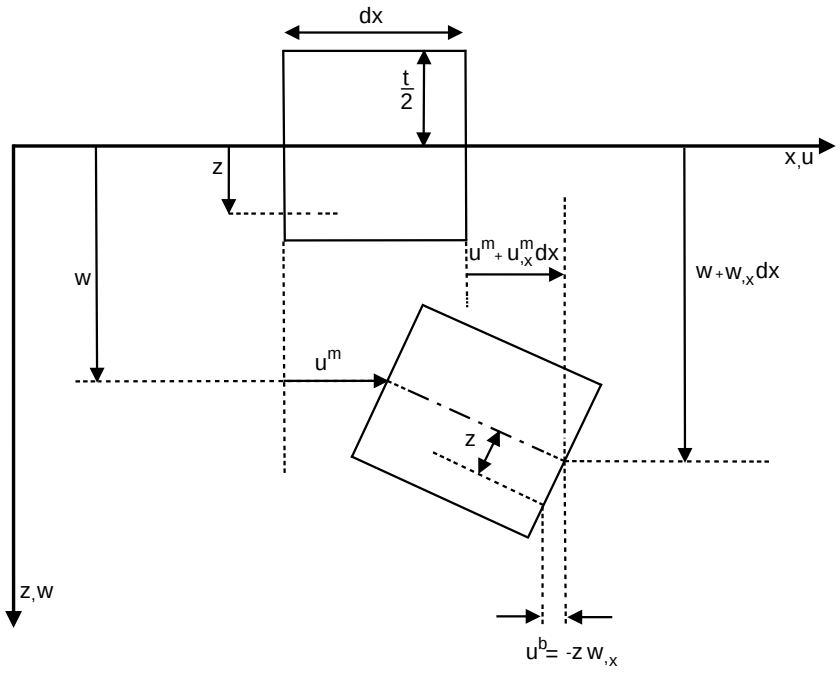

Figure 2.7: Infinitesimal element with contribution of total deformation.

Kinematic continuity between displacements and strains gives, with aspect to Eq.(2.2.6), the total strain definition:

$$\epsilon_x = \epsilon_x^m + \epsilon_x^b \tag{2.2.18}$$

$$\epsilon_y = \epsilon_y^m + \epsilon_y^b \tag{2.2.19}$$

$$\gamma_{xy} = \gamma_{xy}^m + \gamma_{xy}^b \tag{2.2.20}$$

2.2.4 Equilibrium

The forces and moments acting on a plate element can be divided into three separate contributions:

1. In-plane forces
2. Out-of-plane forces
3. Moments

Forces

The in-plane forces on the plate element are given like Fig. 2.8. To implement the contribution of the in-plane forces in the deflection, we seek the equilibrium in z-direction, $\sum F_z$. This gives, as the total result, with the relation that $N_{xy} = N_{yx}$.

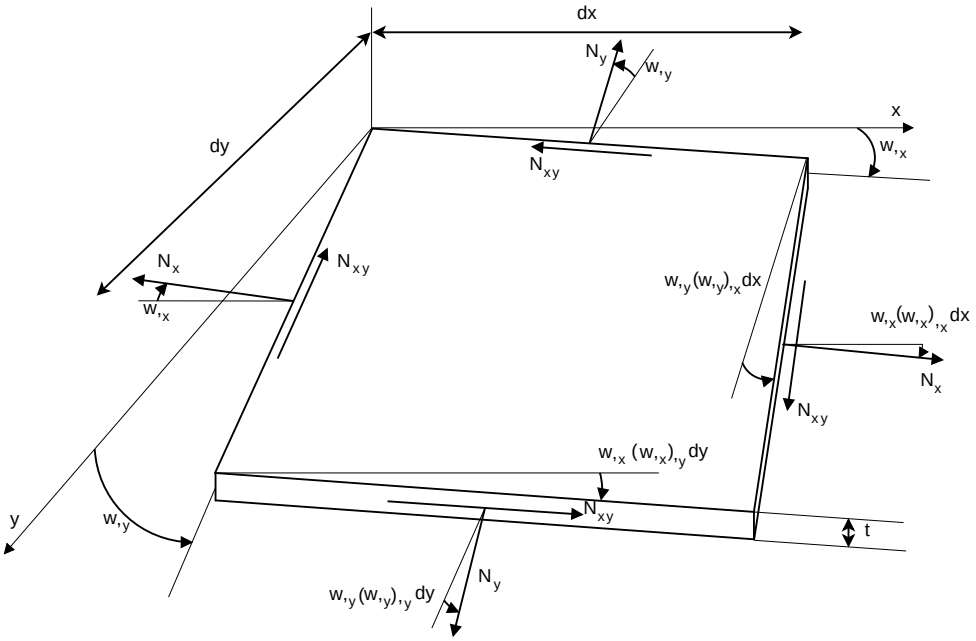

Figure 2.8: In-plane forces on a plate element.

$$\sum F_z = \left(N_x \frac{\partial^2 w}{\partial x^2} + N_y \frac{\partial^2 w}{\partial y^2} + 2N_{xy} \frac{\partial^2 w}{\partial x \partial y} \right) dxdy \tag{2.2.21}$$

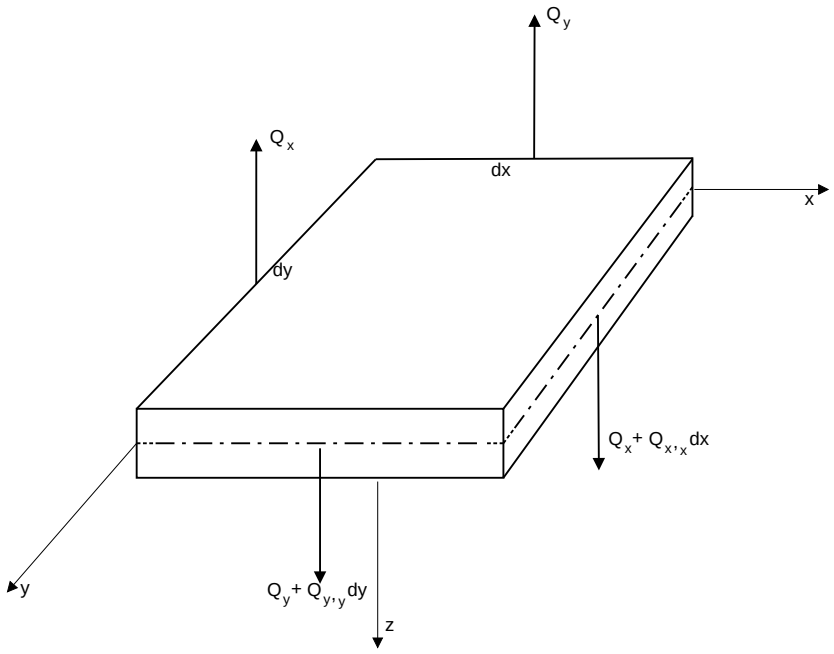

Figure 2.9: Out of plane forces on a plate element.

Considering the forces out of plane, see Fig. 2.9, the equilibrium can be written as

$$-Q_x dy - Q_y dx + \left(Q_x + \frac{\partial Q_x}{\partial x} dx\right) dy + \left(Q_y + \frac{\partial Q_y}{\partial y} dy\right) dx = 0 \qquad (2.2.22)$$

which gives

$$\frac{\partial Q_x}{\partial x} + \frac{\partial Q_y}{\partial y} = 0 \qquad (2.2.23)$$

Eq.(2.2.21) and Eq.(2.2.23) combined, results in the total contribution of forces in z-direction,

$$\frac{\partial Q_x}{\partial x} + \frac{\partial Q_y}{\partial y} + N_x \frac{\partial^2 w}{\partial x^2} + N_y \frac{\partial^2 w}{\partial y^2} + 2N_{xy} \frac{\partial^2 w}{\partial x \partial y} = 0 \qquad (2.2.24)$$

Moments

The moments acting on the element are shown in Fig 2.10, in addition to the contribution of the out of plane forces from Fig. 2.9. By taking equilibrium about the x-axis, $\sum M_x = 0$, we get

$$\frac{\partial M_y}{\partial y} dy dx + \frac{\partial M_{xy}}{\partial x} dx dy - \frac{\partial Q_x}{\partial x} \frac{dx dy dy}{2} - Q_y dx dy - \frac{\partial Q_y}{\partial y} dx dy dy = 0 \qquad (2.2.25)$$

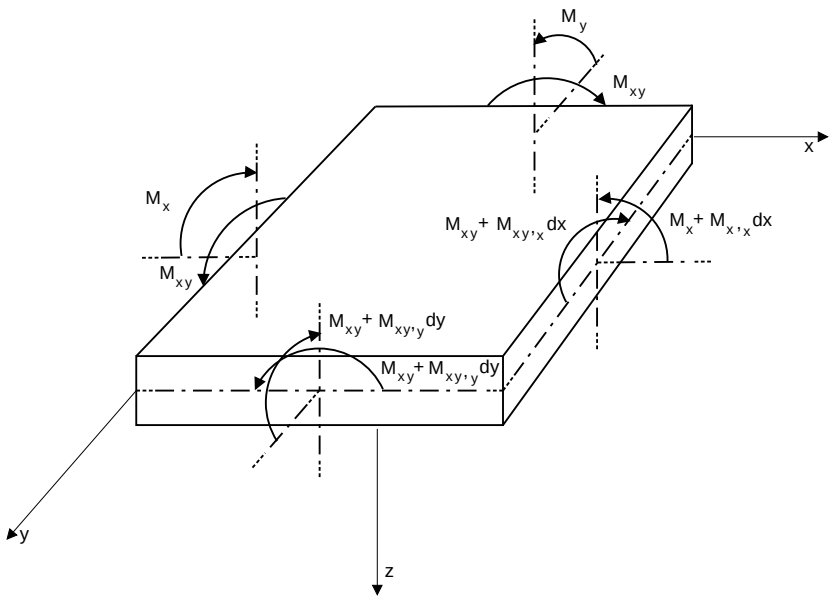

Figure 2.10: Moments acting on the plate element.

By neglecting the higher order terms, the equation can be reduced to

$$\frac{\partial M_y}{\partial y} + \frac{\partial M_{xy}}{\partial x} - Q_y = 0 \tag{2.2.26}$$

Moment equilibrium about the y-axis gives the equivalent expression.

$$\frac{\partial M_x}{\partial x} + \frac{\partial M_{xy}}{\partial y} - Q_x = 0 \tag{2.2.27}$$

In order to substitute these two equations above into Eq. (2.2.24) we must differentiate and solve for Q_x and Q_y, which leads to the differential equation of the plate in form of:

$$\frac{\partial^2 M_x}{\partial x^2} + 2\frac{\partial^2 M_{xy}}{\partial x \partial y} + \frac{\partial^2 M_y}{\partial y^2} + N_x\frac{\partial^2 w}{\partial x^2} + N_y\frac{\partial^2 w}{\partial y^2} + 2N_{xy}\frac{\partial^2 w}{\partial x \partial y} = 0 \tag{2.2.28}$$

Stress and moment relation

To represent the equation above, Eq. (2.2.28), in form of transverse displacement w, we use the stress expression from Eq. (2.2.3) and the bending strain expression Eq. (2.2.9) to find the bending and torsion moments.

$$M_x = \int_{-\frac{t}{2}}^{\frac{t}{2}} \sigma_x z dz \quad M_x = \int_{-\frac{t}{2}}^{\frac{t}{2}} \sigma_y z dz \quad M_{xy} = M_{yx} = \int_{-\frac{t}{2}}^{\frac{t}{2}} \tau_{xy} z dz \tag{2.2.29}$$

$$Q_x = \int_{-\frac{t}{2}}^{\frac{t}{2}} \tau_{xz} dz \qquad Q_y = \int_{-\frac{t}{2}}^{\frac{t}{2}} \tau_{yz} dz \tag{2.2.30}$$

To represent the already established differential equation, Eq. (2.2.28), in form of transverse displacement w, we use the strain equations derived in Section 2.2.3, for bending strain, and the assumption of plane stress, Eq.(2.2.3)-(2.2.5). Then the relations can be rewritten to

$$\begin{aligned} M_x &= -D\left(w_{,xx} + \nu w_{,yy}\right) \\ M_y &= -D\left(w_{,yy} + \nu w_{,xx}\right) \\ M_{xy} &= -D\left(1-\nu\right) w_{,xy} \end{aligned} \tag{2.2.31}$$

where $D = \frac{Et^3}{12(1-\nu^2)}$ is the flexural rigidity for a isotropic plate.

2.2.5 Differential equation

The differential equation of the problem, displacement of the plate, is developed by using Eq. (2.2.28) and insert for the relation for moments, Eq.(2.2.31). We then have

$$D\left(\frac{\partial^4 w}{\partial x^4} + 2\frac{\partial^4 w}{\partial x^2 \partial y^2} + \frac{\partial^4 w}{\partial y^4}\right) = N_x \frac{\partial^2 w}{\partial x^2} + N_y \frac{\partial^2 w}{\partial y^2} + 2N_{xy}\frac{\partial^2 w}{\partial x \partial y} \tag{2.2.32}$$

This expression can also be written as

$$D\nabla^4 w = N_x \frac{\partial^2 w}{\partial x^2} + N_y \frac{\partial^2 w}{\partial y^2} + 2N_{xy}\frac{\partial^2 w}{\partial x \partial y} \tag{2.2.33}$$

∇^2 is called the Laplace-operator and used twice gives $\nabla^2\ \nabla^2 = \nabla^4$. The Laplace-operator is given as:

$$\nabla^2 = \frac{\partial^2}{\partial x^2}\frac{\partial^2}{\partial y^2} \tag{2.2.34}$$

The problem we now are subjected to is a 4.order differential equation and here, in contrast to 2.order theory where the internal stresses are equal to the external stresses, the equation is not disconnected anymore. The sets of equations are depending on each other. We must then have a compatibility equation, which can be derived by derivation and use of Section 2.2.3.

$$\epsilon^m_{x,yy} + \epsilon^m_{y,xx} - \gamma^m_{xy,xy} = \left(\frac{\partial^2 w}{\partial x \partial y}\right)^2 - \frac{\partial^2 w}{\partial x^2}\frac{\partial^2 w}{\partial y^2} \tag{2.2.35}$$

We now have to introduce Airy's stress function, $F(x, y)$, which states

$$N_x = t\sigma_x = F_{,yy} \quad , \quad N_y = t\sigma_y = F_{,xx} \quad , \quad N_{xy} = t\tau_{xy} = -F_{,xy} \tag{2.2.36}$$

With use of Airy's function above and Hooke's law, Section 2.2.2, the von Karman's plate equation, which it is usually called, is derived.

$$D\nabla^4 w = t\left(F_{,yy}\frac{\partial^2 w}{\partial x^2} - 2F_{,xy}\frac{\partial^2 w}{\partial x \partial y} + F_{,xx}\frac{\partial^2 w}{\partial y^2}\right) \tag{2.2.37}$$

or

$$\nabla^4 F = E\left(\left(\frac{\partial^2 w}{\partial x \partial y}\right)^2 - \frac{\partial^2 w}{\partial x^2}\frac{\partial^2 w}{\partial y^2}\right) \tag{2.2.38}$$

Of this we can now find the displacement w which then leads to forces, moments and stresses can be found anywhere on the plate. This differential equation for a plate is valid for plate without any imperfection. Marguerre used von Karman's equation to make it also valid for plate with imperfection [16]. For more complicated plate problems numerical methods are taken in use, with more use of computational power, which we will look at under Chapter 4, but also semi-analytical methods are often an even quicker way to solve problems like these. They take bases on either the differential equation, Eq. (2.2.38) in Galerkins method [23] or on energy principles, potential energy, like in Rayleigh-Ritz, which we will use later on in Chapter 3. The biggest difference between these two semi-analytical methods is that where the Rayleigh-Ritz method only is based on forming a variational problem, see Section 2.4, Galerkin method can provide approximate solutions directly to the differential equation regardless if the problem cannot transform into a variational problem and of this there is no need to find the energy functions. But in a larger view these two solution procedures are quite similar.

2.3 Energy principles

In solid mechanics, laws of physics can be expressed in various forms. One of these is the energy approach. Here the relations between stress, strain, displacement and material properties are expressed in form of energy or work done by forces, internal and external. Later in the thesis the Rayleigh-Ritz method is used to find approximate solutions by variational principles and it is therefore a common practice to use energy methods to obtain these solutions.

2.3.1 Virtual work

Virtual work arise in relation with principle of stationary action, which is a variational principle, at when action is applied a mechanical system. Virtual work is used to achieve an equation that describes behaviour for a physical system and to find the solution for an equilibrium problem. Its task is to study forces and motion to a mechanical system. Virtual work can be expressed in two ways, one where the actual load is acting on a body with virtual displacement, called *virtual displacements*, and the other where virtual load acting on a body with actual displacement, called *virtual forces*. Because of the Rayleigh-Ritz approach later on the virtual displacements will be used further on and is expressed as:

$$\delta W = \int \mathbf{F} \cdot \delta \mathbf{u} dv \tag{2.3.1}$$

where $\mathbf{F}$ is the actual force, $\delta \mathbf{u}$ is the virtual displacement and dv is the volume of the element.

Virtual work principle states that: *If a continuous body is in equilibrium, the virtual work of all actual forces in moving through a virtual displacement is zero* [30].

$$\delta W = \delta W_I + \delta W_E = 0 \tag{2.3.2}$$

Where W_I is the internal virtual work and W_E is the external virtual work.

Internal virtual work

When internal virtual work is described, many types of forces can be assembled, but here the internal energy will be considered only by the internal strain energy, which is the energy stored in the body when deformation occurs. Therefore $\delta W_I = \delta U$.

The strain energy is expressed as:

$$U = \int_V U_0 dV \tag{2.3.3}$$

where U_0 is the strain energy density. For elastic materials the energy, U_0, is stored in the material and can be regained after unloading.

$$U_0 = \int_0^{\epsilon} \boldsymbol{\sigma}^T d\boldsymbol{\epsilon} \tag{2.3.4}$$

For a linear elastic material U_0 is:

$$\begin{aligned} U_0 = &\int \sigma_x d\epsilon_x + \int \sigma_y d\epsilon_y + \int \sigma_z d\epsilon_z \\ &+ \int \tau_{xy} d\gamma_{xy} + \int \tau_{yz} d\gamma_{yz} + \int \tau_{zx} d\gamma_{zx} \end{aligned} \tag{2.3.5}$$

But with use of the assumptions for plane stress, Section 2.2.2, the expression becomes more simple.

$$U_0 = \int \sigma_x d\epsilon_x + \int \sigma_y d\epsilon_y + \int \tau_{xy} d\gamma_{xy} \tag{2.3.6}$$

By integration of Eq.(2.3.4) and use of Hook's law, U_0 becomes:

$$U_0 = \frac{1}{2}\{\boldsymbol{\sigma}\}^T\{\boldsymbol{\epsilon}\} = \frac{1}{2}\{\boldsymbol{\epsilon}\}^T [\mathbf{E}] \{\boldsymbol{\epsilon}\} \tag{2.3.7}$$

With combination of Eq.(2.3.3) and Eq.(2.3.7) the total strain energy can be expressed as:

$$U = \frac{1}{2}\int_V \{\boldsymbol{\epsilon}\}^T [\mathbf{E}] \{\boldsymbol{\epsilon}\} dV \tag{2.3.8}$$

$$\delta W_I = \delta U = \frac{1}{2}\int_V \{\boldsymbol{\epsilon}\}^T [\mathbf{E}] \{\delta\boldsymbol{\epsilon}\} dV \tag{2.3.9}$$

As described in Section 2.2.3, the strain consists of two terms, one from membrane and the other one from bending. These have to be added to get the potential energy:

$$U^p = U^m + U^b \tag{2.3.10}$$

with

$$U^m = \frac{1}{2}\int_V \{\boldsymbol{\epsilon}^m\}^T [\mathbf{E}] \{\boldsymbol{\epsilon}^m\} dV \tag{2.3.11}$$

and

$$U^b = \frac{1}{2}\int_V \{\boldsymbol{\epsilon}^b\}^T [\mathbf{E}] \{\boldsymbol{\epsilon}^b\} dV \tag{2.3.12}$$

Expressions for ϵ^b and ϵ^m is derived in Section 2.2.3.

External virtual energy

The external forces acting on a body can be split into two contributions:

- body forces per unit volume, $\mathbf{f}$.
- surface tractions per unit area, $\mathbf{T}$ or $\mathbf{\Phi}$.

$$\delta W_E = -\left(\int_V \mathbf{f} \cdot \delta\mathbf{u} dv + \int_{S_\sigma} \mathbf{T} \cdot \delta\mathbf{u} ds\right) \tag{2.3.13}$$

where V is the volume of the body, S_σ is the area of the surface where the surface tractions are valid and ds is the surface element. By setting a negative sign on the external energy expression, it is expressed that the work is done on the element. This can be written as:

$$\begin{aligned} H &= -\int_V (f_x u + f_y v + f_z w)\, dV - \int_{S_\sigma} (T_x u + T_y v + T_z w)\, dS \\ &= -\int_V \mathbf{u}^T \mathbf{f} dV - \int_{S_\sigma} \mathbf{u}^T \mathbf{T} dS \end{aligned} \tag{2.3.14}$$

Where H is the load potential.

2.3.2 Principle of minimum potential energy

The principle of minimum potential energy is valid for linear static systems. The principle can be derived from the principle of virtual work, which is the integrated expression for an equilibrium condition to a body. The total potential energy, Π, can be found by sum of the strain energy and load potential.

$$\Pi = U + H \tag{2.3.15}$$

At static equilibrium, the displacements will adjust in a way that the total potential energy gets a minimum and the derivative with respect of displacements equals zero, principle of minimum total potential energy.

$$\delta\Pi = \delta U + \delta H = 0 \tag{2.3.16}$$

δ symbolises variation. The deformation must in addition satisfy the essential boundary conditions, and the internal kinematic compatibility must be fulfilled.

For linear systems the total potential energy, Π, always comes out as quadratic function of displacement and has only one point where the conditions are satisfied. From this, a linear system has only one possible solution for a linear static problem.

2.4 Variational methods

The methods are ways to find an approximate solution for the eigenvalue. It has basis in the variational principle which is a method that finds extremes, like minimum or maximum, of a function. The method simplifies a function with one or more unknown parameters, to be expressed in the way of getting the lowest possible value. This is done by approximating some of the unknown parameters.

2.4.1 Rayleigh-Ritz method

There exist many numerical methods that solve complex problems. These methods use a final number of degrees of freedom. For a continuous system, an elastic body with infinite degrees of freedom, it is difficult or more or less impossible to determine a field, displacement or stress, which solves the partial differential equation, that describes the continuous system and that satisfy the boundary conditions. As where the analytical solution generates an exact solution, numerical methods give an approximate solution by assuming a displacement field. The problem then reduces to exist of a final number of degrees of freedom.

The displacement fields exist of a sum of functions, where the accuracy to the solution increases with the number of degrees of freedom, how well the field describe the deformation of the body and the more shape functions takes part in the displacement field. The basis of the Rayleigh-Ritz method is to use the assumed displacement field with the principle of stationary or minimum potential energy. The shape functions must be linear independent and the essential boundary conditions must be fulfilled. The method forces the body through the displacement field to deform in a particular form, which makes the body act stiffer than in reality. This result in making Rayleigh-Ritz overestimate the system, by underestimating the deformation and the solution will converge from above. This gives the solution from Rayleigh-Ritz to have exact or overestimated stiffness.

Procedure

Every point in the body can move in u, v and w direction. The method starts with defining approximate fields for these components.

$$u = \sum_{i=1}^{N_u} a_i f_{u,i} \quad v = \sum_{i=1}^{N_v} a_i f_{v,i} \quad w = \sum_{i=1}^{N_w} a_i f_{w,i} \tag{2.4.1}$$

where f is the assumed shape functions and a_i is the amplitude that the problem is reduced to be found. For thin plates with deflection out of plane, the displacement field can be written as:

$$w(x,y) = \sum_{i}^{m} \sum_{j}^{n} a_{ij} f_i(x) f_j(y) \tag{2.4.2}$$

Together with the potential energy principle we get an equation system, that by solving the displacements is fully defined.

$$\frac{\partial \Pi}{\partial a_{ij}} = 0 \tag{2.4.3}$$

To express potential energy we need both the strain energy and the load potential, from Eq.(2.3.15).

$$U = \frac{1}{2} \int_l EI \left(w''\right)^2 dx \quad \textit{and} \quad H = -\frac{P}{2} \int_l \left(w'\right)^2 dx \tag{2.4.4}$$

where w is the assumed displacement field.

$$w = \sum_{i=1}^{N_w} a_i f_i = a_1 x + a_2 x^2 + \cdots + a_{N_w} x^{N_w} \tag{2.4.5}$$

From Eq.(2.3.16) we then can write

$$\delta\Pi = \delta U + \delta H = \frac{\delta\Pi}{\delta a_1}\delta a_1 + \frac{\delta\Pi}{\delta a_2}\delta a_2 + \cdots + \frac{\delta\Pi}{\delta a_{N_w}}\delta a_{N_w} = 0 \tag{2.4.6}$$

All small variations, δa_{N_w}, must satisfy the equilibrium, then all partial derivations must equal zero.

$$\begin{aligned}
\frac{\delta\Pi}{\delta a_1} &= \frac{\delta U}{\delta a_1} + \frac{\delta H}{\delta a_1} = 0 \\
\frac{\delta\Pi}{\delta a_2} &= \frac{\delta U}{\delta a_2} + \frac{\delta H}{\delta a_2} = 0 \\
\vdots \quad & \quad \vdots \quad \vdots \quad \vdots \\
\frac{\delta\Pi}{\delta a_{N_w}} &= \frac{\delta U}{\delta a_{N_w}} + \frac{\delta H}{\delta a_{N_w}} = 0
\end{aligned} \tag{2.4.7}$$

The above equation, Eq.(2.4.7), can be simplified to

$$\frac{\delta\Pi}{\delta \mathbf{a}}\delta\mathbf{a} = \left(\frac{\delta U}{\delta \mathbf{a}} + \frac{\delta H}{\delta \mathbf{a}}\right)\delta\mathbf{a} = 0 \tag{2.4.8}$$

This leads to the eigenvalue equation

$$\left(\mathbf{K^M} - \lambda_p \mathbf{K}^G\right)\mathbf{a} = \mathbf{0} \tag{2.4.9}$$

where $\mathbf{K^M}$ is the material stiffness matrix and $\mathbf{K^G}$ is the geometric stiffness matrix. While $\mathbf{a}$ is the eigenvector and λ_p is introduced as the load factor and is the one we search for.

Chapter 3

Eigenvalue calculation

This chapter contains theory of how eigenvalue calculations are performed. The theory is based on Rayleigh-Ritz method, Section 2.4. The calculations are performed with help from the computerized mathematical programs Matlab and Maple. The calculations are based on theory from Chapter 2 with additional supplementation from Cook [21], Hareide [26], Brubak [22], Byklum [20] and Matlab help function [31].

3.1 Displacement field

To conduct the eigenvalue calculation that leads to critical load, we use the approximation method Rayleigh-Ritz, described in detail in Section 2.4.1. We start with defining a displacement field, which will approximately have the same shape as the exact problem. In our case with double plates we assume that the doubler plate is thinner than the original plate in the already existing construction. We further assume that only the doubler plate will buckle out and we must assume a displacement function that only deflects in the positive direction. Some possible functions can be:

$$f_i = sin^2\left(\frac{i\pi x}{L}\right) \tag{3.1.1}$$

$$f_i = \left(1 - cos\left(2\frac{i\pi x}{L}\right)\right) \tag{3.1.2}$$

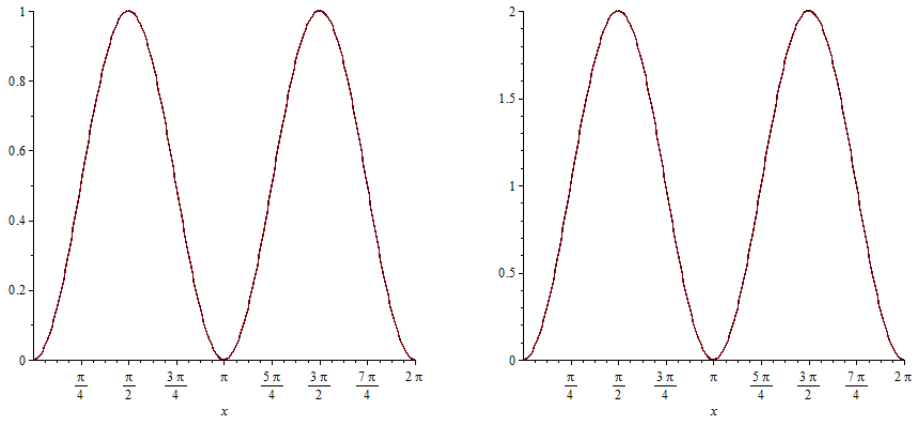

(a) (b)

Figure 3.1: (a) Shape of the *sin*-function and (b) Shape of the *cos*-function.

By plotting these functions we can see how they occur, Fig. 3.1. In our problem the plate, which is analysed, is being a part of a larger construction. We will only look at a small section of this, that is a full plate between two stiffeners, see Fig. 3.2. By the means that all the edges to the analysed plate are coupled with other plate and stiffeners we must assume a clamped boundary condition. If we look at the shape of the function Eq. (3.1.2), this function fulfils all requirements. The other function Eq. (3.1.1) also meets the demands but here we have a quadratic function and to make the calculations as simple as possible we choose Eq. (3.1.2) as our displacement function. With use of the general expression for displacement function, Eq. (2.4.2), we get:

$$w(x,y) = \sum_{i=1}^{m}\sum_{j=1}^{n} a_{ij}\left(1 - cos\left(2\frac{i\pi x}{L}\right)\right)\left(1 - cos\left(2\frac{j\pi y}{s}\right)\right) \tag{3.1.3}$$

where L is the length of the plate and s is the width between stiffeners.

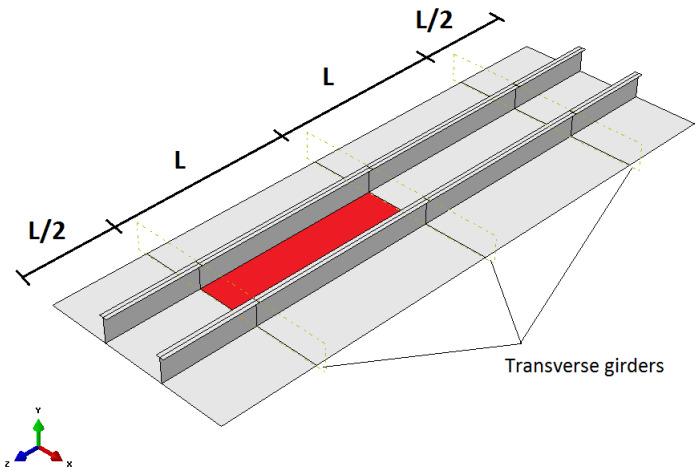

Figure 3.2: The red area marks the section we will analyse.

3.2 Potential energy

By following the procedure given in Section 2.4.1, the next step is to establish an equation system with help for the potential energy principle from Section 2.3. The total potential energy is found by the sum of the strain energy and load potential, see Section 2.3.2.

$$\Pi = U + H \tag{3.2.1}$$

3.2.1 Strain energy

From Eq.(2.3.10) we have

$$U^p = U^m + U^b = \frac{1}{2}\int_V \{\epsilon^m\}^T [\mathbf{E}] \{\epsilon^m\} dV + \frac{1}{2}\int_V \{\epsilon^b\}^T [\mathbf{E}] \{\epsilon^b\} dV \tag{3.2.2}$$

These two contributions can separately be calculated with use of Hook's law, Section 2.2.2 and the kinematic relations, Section 2.2.3.

$$U^b = \frac{D}{2}\int_0^L \int_0^s \left[(w_{,xx} + w_{,yy})^2 - 2(1-\nu)\left(w_{,xx}w_{,yy} - w_{,xy}^2\right)\right] dydx \tag{3.2.3}$$

$$U^m = \frac{t}{2E}\int_0^L \int_0^s \left[(F_{,yy} + F_{,xx})^2 - 2(1-\nu)\left(F_{,x}F_{,y} - F_{,xy}^2\right)\right] dydx \tag{3.2.4}$$

U^m can be rewritten by use of the relations for Airy's stress function, Eq.(2.2.36).

$$U^m = \frac{t}{2E}\int_0^L \int_0^s \left[(S_x + S_y)^2 - 2(1-\nu)\left(S_x S_y - S_{xy}^2\right)\right] dydx \tag{3.2.5}$$

Here S_x, S_y and S_{xy} are the applied stress on the plate section, see Fig. 3.3. From these equations we can see that only U^b will give contribution in the principle of stationary potential energy and the membrane strains can be neglected, since the Airy's stress function does not imply the amplitude, a_{ij}.

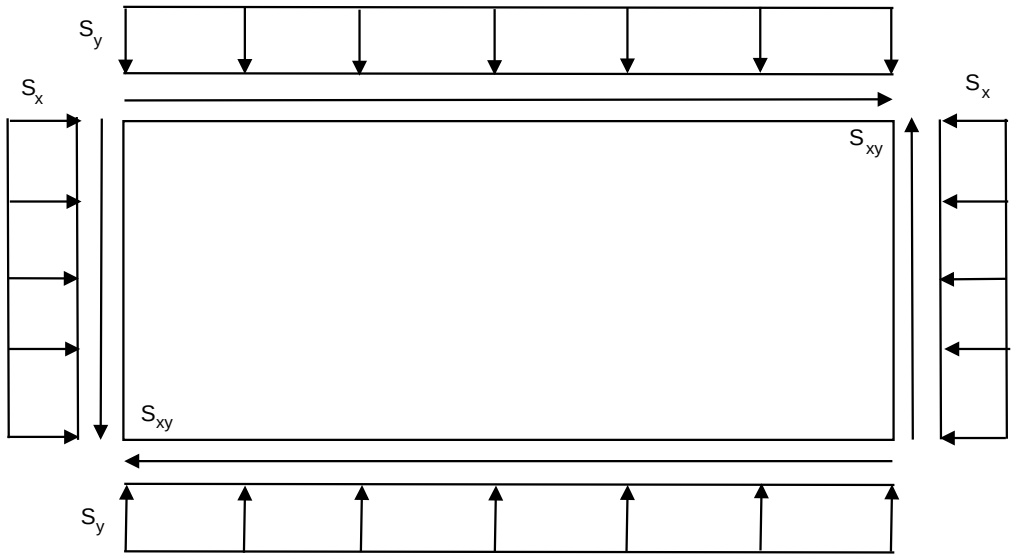

Figure 3.3: Applied stress.

3.2.2 Load potential

In general we use the Eq. (2.3.14), but in our problem the plate is only exposed to surface traction and the load potential expression is then simplified to

$$H = -\int_{S_\sigma} \mathbf{u}^T \mathbf{T} dV \tag{3.2.6}$$

The contribution of the external loads also called the load potential can be divided into three, one for each component of applied load.

$$H = H_{S_x} + H_{S_y} + H_{S_{xy}} \tag{3.2.7}$$

Each of these components can be expressed as

$$H_{S_x} = \int_0^s \int_{-\frac{t}{2}}^{\frac{t}{2}} S_x \Delta u(y)\, dzdy \tag{3.2.8}$$

where $\Delta u\,(y)$ is the end shortening in x-direction. Written with respect to stress it gives positive (pressure) contributions to the system:

$$\Delta u\,(y) = \int_0^L u^m_{,x} dx = \int_0^L \left(\epsilon^m_x - \frac{1}{2} w^2_{,x}\right) dx \tag{3.2.9}$$

We can neglect higher order terms, which means that ϵ^m does not contribute in the potential. This yields equal for the two other components and this gives us the relation

$$\begin{aligned} H = &-\frac{t}{2}\int_0^L \int_0^s \left(S_x w^2_{,x} + 2S_{xy} w_{,x} w_{,y} + S_y w^2_{,y}\right) dydx \\ &+t\int_0^L \int_0^s \left(S_x \epsilon^m_x + S_y \epsilon^m_y + S_{xy}\gamma^m_{xy}\right) dydx \end{aligned} \tag{3.2.10}$$

By inserting the approximated displacement field, Eq. (3.1.2), and Airy's stress function, the load potential can be derived exactly. As for the strain energy the last integral can be neglected also for the load potential expression, as for the linear expression of $F(x, y)$, that would not be of any contribution in the minimum potential energy principle where we must differentiate the total potential energy expression twice.

3.2.3 Stiffness matrices

Our next job is to find the two stiffness matrices, material and geometric, that completes the eigenvalue problem, Eq. (2.4.9).

$$\begin{aligned} \mathbf{K}^M &= \frac{\partial^2 U}{\partial \mathbf{a}^2} \\ \mathbf{K}^G &= \frac{\partial^2 H}{\partial \mathbf{a}^2} \end{aligned} \tag{3.2.11}$$

Material stiffness matrix

We start with defining our system:

$$\mathbf{K}^M = \frac{\partial^2 U}{\partial a_{pq}\partial a_{rt}} = \begin{bmatrix} \frac{\partial^2 U}{\partial a_{11}\partial a_{11}} & \cdots & \frac{\partial^2 U}{\partial a_{11}\partial a_{mn}} \\ \vdots & & \vdots \\ \frac{\partial^2 U}{\partial a_{mn}\partial a_{11}} & \cdots & \frac{\partial^2 U}{\partial a_{mn}\partial a_{mn}} \end{bmatrix} \tag{3.2.12}$$

From Section 3.2.1 we have the expression for the strain energy:

$$U = \frac{D}{2}\int_0^L \int_0^s \left[\left(w_{,xx} + w_{,yy}\right)^2 - 2\left(1-\nu\right)\left(w_{,xx}w_{,yy} - w^2_{,xy}\right)\right] dydx \tag{3.2.13}$$

By inserting the displacement function, Eq. (3.1.3) and solve the integral we end up with an expression for the strain energy. The whole calculation is shown in Appendix A.2, with use of the integrals from Appendix A.1.

$$
\begin{aligned}
U =& \frac{D}{2}\left[\sum_{i=1}^{m}\sum_{j=1}^{n}\sum_{k=1}^{p}\sum_{l=1}^{q} a_{ij}a_{kl}\left(2\frac{i\pi}{L}\right)^2\left(2\frac{k\pi}{L}\right)^2\cdot\frac{3}{4}\cdot L\cdot s\delta_{ik}\delta_{jl}\right. \\
&+\sum_{i=1}^{m}\sum_{j=1}^{n}\sum_{k=1}^{p}\sum_{l=1}^{q} a_{ij}a_{kl}\left(2\frac{i\pi}{L}\right)^2\left(2\frac{k\pi}{L}\right)^2\cdot\frac{L\cdot s}{2}\delta_{ik}I_{jl} \\
&+\sum_{i=1}^{m}\sum_{j=1}^{n}\sum_{k=1}^{p}\sum_{l=1}^{q} a_{ij}a_{kl}\left(2\frac{j\pi}{s}\right)^2\left(2\frac{l\pi}{s}\right)^2\cdot\frac{3L}{2}\cdot\frac{s}{2}\delta_{ik}\delta_{jl} \\
&+\sum_{i=1}^{m}\sum_{j=1}^{n}\sum_{k=1}^{p}\sum_{l=1}^{q} a_{ij}a_{kl}\left(2\frac{j\pi}{s}\right)^2\left(2\frac{l\pi}{s}\right)^2\cdot L\cdot\frac{s}{2}I_{ik}\delta_{jl} \\
&+2\nu\sum_{i=1}^{m}\sum_{j=1}^{n}\sum_{k=1}^{p}\sum_{l=1}^{q} a_{ij}a_{kl}\left(2\frac{i\pi}{L}\right)^2\left(2\frac{l\pi}{s}\right)^2\cdot\frac{L\cdot s}{4}\delta_{ik}\delta_{jl} \\
&\left.+2(1-\nu)\sum_{i=1}^{m}\sum_{j=1}^{n}\sum_{k=1}^{p}\sum_{l=1}^{q} a_{ij}a_{kl}\left(2\frac{i\pi}{L}\right)\left(2\frac{k\pi}{L}\right)\left(2\frac{j\pi}{s}\right)\left(2\frac{l\pi}{s}\right)\cdot\frac{L\cdot s}{4}\delta_{ik}\delta_{jl}\right]
\end{aligned}
\tag{3.2.14}
$$

Here δ refers to Kronecker's delta, which is an indicator for the integral to only be non-zero when the terms are equal and I indicate the same when the terms are unequal. Further this expression must be differentiated twice in order to complete the matrix. We divide the total expression into six separate parts and differentiate them separately. The first term is derived here, the rest is derived in Appendix A.4.

$$
\begin{aligned}
\mathbf{K}_1^M =& \frac{\partial^2}{\partial a_{pq}\partial a_{rt}}\left[\frac{D}{2}\sum_{i=1}^{m}\sum_{j=1}^{n}\sum_{k=1}^{p}\sum_{l=1}^{q} a_{ij}a_{kl}\left(2\frac{i\pi}{L}\right)^2\left(2\frac{k\pi}{L}\right)^2\cdot\frac{3}{4}\cdot L\cdot s\delta_{ik}\delta_{jl}\right] \\
=& \frac{\partial}{\partial a_{pq}}\frac{D}{2}\left[\sum_{k=1}^{p}\sum_{l=1}^{q} a_{kl}\left(2\frac{r\pi}{L}\right)^2\left(2\frac{k\pi}{L}\right)^2\cdot\frac{3}{4}\cdot L\cdot s\delta_{rk}\delta_{tl}\right. \\
&\left.+\sum_{i=1}^{m}\sum_{j=1}^{n} a_{ij}\left(2\frac{i\pi}{L}\right)^2\left(2\frac{r\pi}{L}\right)^2\cdot\frac{3}{4}\cdot L\cdot s\delta_{ir}\delta_{jt}\right] \\
=& \frac{D}{2}\left[\left(2\frac{r\pi}{L}\right)^2\left(2\frac{p\pi}{L}\right)^2\cdot\frac{3}{4}\cdot L\cdot s\delta_{rp}\delta_{tq}+\left(2\frac{p\pi}{L}\right)^2\left(2\frac{r\pi}{L}\right)^2\cdot\frac{3}{4}\cdot L\cdot s\delta_{pr}\delta_{qt}\right]
\end{aligned}
\tag{3.2.15}
$$

The five others will come out as:

$$\mathbf{K}_2^M = \frac{D}{2}\left[\left(2\frac{r\pi}{L}\right)^2\left(2\frac{p\pi}{L}\right)^2\cdot\frac{L\cdot s}{2}\delta_{rp}I_{tq} + \left(2\frac{p\pi}{L}\right)^2\left(2\frac{r\pi}{L}\right)^2\cdot\frac{L\cdot s}{2}\delta_{pr}I_{qt}\right] \tag{3.2.16}$$

$$\mathbf{K}_3^M = \frac{D}{2}\left[\left(2\frac{t\pi}{s}\right)^2\left(2\frac{q\pi}{s}\right)^2\cdot\frac{3L}{2}\cdot\frac{s}{2}\delta_{rp}\delta_{tq} + \left(2\frac{q\pi}{s}\right)^2\left(2\frac{t\pi}{s}\right)^2\cdot\frac{3L}{2}\cdot\frac{s}{2}\delta_{pr}\delta_{qt}\right] \tag{3.2.17}$$

$$\mathbf{K}_4^M = \frac{D}{2}\left[\left(2\frac{t\pi}{s}\right)^2\left(2\frac{q\pi}{s}\right)^2\cdot L\cdot\frac{s}{2}I_{rp}\delta_{tq} + \left(2\frac{q\pi}{s}\right)^2\left(2\frac{t\pi}{s}\right)^2\cdot L\cdot\frac{s}{2}I_{pr}\delta_{qt}\right] \tag{3.2.18}$$

$$\mathbf{K}_5^M = D\nu\left[\left(2\frac{r\pi}{L}\right)^2\left(2\frac{t\pi}{s}\right)^2\cdot\frac{L\cdot s}{4}\delta_{rp}\delta_{tq} + \left(2\frac{p\pi}{L}\right)^2\left(2\frac{q\pi}{s}\right)^2\cdot\frac{L\cdot s}{4}\delta_{pr}\delta_{qt}\right] \tag{3.2.19}$$

$$\begin{aligned}\mathbf{K}_6^M =& \frac{D}{2}\cdot 2\left(1-\nu\right)\left[\left(2\frac{r\pi}{L}\right)\left(2\frac{p\pi}{L}\right)\left(2\frac{t\pi}{s}\right)\left(2\frac{q\pi}{s}\right)\cdot\frac{L\cdot s}{4}\delta_{rp}\delta_{tq}\right. \\ &\left. + \left(2\frac{p\pi}{L}\right)\left(2\frac{r\pi}{L}\right)\left(2\frac{q\pi}{s}\right)\left(2\frac{t\pi}{s}\right)\cdot\frac{L\cdot s}{4}\delta_{pr}\delta_{qt}\right]\end{aligned} \tag{3.2.20}$$

Geometric stiffness matrix

The procedure above applies in the same way for the geometric stiffness matrix.

$$\mathbf{K}^G = \frac{\partial^2 H}{\partial a_{pq}\partial a_{rt}} = \begin{bmatrix} \frac{\partial^2 H}{\partial a_{11}\partial a_{11}} & \cdots & \frac{\partial^2 H}{\partial a_{11}\partial a_{mn}} \\ \vdots & & \vdots \\ \frac{\partial^2 H}{\partial a_{mn}\partial a_{11}} & \cdots & \frac{\partial^2 H}{\partial a_{mn}\partial a_{mn}} \end{bmatrix} \tag{3.2.21}$$

Where we insert the expression for the load potential from Eq.(3.2.10).

$$H = -\frac{t}{2}\int_0^L\int_0^s \left(S_x w_{,x}^2 + 2S_{xy}w_{,x}w_{,y} + S_y w_{,y}^2\right)dydx \tag{3.2.22}$$

In the assumed displacement field, Eq. (3.1.3), we have a function only containing cosine functions. A cosine function will only be able to describe symmetrical

shapes. Shear behaviour will need asymmetrical shapes and because of this our approximation cannot perform an analysis with shear forces. We can then neglect the shear term, S_{xy} from the Eq. (3.2.22). The full calculation of this matrix, with integrals and differentiation, can be found in Appendix A.3 and A.5.

$$\mathbf{K}_1^G = \left(-\frac{t}{2}\right) S_x \left[\left(2\frac{r\pi}{L}\right)\left(2\frac{p\pi}{L}\right)\cdot\frac{L}{2}\cdot\frac{3s}{2}\delta_{rp}\delta_{tq} + \left(2\frac{p\pi}{L}\right)\left(2\frac{r\pi}{L}\right)\cdot\frac{L}{2}\cdot\frac{3s}{2}\delta_{pr}\delta_{qt}\right] \tag{3.2.23}$$

$$\mathbf{K}_2^G = \left(-\frac{t}{2}\right) S_x \left[\left(2\frac{r\pi}{L}\right)\left(2\frac{p\pi}{L}\right)\cdot\frac{L}{2}\cdot s\delta_{rp}I_{tq} + \left(2\frac{p\pi}{L}\right)\left(2\frac{r\pi}{L}\right)\cdot\frac{L}{2}\cdot s\delta_{pr}I_{qt}\right] \tag{3.2.24}$$

$$\mathbf{K}_3^G = \left(-\frac{t}{2}\right) S_y \left[\left(2\frac{t\pi}{s}\right)\left(2\frac{q\pi}{s}\right)\cdot\frac{3L}{2}\cdot\frac{s}{2}\delta_{rp}\delta_{tq} + \left(2\frac{q\pi}{s}\right)\left(2\frac{t\pi}{s}\right)\cdot\frac{3L}{2}\cdot\frac{s}{2}\delta_{pr}\delta_{qt}\right] \tag{3.2.25}$$

$$\mathbf{K}_4^G = \left(-\frac{t}{2}\right) S_y \left[\left(2\frac{t\pi}{s}\right)\left(2\frac{q\pi}{s}\right)\cdot L\cdot\frac{s}{2}I_{rp}\delta_{tq} + \left(2\frac{q\pi}{s}\right)\left(2\frac{t\pi}{s}\right)\cdot L\cdot\frac{s}{2}I_{pr}\delta_{qt}\right] \tag{3.2.26}$$

3.2.4 Solution of the eigenvalue problem

We now know all the parameters that lead to the eigenvalue problem and we use the eigenvalue equation, Eq. (2.4.9), to solve the system with respect to the unknown parameter λ_p, which represents the eigenvalue. A Matlab script is provided for the solution and can be found in Appendix B. Matlab's eigenvalue calculation procedure have bases in the eigenvalue equation being solved like this:

$$\mathbf{K^M a} = \lambda_p \mathbf{K}^G \mathbf{a} \tag{3.2.27}$$

Chapter 4

Finite element method

4.1 Introduction

Finite element method (FEM) is a numerical method that in the recent years has become one of the most important methods to carry out strength and deformation calculations of constructions. The method is based on approximated solutions of defined problems within advanced mathematics, that can not be solved analytically. Such problems for example are partial differential equations (PDE). These can be solved by approximating the PDE in a system of ordinary differential equations (ODE) that can be solved with use of standard techniques. The challenge with this method is to decide such a system.

In element method (EM) the construction/structure/body is divided into smaller parts that as whole define the total area of what should be analysed. The parts which the construction is divided into are called elements and a composition of these, decided by the engineer/constructor in the purpose of analyse, is named mesh. A mesh can exist of different elements, regarding size and types of elements. Elements link up in a mesh through nodes, intersections, that is stated discreet points. The mesh is represented by a system of algebraic equations, which are solved for the unknowns at the nodes. FEM can be used on every field analysis and can solve problems within stability, dynamics, heat transfer, hydrodynamics and non-linear behaviour of constructions. This is one of the advantages with FEM, but several others make this method stronger in relation to other numerical methods:

- No geometrical limitations. A body can have all kinds of moulds and sizes.
- Boundary condition and loading is not limited.

- The material properties are not bound to be isotropic and can have different properties between parts in the assembly.
- Various types of elements can be combined, in form of types and degree of freedom. Column, beam, plate, shell, volume, etc.
- The FE-model is closely similar to the real construction, which is analysed.
- The element size can be changed, in the way that more elements are defined in the same area. This leads to even better stress distribution.

The method has, as mentioned earlier, a wide range of application and can be used for lots of applications, from strength calculations of ship hull to predicting the weather. The theories take bases from Cook [21], Brubak [22], Hareide [26], Kippenes [32] and Abaqus User Manual [33].

4.2 Principles of the element method

The method is based on the same total potential energy expression found earlier, Eq. (2.3.15) and the expressions for strain energy and potential load energy, Eq. (2.3.8) and Eq. (2.3.14) respectively. Instead of the classical Rayleigh-Ritz method which defines one element for the whole body, the FEM approach divides the body into an assembly of smaller elements and defines separately interpolation for each element.

$$\Pi = \frac{1}{2}\sum_{e=1}^{n}\int_{V_e}\epsilon_e^T\mathbf{E}\epsilon_e dV_e - \sum_{e=1}^{n}\int_{V_e}\mathbf{u}_e^T\mathbf{f}dV_e - \sum_{e=1}^{n}\int_{S_{\sigma_e}}\mathbf{u}_e^T\mathbf{T}dS_{\sigma_e} \tag{4.2.1}$$

were n is number of elements the body is divided into. We know from earlier that

$$\epsilon = \delta\mathbf{u} \tag{4.2.2}$$

In the element method $\mathbf{u}$ is a set of polynomials, $\mathbf{u} \in \mathbf{P}^n$ and is assumed as

$$\begin{aligned}\mathbf{u} &= c_0 + c_1\mathbf{x} + c_2\mathbf{x}^2 + \ldots + c_n\mathbf{x}^n \\ &= d_1\left(1 + x + \ldots x^n\right) + d_2\left(1 + x + \ldots x^n\right) + d_m\left(1 + x + \ldots x^n\right) \\ &= d_1 \cdot P_1 + d_2 \cdot P_2 + \ldots d_m \cdot P_m\end{aligned} \tag{4.2.3}$$

This can then be written as

$$\mathbf{u} = \begin{bmatrix}P_1 & P_2 & \ldots & P_m\end{bmatrix} \cdot \begin{bmatrix}d_1 \\ d_2 \\ \vdots \\ d_m\end{bmatrix} = \mathbf{Nd} \tag{4.2.4}$$

This leads to, with use of Eq.(4.2.2).

$$\epsilon = \delta \mathbf{N}\mathbf{d} \tag{4.2.5}$$

where $\delta\mathbf{N} = \mathbf{B}$, which is the unit displacement-strain matrix. From these relations the potential energy expression can be derived once again. $\mathbf{a}_e$ is the topology matrix, which is a tool that gives relations between displacement, $\mathbf{d}_e \sim \mathbf{D}$, stiffness, $\mathbf{k}_e \sim \mathbf{K}$ and load, $\mathbf{r}_e \sim \mathbf{R}$.

$$\Pi = \sum_{e=1}^{n} \left[\frac{1}{2} \int_{V_e} \mathbf{D}^T \mathbf{a}_e^T \mathbf{B}_e^T \mathbf{E} \mathbf{B}_e \mathbf{a}_e \mathbf{D} dV_e - \int_{V_e} \mathbf{D}^t \mathbf{a}_e^T \mathbf{N}_e^T \mathbf{f} dV_e - \int_{S_{\sigma_e}} \mathbf{D}^T \mathbf{a}_e^T \mathbf{N}_e^T \mathbf{T} dS_{\sigma_e} \right] \tag{4.2.6}$$

where $\mathbf{D}^T \mathbf{a}_e^t \mathbf{B}_e \mathbf{E} \mathbf{B}_e \mathbf{a}_e \mathbf{D}$ is a scalar and equal to $\left(\mathbf{D}^T \mathbf{a}_e^T \mathbf{B}_e \mathbf{E} \mathbf{B}_e \mathbf{a}_e \mathbf{D}\right)^T$. By using the principle of minimum potential energy, Section 2.3.2, the following expression is derived:

$$\delta\Pi = \sum_{e=1}^{n} \left[\int_{V_e} \mathbf{a}_e^T \mathbf{B}_e^T \mathbf{E} \mathbf{a}_e \mathbf{B} dV_e \mathbf{d}_e - \int_{V_e} \mathbf{a}_e^T \mathbf{N}_e^T \mathbf{f} dV_e - \int_{S_{\sigma_e}} \mathbf{a}_e^T \mathbf{N}_e^T \mathbf{T} dS_{\sigma_e} \right] = 0 \tag{4.2.7}$$

This can be written as

$$\mathbf{K}\mathbf{D} = \mathbf{R} \tag{4.2.8}$$

With this we have gathered each element into a global system, where the contribution of the elements are collected by

$$\begin{aligned} \mathbf{K} &= \sum_{e=1}^{n} \mathbf{a}_e^T \mathbf{k}_e \mathbf{a}_e \\ \mathbf{R} &= \sum_{e=1}^{n} \mathbf{a}_e^T \mathbf{r}_e \end{aligned} \tag{4.2.9}$$

where $\mathbf{k}_e$ and $\mathbf{r}_e$ are the element stiffness matrix and element load vector, that are expressed for each element as

$$\begin{aligned} \mathbf{k}_e &= \int_V \mathbf{B}^T \mathbf{E} \mathbf{B} dV \\ \mathbf{r}_e &= \int_V \mathbf{N}^T \mathbf{f} dV + \int_{S_\sigma} \mathbf{N}^T \mathbf{T} dS_\sigma \end{aligned} \tag{4.2.10}$$

4.3 Finite Element Method in Abaqus

There are numerous programmes developed for Finite Element Analysis, like for instance Ansys, Abaqus and Solid Works, and in this thesis we will use Abaqus to perform our modelling and analysis of the plate problem. Abaqus started out as a tool for non-linear behaviour and has for this reason a wide range of material models and is very popular among academics and researchers because of its ability to be customized.

4.3.1 Types of elements

Abaqus has a library with a wide range of elements to pick from. The elements are allocated in "families". The difference between them depends of how the geometry is assumed. The number of degrees of freedom are the vital variable to be calculated. The degrees of freedom varies between the "families". Equal for all are the translations, and for shell, beam and pipe also rotations are included. We can in addition have a look at heat transfer and temperature.

All the degrees of freedom are being calculated at the nodes. Results at any other point on an element deformation are calculated by interpolation of the nodal deformation. Elements with nodes only in the corners use linear interpolation and they are because of this called linear elements or first-order elements. Some elements have a mid-node, which means that they have a node between the corner nodes. They use quadratic interpolation and are being called quadratic elements or second-order elements. Triangular elements with a mid-node use a modified second-order interpolation, from this the name modified second-order elements. To achieve different kinds of behaviour, some of the "families" have several formulations, like for the type of element that will be used in this thesis, shell elements, which can be categorized into three classes:

1. General
2. Thin shells
3. Thick shells

The thin shell elements in Abaqus is based on Kirchhoff's classical plate theory, Section 2.2.1, the thick shell elements is based on Mindlin-Reissner theory of plates [30] and are therefore quite suitable when shear behaviour encounter. The last category can work for both thick and thin elements and cannot have shear locking. These can handle large deflections as well as non-linearity in material

or geometry. In this thesis we will use a general element called $S8R$, this is an 8 node doubly curved thick element which uses reduced integration. Shell elements are chosen because of their properties for isotropic plates, they can describe bending/buckling accurate.

In addition to this, Abaqus can model continuous shell elements, which have nodal contact like continuous elements, but is formulated to model shell behaviour with as few as one element through the thickness. This application is allowed for both thick and thin plates, linear and non-linear behaviour and high ratio between in-plane dimensions and thickness. This gives us more accurate contact modelling. The program integrates numerically and can use both full and reduced integration. Reduced integration uses low-order integration to establish the element stiffness. The mass matrix and the distributed load use full integration. Reduced integration reduces the calculation time, especially for three dimensional problems.

4.3.2 Boundary conditions

Boundary conditions are classified into two forms, one called *essential* (principal) boundary condition and the second called *non-essential* (natural) boundary condition. From a structural mechanics point of view these two can be separated by the direct involvement of the nodal freedom, like displacement or rotations, which are the essential boundary conditions and all others will then be non-essential boundary conditions. We have in this thesis used a variational method to develop our analytical model, which is an approximation method that weakens the physical problem and this also influences the boundary conditions. In Abaqus we insert this nodal restriction, displacement and rotation, directly in the modelling of the problem, which we shall describe next.

4.3.3 Modelling the plate problem

For modelling the problem in Abaqus a DNV/IACS technical report has been used [32], which explains in detail how a single plate should be modelled in Abaqus. The model consists of $\frac{1}{2}$, 1, 1 and $\frac{1}{2}$ plates, with two stiffeners, like shown in Fig. 1.1. This to insure the effects of neighbouring plates are taken into account and to prevent collapse of panels. The doubler plate is sectioned in the same manner and placed under the original plate. The properties of the problem are shown in Table 4.1.

Table 4.1: Plate properties

Properties	
L (in mm)	2400
s (in mm)	830
h_f (in mm)	315
b_w (in mm)	100
t_p (in mm)	15/20
t_d (in mm)	15/10
t_f (in mm)	12
t_w (in mm)	15
E (in MPa)	208000
ν	0.3
f_y (in MPa)	235

Here L is the length of one plate, s is the spacing between stiffeners, h_f is the height of the flange in the stiffener, b_w is the width of the web, t_p, t_d, t_f and t_w is the respective thickness to the plate, doubler, flange and web, E is the elasticity module, ν is the Poisson's ratio and f_y is the yield stress. The properties for the stiffener are taken from the library of stiffeners included in PULS. We will analyse this plate problem with focus on the effect of the doubler plate.

In modelling a problem in Abaqus, or in another element program, there are some basic steps to be followed. First the problem has to be modelled in something called a pre-processor. Here the geometry, element type, mesh size, material properties, boundary conditions, constraints, loads and analyse type are assigned. Next the solution itself is performed. Before the last step, in the post-processor, we can read and see, graphically, the results of the deformations and stress fields. All results can be handled in many different ways and the output is chosen regarding on what we are interested in. With use of the manual DNV/IACS have provided [32], our first job is to create an analysis for a single plate with two stiffeners,

this analysis will give us a reference to see fully how the effect of the doubler will encounter. This analyse can also be verified by PULS, to check for possible errors in the modelling. We use the same boundary conditions and constraints like as the manual. This means for instance the introduction of multi-point-constraint (MPC) of SLIDERS. These are important when we have impact of shear. The slider function is assigned to the edges that run parallel with the stiffeners. These will constrain the edges to move in a straight line between the end points. In addition to the sliders we must make sure that this two edges, stays parallel to each other by constrain the end points to rotate and displace in the same way as a third end point. This will provide the whole system/problem to just be a section of a whole ship hull and also these edges will have "neighbouring" plates. The constraint to provide this can be expressed as an equation:

$$\begin{aligned} \delta_y^{C2} &= 3l\theta_z^{C4} \\ \delta_y^{C3} &= 3l\theta_z^{C4} + \delta_y^{C4} \end{aligned} \tag{4.3.1}$$

To simplify the explanation above, we can look at a sketch from the manual, Fig.4.1. Here the end point or corner nodes $C2$ and $C3$ are the ones that are given the constraint.

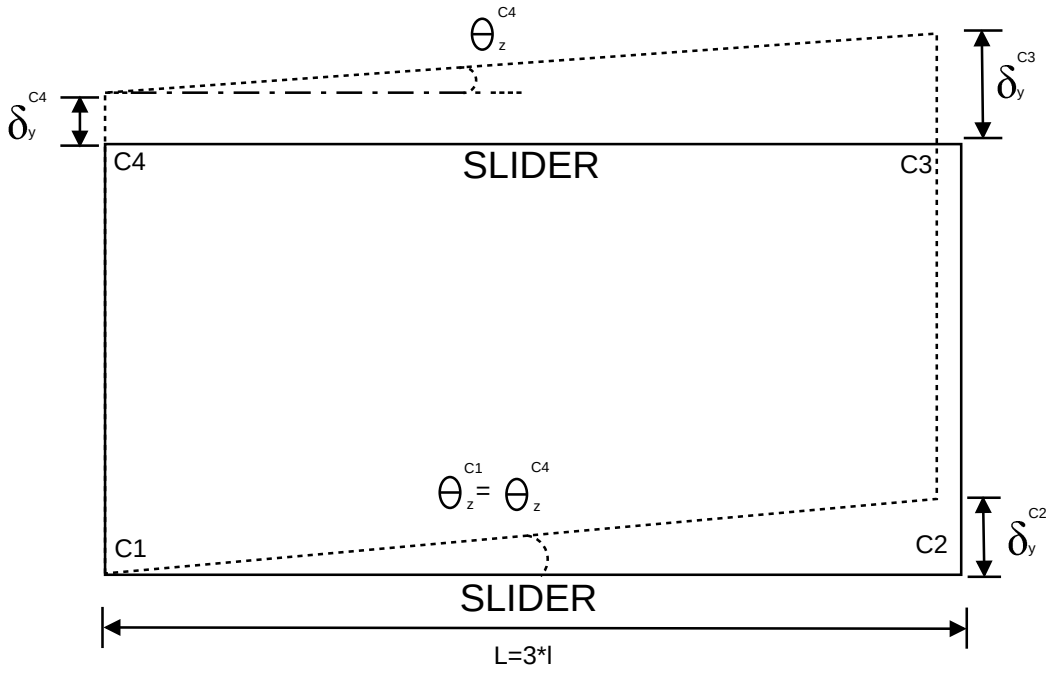

Figure 4.1: Definition of edges kept parallel.

There is not a big difference between modelling a single and a double plate. But in modelling a double plate some difficulties will occur. When two plates

are assembled we must ensure that the plates will behave like a real construction. Without any interaction properties assigned, the plates will act like they both are free and that they have no surroundings. Therefore it is important to make the environment as like a real construction as possible. We must set the interaction properties in a way that the two plates recognize each other, so that now the plates will not buckle through each other, but have boundaries. In Fig. 4.2 and Fig. 4.3 we can see the difference between having defined interactions or not.

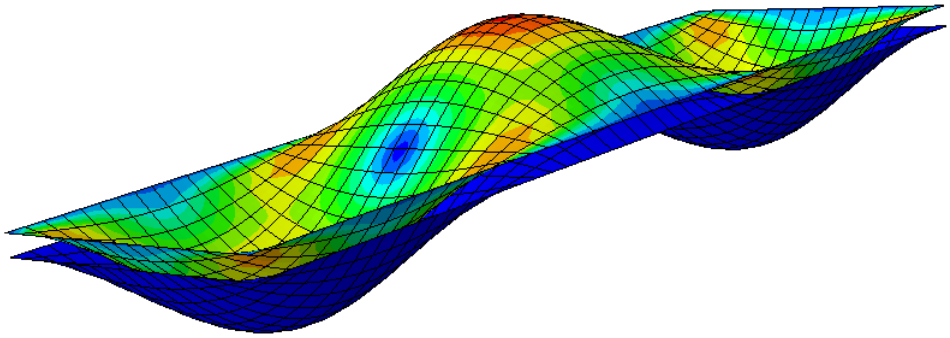

Figure 4.2: Interaction defined.

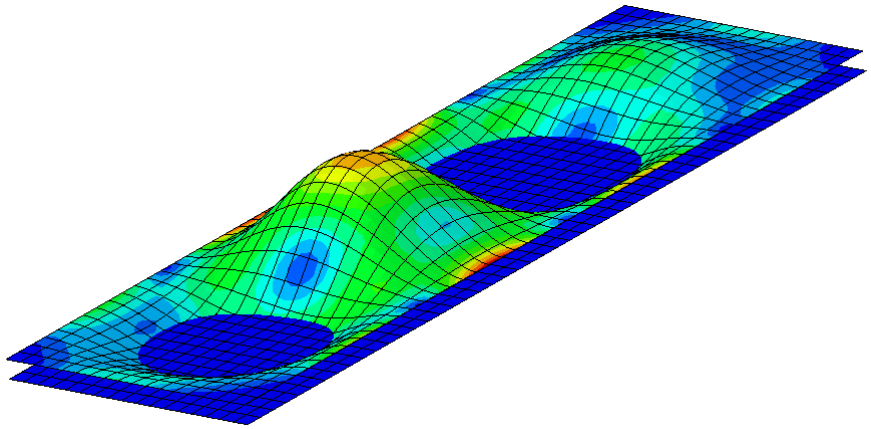

Figure 4.3: Without defined interactions.

Defining interaction properties in Abaqus is for this problem done by defining frictionless tangential behaviour and "Hard" contact with default constraints. In selection of which area that is bounded by these properties, we must select one

master and one slave surface. The master surface is the one that is the main part and is the one that in a way controls the slave surface. The master and slave surfaces are selected as the two which will be in contact with each other during the buckling analysis. In the plate with the stiffeners, the bottom surface is selected as the master surface and the top surface for the double plate that lies underneath is assigned as the slave.

Further on, the plates are welded in the corners and in intersections where the stiffeners are located. This information was given by reviewing some drawings DNV had got from shipbuilders, about double plating, but since these are property of the shipbuilder these cannot be shown or referred to in this thesis. The set up of the system insures the effect of neighbouring plates and the half plates at both ends ensures that the system responds to this feature. The ends will then require symmetrical conditions to represent these as a part of a larger structure. This can be defined by tying the ends of the doubler to the original stiffened plate, done by the multi-point constraint, TIE. Along the stiffeners we also have to use a MPC called LINK, this ensures that the doubler is welded into the the section where the stiffener lies.

When defining the in-plane loads axial, transverse and shear, we use Shell Edge Load and define the magnitude of the load to be 1 MPa. The axial load will be applied on both plates as well as the stiffeners. Transverse and shear load will only affect the two plates. When we speak of the loading direction, we in this thesis mean with axial loading, the normal force that acts in the stiffener direction and by transverse this often can be interpreted as a lateral force, but here we mean the normal force, working in the mid-plane of the plate, that acts perpendicular on the plate, y-direction, see Fig. 4.4.

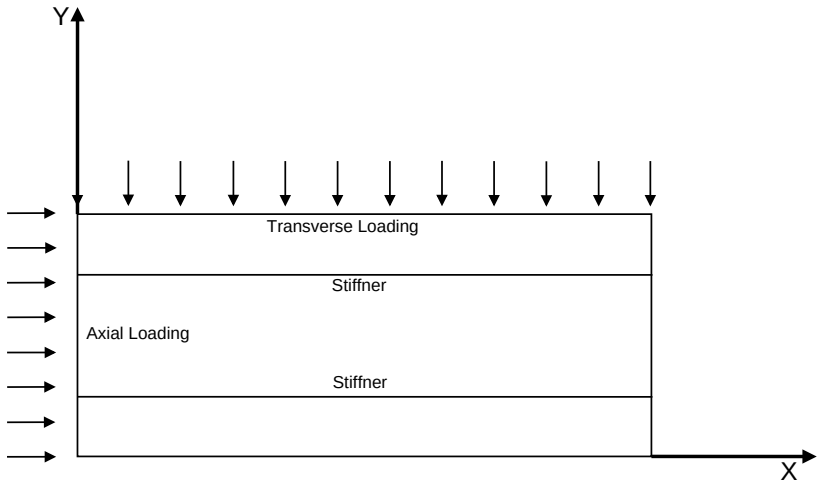

Figure 4.4: Definition of the load directions.

4.3.4 Steps

The total analyse is divided into two separate steps. As mentioned earlier all plates have some imperfection and we use the eigenvalue analyse as an imperfection in the non-linear step. When running the linear eigenvalue calculation we get in addition to an imperfection field for our next step also our critical loads, buckling loads. The imperfection is scaled up by the normal production estimate, $\frac{s}{200}$. The linear calculation is done by using the step called BUCKLE under linear perturbation procedure, while the non-linear calculation is performed by the STATIC, RIKS step under general procedure.

4.3.5 Challenges in modelling the problem

In making the model for stiffened plates with doublers attached some difficulties arises through the development of the thesis. It is crucial to have the right boundary conditions and constraint, such that the problem is as close to the real systems as possible. The IACS report is given for a single plate and the environment to the doubler is not given at any specific place. The link-up/weld between these two plates has to be arranged in a correct manner. Therefore they are based on drawings from a shipyard.

The kind of constraint is also important to get right, with the wrong definition the results and performance of the system can get quite abnormal. Under constraints there are a numerous selection of different kinds of possible types. In modelling a problem consisting of more than one plate, the constraints at the edges can be quite strict without giving an answer that is totally out of context, this can be done simply because of the definition of the modelling procedure, where two hole plates in center of the section only have restriction of other plates and will buckle out as they should, as can be seen by Fig. 4.5. This gives us an advantage in the modelling process when modelling a problem consisting of double plates, but with tying up the edges we can represent the symmetrical conditions that are necessary to have a complete model, in reference to a problem with a single plate where the edge constraints are only the ones given by the report from IACS and the buckling shape goes through the whole model, Fig. 4.6.

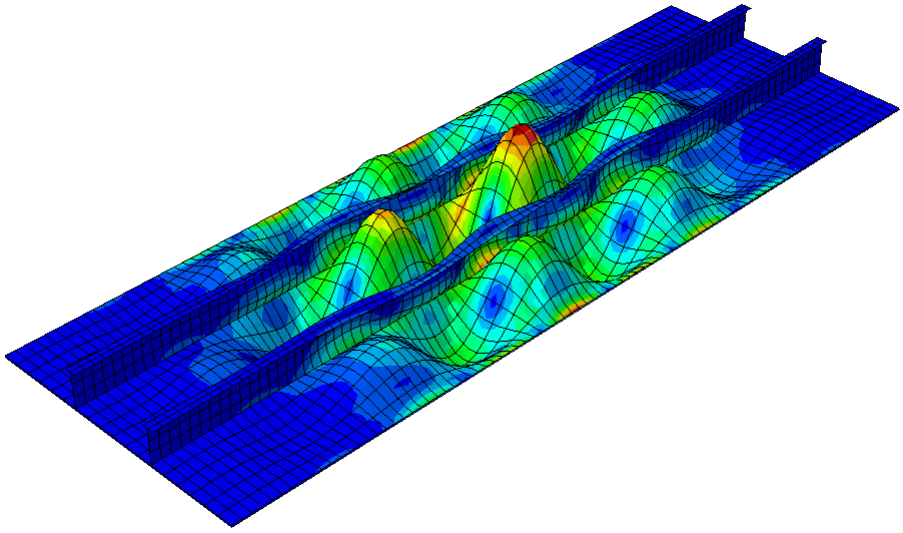

Figure 4.5: Strict constraints at the edges for double plate problems, axial loading.

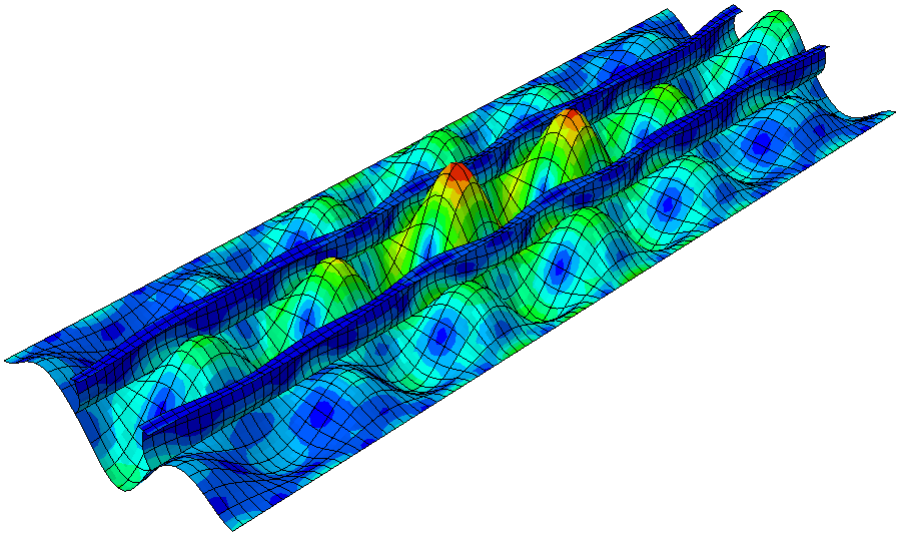

Figure 4.6: Buckling shape for a single plate, axial loading.

The location and size of the external loads are also given by the IACS report. The loads are given to represent a magnitude of 1 MPa over the length. This is in the report done by having a master node at one corner and let the rest of the side follow the corner node by an equation constrain. For our model this is not possible due to the introduction of the SLIDER command. We will because of this have two constraints which do not correspond. We must therefore use Shell Edge Load, but we assign this in the same manner, with magnitude of 1 MPa.

In our analyse we preform two separate kinds of steps, Section 4.3.4. The linear analysis is quite straight forward, but in the non-linear analyse it can be a little bit tricky to get stable response in the solution, which is an answer to having a well preformed analyse. By adjusting the step size, number of increments and the minimum arc length this can be achieved. When adding load to this model we, in some cases, can encounter a problem with achieving a stable response, this refers to the aspect of material yielding, the von Mises yield criterion, explained in Section 2.1.4. This arises when the applied load reaches the maximum of what the system can carry before yielding of the material starts, the system has reached its peak performance in definition of buckling. We then experience something called squash yield. Squash yield addresses to the compressive load at which the section is fully yielded. In our analysis this leads to removing the tangent specified under the material plasticity properties, which is a value for hardening of the material, since the problem are then not able to deform further. This problem primarily occurs where shear force encounter.

Chapter 5

Verification of the semi-analytical model

In Chapter 3 we developed a model for a semi-analytical method for calculation of the eigenvalues, also called buckling loads for a plate problem, described in Section 3.1. The analytical model needs to be verified to secure the output from the model. To conduct the verification of our calculations and model we compare with the element calculation in Abaqus.

5.1 Control of displacement field

The defined displacement field, Eq. (3.1.3), was chosen on the basis of having a displacement function that would only describe displacement in one direction, the positive region. That means a deformation that only buckles unidirectional and is retained by a second, thicker and stronger, plate in the other direction. From the boundary conditions the displacement function was also chosen by how the environment to a single plate would be. A single plate will have neighbouring plates, stiffeners and girders that will make the conditions clamped, with zero rotation at the ends. The amplitude, $\mathbf{a_{ij}}$ had so far not been thought of. The amplitude can and will have both positive and negative signs, which leads to having buckling shape that deforms in both directions, Fig. 5.1. This is a state which we are not interested in having, we are looking for unidirectional buckling, Fig. 5.2.

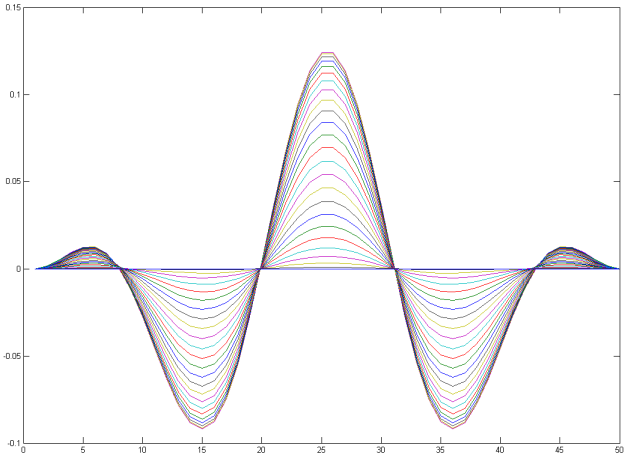

Figure 5.1: Deflection in both directions.

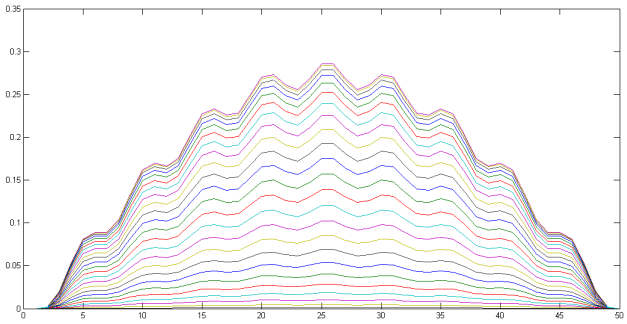

Figure 5.2: Deflection in only one direction.

To have the same buckling modes that we are looking for in our system we must "search" through the eigenmodes the model calculates to find those shapes that satisfy our problem. This is possible to let Matlab do, by scripting through all the modes and only print those with positive amplitude. This problem with the negative sign for amplitude will only encounter with axial and shear loads, but later we will see that in reality only axial loads is of concern. For transverse load the buckling shape will give a correct shape at once, in the first mode. As from the geometry, length is four times longer than the width, the buckling shape will only be one half wave, in positive direction.

5.1.1 Abaqus model for verification

In Abaqus, numerous attempts are done to model a system which describes the problem where only one plate deflects/deforms, from the assumptions made in Section 3.1. The different types of modelling techniques attempted for calculation of the critical load, is for example two plates were one is infinitely stiff/rigid or that one plate has a high Young's modulus and is much thicker than the other.

In both these cases contact or interaction must be defined. Without this constrain the two plates will not be able to recognize each other, as described is Section 4.3.3. By defining these contacts, the problem transforms from being a linear eigenvalue problem to be a non-linear problem. This happens because the definition of the contact interaction in Abaqus is a non-linear problem. To solve this we had to go back to solve the problem much in the same way as for the semi-analytical model, by having a normal plate, with clamped boundary conditions, like the cosine function in the analytical method, like shown in Fig. 5.3. To find the eigenvalues we are seeking we must take out as many eigenvalues as possible and search for those who have the buckling shape we are looking for, Fig 5.2.

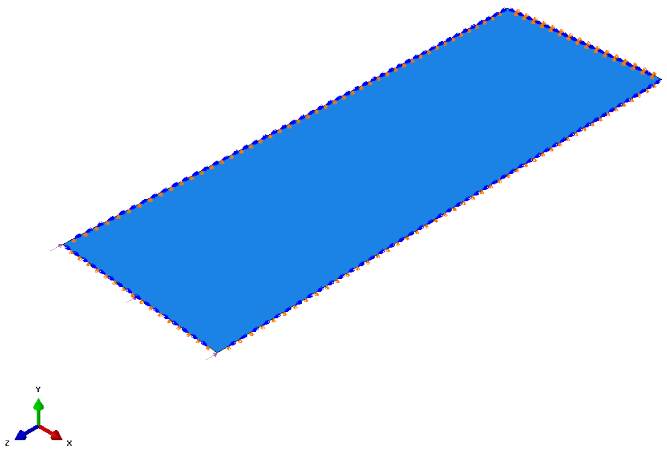

Figure 5.3: Abaqus model for verification of the semi-analytical method, with boundary conditions assigned.

5.2 Pure axial load

As described we will have problems with the eigenmodes and we must search for the right ones. That was done for both the semi-analytical model and the model in Abaqus. The eigenvalue results and corresponding eigenmodes are given in Table 5.1.

Table 5.1: Results for pure axial load.

Semi-analytical		Abaqus	
Eigenmode	Eigenvalue	Eigenmode	Eigenvalue
9	1273.3	34	1234.1
11	1672.6	49	1635.2
13	2288	72	2242.2
15	3015.8	94	2967.6

By comparing the results Matlab and Abaqus, we can see that

1. For all the values given by Matlab there exists a Abaqus value that matches.

2. The lowest value (the critical value) is equal for both.

3. Abaqus gives even more possible solutions for the buckling shape we are searching for, where we have only one directional buckling, for instance that it can have two buckling waves over the width. This is a form the analytical model is not able to describe. In addition Abaqus can have a mix of both one and two half waves over the width at the same time.

4. From what is described in the previous point, Abaqus gives the lowest eigenvalue at eigenmode 34, while Matlab already at mode 9 shows the critical value.

If we compare the first eigenmode in Abaqus and Matlab we can also see that they give us the same result and they give out the same buckling shape, as can be seen in Fig. 5.8 and 5.9. Another type of verification process that can be performed is by varying the thickness. The results of this can be found in Table 5.2.

Table 5.2: Results for pure axial, by varying the thickness.

	Semi-analytical	Abaqus
Thickness(t)	Eigenvalue	Eigenvalue
5	318.32	310.98
8	814.91	792.80
10	1273.3	1234.1
12	1833.6	1768.9
15	2864.9	2740
20	5093.2	4776.6

5.3 Pure transverse load

Up till now all comparison has been done with regard to pure axial load. What about other directional loads? Like outlined earlier, the thesis implies to survey in-plane forces, so transverse and shear must also be controlled. With transverse loaded plate, as described earlier in this chapter, we have a plate that is four times longer than it is wide and therefore the plate will buckle with one half wave at the first mode. This leads to a much easier retrieval of the results both for element method in Abaqus and semi-analytical method in Matlab. One half wave gives automatically deformation in one direction and we find what we are searching for at once.

To verify the issue of this load direction, we seek different eigenvalues by varying the plate size properties, length and width. We do this by varying one property at the time and the results can be seen in Table 5.3 and 5.4.

Table 5.3: Results for pure transverse load, by varying the length.

	Semi-analytical	Abaqus
Length(L)	Eigenvalue	Eigenvalue
830	274.91	274.06
1000	203.49	203.00
1500	138.95	138.69
2000	123.33	123.11
2400	118.24	118.05
2500	117.40	117.21
3000	114.55	114.36

Table 5.4: Results for pure transverse load, by varying the width.

	Semi-analytical	Abaqus
Width(s)	Eigenvalue	Eigenvalue
400	477.52	474.62
830	118.24	118.05
1200	63.12	63.06
1600	42.78	42.75
2000	35.24	35.23
2400	32.88	32.87

5.4 Pure shear load

When we investigate the shear behaviour in our semi-analytical model, we encounter some problems, also mentioned in Section 3.2.3. When we defined and selected our displacement field, we chose a field containing only cosine terms. Cosine terms are always symmetrical and can therefore not be used to describe shear deformations. To perform analysis containing shear forces we need to add sine terms in the displacement field. To overcome this problem in analysis where we have clamped boundary conditions a coupling between cosine and sine terms can be implemented. Hence our semi-analytical model cannot perform a shear force analysis.

5.5 Verification

We now have the results from our check of the semi-analytical model and can then complete the verification process by plotting the result for pure axial load and pure transverse load separately. The first plot shows how the eigenvalues with pure axial load will change both in Abaqus and in our model with correspondence with each eigenmode, Fig. 5.4.

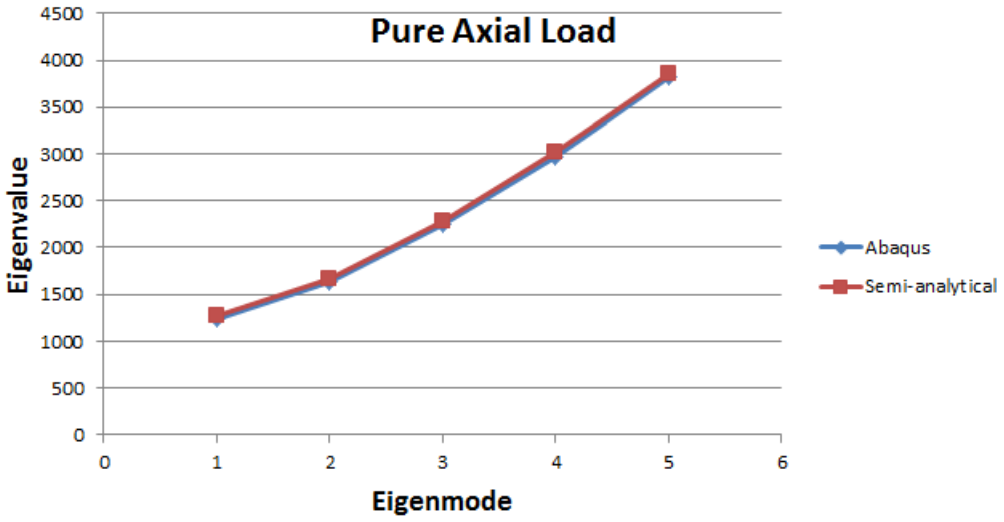

Figure 5.4: Results for pure axial load with different eigenmodes.

Here we can see that by picking out the eigenmodes that correspond to the buckling shape we look for, both the semi-analytical and element method show good compliance in order of eigenvalues. The second plot reviews the varying thickness of the plate, Fig. 5.5.

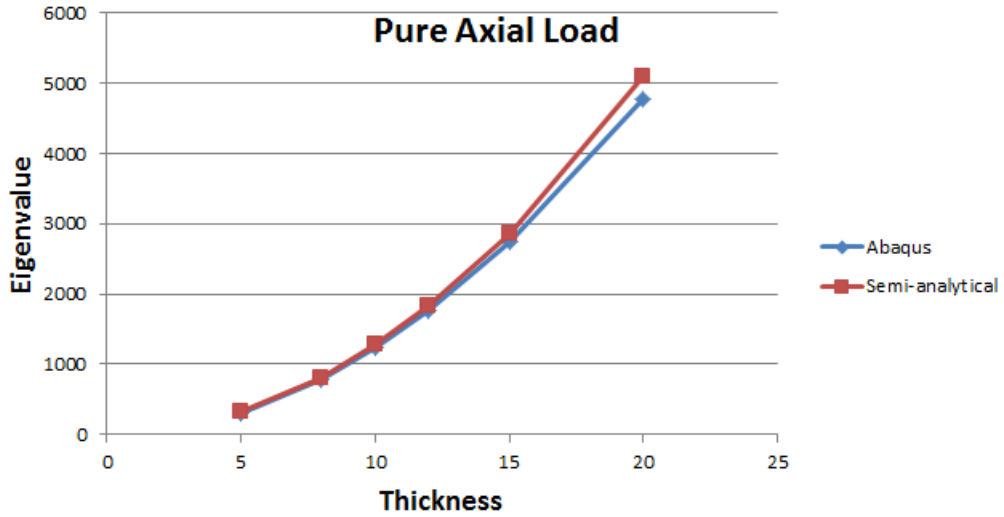

Figure 5.5: Results for pure axial load with varying thickness.

The semi-analytical method gives a slightly higher estimate for the eigenvalues, but the difference is quite small and it does not appear clearly before the thickness becomes in a high rate. For the transverse load case we plot the Tables 5.3 and 5.4, where we have looked at variable length and width, Fig. 5.6 and 5.7.

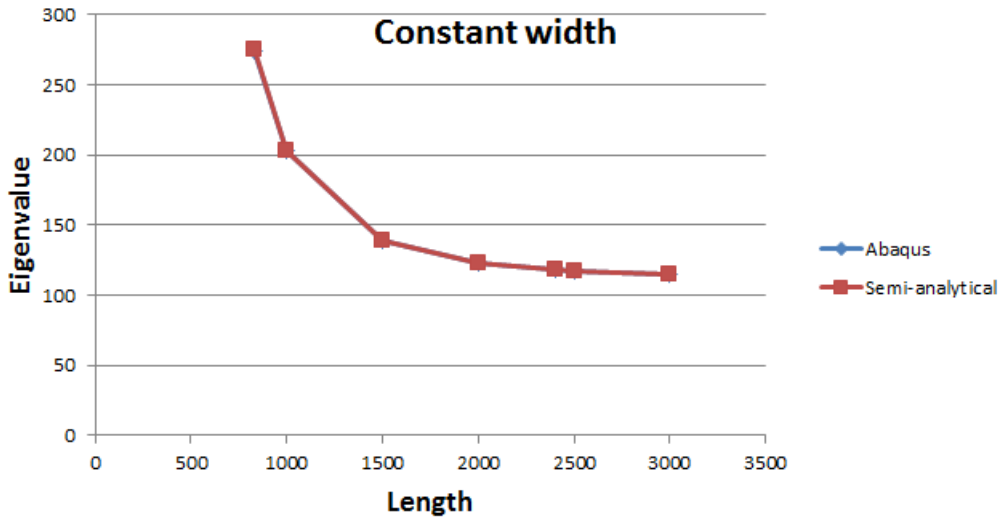

Figure 5.6: Results for pure transverse load with variable length.

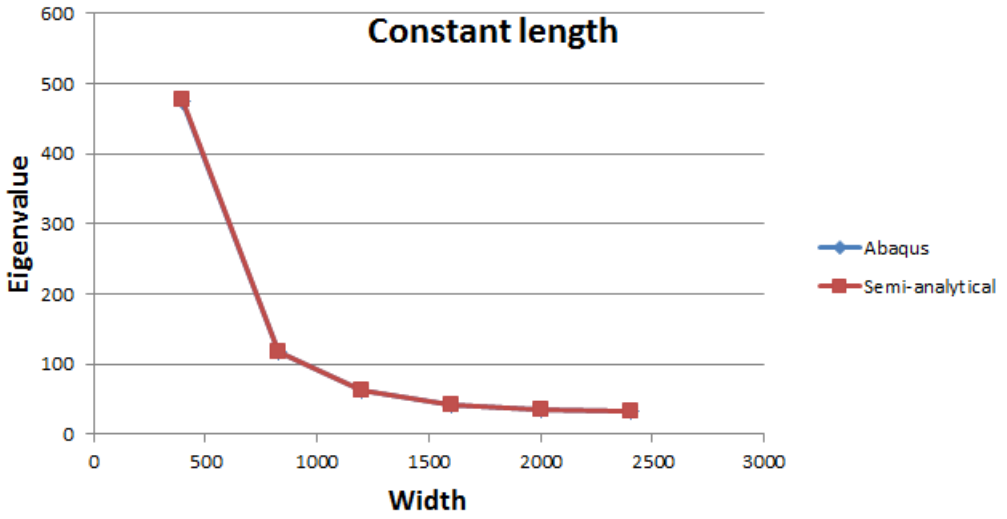

Figure 5.7: Results for pure transverse load with variable width.

It can be difficult to see the difference for the transverse load cases, but this is because of, as shown in Table 5.3 and 5.4, a very good correspondence between the two methods. By both looking at the plots and the results posted in Table 5.1, 5.2, 5.3 and 5.4 we can see a good compliance between the semi-analytical model, at which resulted from our work in Chapter 3, and the finite element method, in Abaqus.

For all these four cases we can see that the semi-analytical method gives a slightly higher result. The formulation of the Rayleigh-Ritz method, Section 2.4.1, states that the method always overestimates the system and the solution will converge from above, which is a good explanation for the results. By letting the analytical model run with few degrees of freedom, the result will have a poorer estimate of the eigenvalue and cannot be accepted. It is therefore very important to check for convergence in the run of the model/script. For calculation of forces in axial and transverse direction, we can then say that the semi-analytical model safely can be used, but eigenmodes must be controlled to check for the right shapes.

5.5.1 The eigenmodes

To compare the eigenmodes for the same critical value, the lowest eigenvalue, in Abaqus and the semi-analytical model the plots, Fig 5.8 and 5.9, show how the methods equals each other in order of buckling shape for both axial and transverse loading. The shapes are symmetrical, brought in by the clamped condition. In the other eigenmodes we have chosen, Table 5.1, 5.3 and 5.4, the buckling shapes correspond as well.

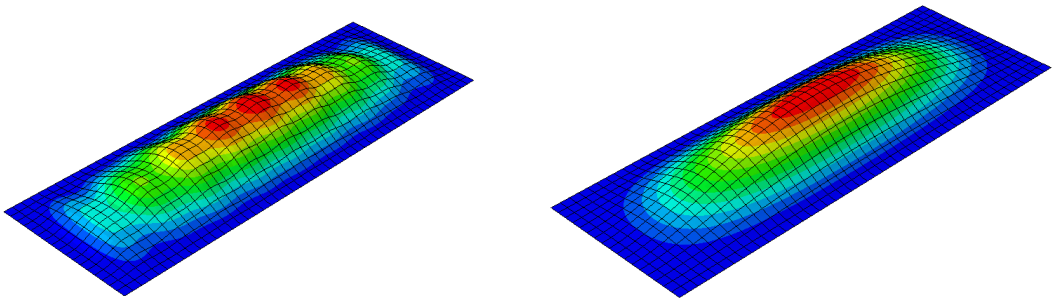

(a) (b)

Figure 5.8: Abaqus (a) Axial force and (b) Transverse force.

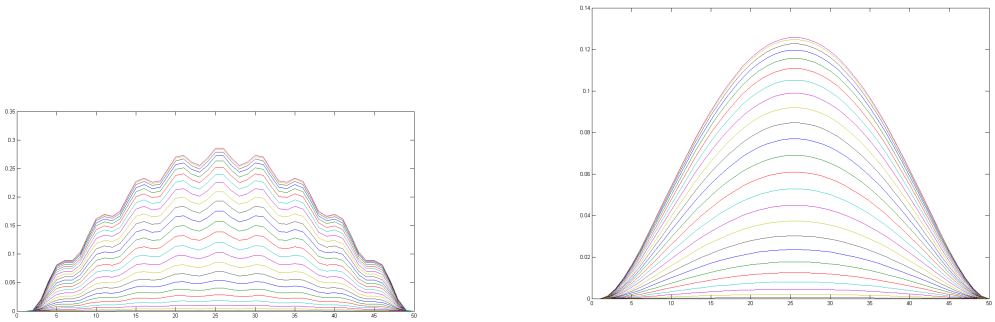

(a) (b)

Figure 5.9: Analytical (a) Axial force and (b) Transverse force.

5.6 Remarks

Stating that the semi-analytical model can be used to calculate eigenvalues for a double plate problem is only partly true. The model can be used to calculate eigenvalues for problems with a single direction deflection/deformation, which only encounters with transverse loading, but for a real doubler problem we will experience two ways deflection with axial loading. A plate is never as stiff or rigid as assumed in this model. Therefore this model cannot be used to calculate the strength of a real double plate repair.

A second thing worth noticing is that by having too few degrees of freedom, for axial loading, the model gives results for the eigenvalue that do not corresponds to the element method and the system does not start to converge before at least ten degrees of freedom is included. This can be seen by looking at the Fig. 5.10. This behaviour we have not been able to conclude on, but with enough degrees of freedom, ten or more, the system converges and gives output in a correct manner.

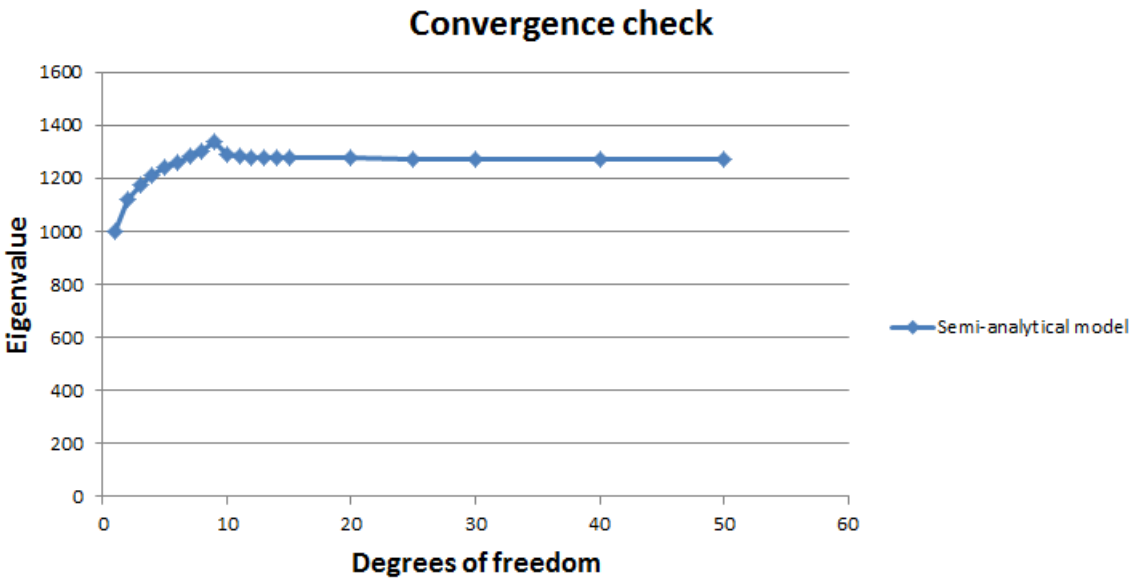

Figure 5.10: Convergence check of the semi-analytical model.

Chapter 6

Intact stiffened plate

We will now focus on at the contribution a double plate will have on a structure. In this chapter an undamaged plate model with stiffeners will be calculated both regarding eigenvalues/buckling loads and capacity/ultimate strength. The problem is defined to look at how double plates contribute to the strength of a ship hull. We will look at the difference between having only a single plate compared to a double, the influence of the thickness of the doubler and look at different kinds of imperfection. This intact structure with double plating will give us a better understanding in the behaviour of this contribution and gives us a great advantage in handling repair of a damage structure, as we will perform in the next chapter.

6.1 Impact of double plates

We have two similar plate systems with stiffeners, one with and one without a double plate. The imperfection size is the same, $\frac{s}{200}$, but the loads are different. Like stated in Section 4.3.3 the loads are added by the magnitude of 1 MPa. This leads to having more loads assigned to the double plate problem, as it has more area that will be affected. In this thesis we focus on the capacity of the plate and will then plot the stresses, but if we instead had plotted the force, we get the real view of how the different thickness ratios will change the properties. Several load cases/directions have been looked at, this is a result of the IACS technical report, [32], where it is stated that different load combinations trigger different buckling behaviour in a stiffened panel. This must be taken into account when selecting an imperfection pattern for the non-linear collapse analysis. As from the buckling theory in Section 2.1.3 we select the imperfection from the first eigenmode. The combinations of imperfections and loads in the post-buckling region can be seen

in Table 6.1 below. For almost all load combinations the results will be found between the first and fourth quadrant.

Table 6.1: Load combinations, compression loads.

Imperfection	Load combination
Pure Axial	Bi-axial
Pure Axial	Axial and Shear stress
Pure Axial	Transverse and Shear stress
Pure Transverse)	Bi-axial)
Pure Transverse	Axial and Shear stress
Pure Transverse	Transverse and Shear stress
Bi-axial	Bi-axial
Axial and Shear stress	Axial and Shear stress
Transverse and Shear stress	Transverse and Shear stress
Pure Axial	Pure Axial
Pure Transverse	Pure Transverse
Pure Shear stress	Pure Shear stress

To get a more complete picture of how a double plate affects a structure, several cases of thickness ratio between the plate with stiffeners and the doubler have been examined against the single plate, Table 6.2.

Table 6.2: Cases examined, Plate with stiffener vs Double plate.

Cases	Thickness ratio
CASE A	15-15 [mm]
CASE B	20-10 [mm]
CASE C	15-10 [mm]

For all cases the different load combinations, Table 6.1, have been examined, but the most critical and important combinations will be where both normal and shear forces act simultaneously, with so called "real" imperfection. This real imperfection is referring to the case when the imperfection is equal to the load direction in the post-buckling analyse. For analyse in first and fourth quadrant the imperfection will then change according to the angle of the load. To conduct a full review and ensure a satisfying validation of the results, the IACS technical report [32] has given some advice in how to handle the results:

- Plot of the imperfection mode, to ensure that the imperfection used is reasonable in order to describe the physical behaviour that are not dominated by boundary conditions and effects of constraints.
- The failure mode should be plotted in form of stress and deformation, both for the mode that gives collapse and the last increment in the analysis. This to ensure and verify that the buckling behaviour both are physical and that the plate has actually collapsed.
- The collapse stress is our main goal to find in the non-linear analyse. This gives the ultimate capacity of the plate and a stress plot of this mode should be presented.
- In addition the load-shortening curve, applied load against displacement, must be plotted to look for stable response in our analysis.

6.1.1 Single plate

In Section 4.3.5 we explained how an analysis of this problem is modelled. We use the symmetrical condition at the ends of the two half plates to insure that the model can represent a section of an entire ship hull structure, Fig 6.1. We analyse this simple system so that the result can be used as a reference to the doubler system.

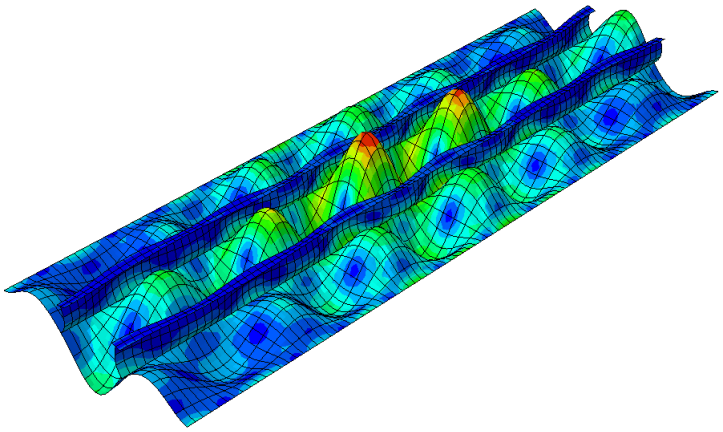

Figure 6.1: Complete buckled shape of a single plate, pure axial, enlarged $\times 720$.

For this single plated system with stiffeners, there already exists a semi-analytical tool, PULS, developed by DNV. This can be used to secure and control our model,

this is applicable since the two programs use different methods, Abaqus use the element method, Section 4.2, and PULS is based on the variational method of Rayleigh-Ritz, Section 2.4.1. In the determination of the critical load and from this the imperfection mode we shall be using in the non-linear post-buckling analyse, we can see that for pure axial, Fig. 6.1, pure transverse, Fig. 6.2a, and pure shear, Fig. 6.2b, they all give reasonable buckling shapes.

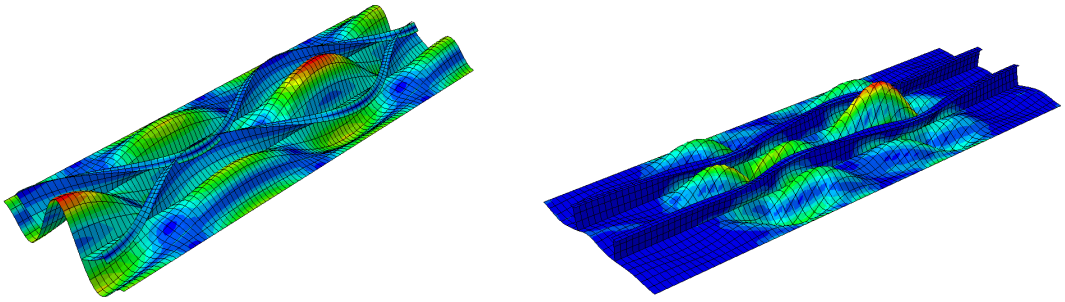

(a) (b)

Figure 6.2: Enlarged, ×720,imperfection shapes for (a) Pure transverse and (b) Pure shear.

We summit the control by analysing one load combination, for example one of the more important combinations with both normal and shear load, see Fig. 6.3.

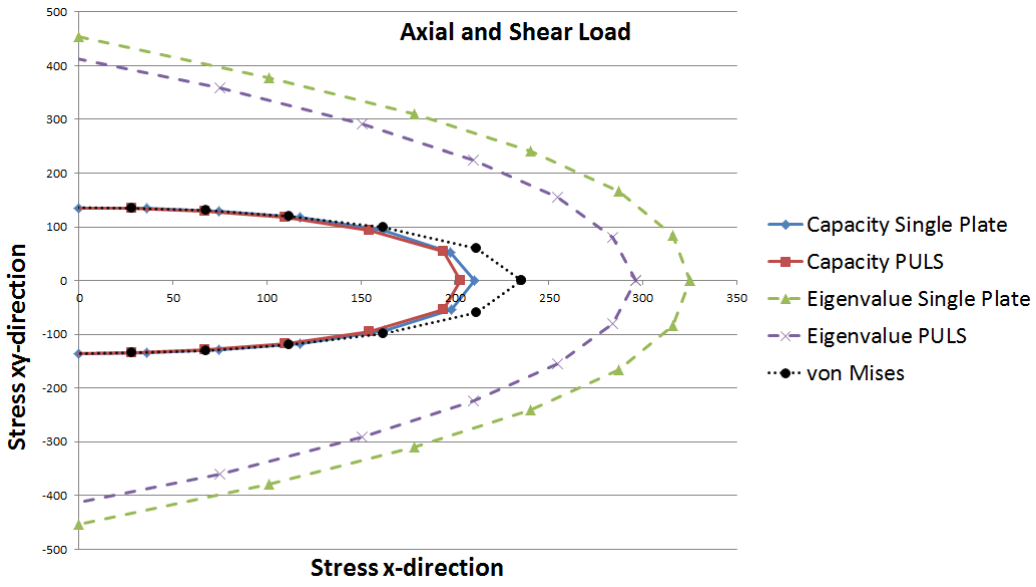

Figure 6.3: Comparison between Abaqus and PULS, for a single plate.

From these results we can see that there is good compliance between our Abaqus model and PULS. For both capacity and eigenvalue, Abaqus are slightly more conservative, but still the results are acceptable. We have in this diagram also plotted the von Mises stress limit, which indicates where the plate problem reaches the ultimate capacity due to material yield, described in Section 2.1.3 and 2.1.4.

In this thesis we will conduct a buckling analysis for doubler plates, where only buckling of the plate is the issue and we exclude the material problem. Therefore we set the von Mises stress as our limit for all the analysis preformed. To secure the verification of the results we shall plot the deformation for the failure mode both at collapse and at the last increment in the analysis to ensure that the plate has completely collapsed. In our analysis we check not only for pure loads but also a combination of them, through first and fourth quadrant, like shown in Fig. 6.3, but we select to view only one load direction for simplicity, as seen in the axial load direction collapse mode Fig. 6.4, but there are conducted a full check for all load directions, in every case.

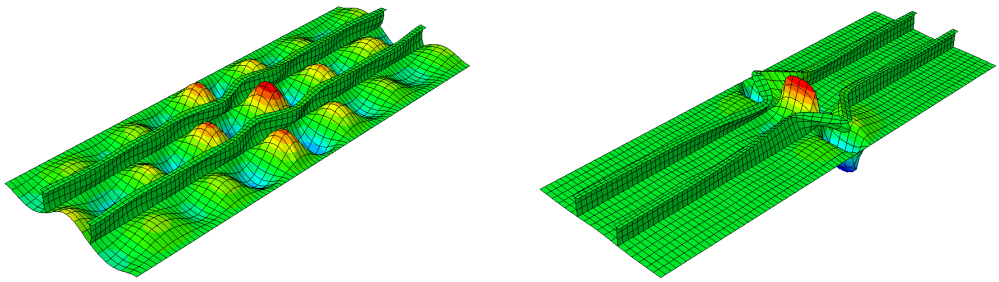

(a) (b)

Figure 6.4: Up-scaled deformation plot, $\times 10$,with axial loading for (a) Increment of collapse and (b) Last increment in the analyse.

Fig. 6.4a shows the shape of the plate when the plate collapses and in Fig. 6.4b the plate is fully collapsed and the deformation shape are drastically changed, with this we have an analyse that has been fully implemented.

The last check is to find out if our analysis gives a stable response. This is conducted by plotting the load-shortening curve, applied load against displacement. By looking at Fig. 6.5 we can see that both pure load directions, axial and transverse, are performing a stable response. A stable response is given to be when the curve plotted is not giving out any local peaks. If we have local peaks, the curve ends with the maximum value, we have unstable response and the possibility of mode snapping. In addition, we have also plotted the eigenvalue for the direction of concern in the load-shortening curve, dotted lines, and the

von Mises stress limit which indicates the material yielding limit. These gives us a view to see if the highest load the system is exposed to have exceeded the eigenvalue or the limit where yielding of the material arises. By doing this we can see if the system has some reserve strength.

The eigenvalue limit is also often called the ELS, Elastic limit state. As stated in Section 2.1.2 the eigenvalue is often set, in design calculations, as the conservative limit. If then the load is higher than the eigenvalue we have a system with reserve strength. This can be checked by both looking at the load-shortening diagram, Fig. 6.5, and the capacity/eigenvalue diagram, Fig. 6.3. For all three pure load directions, axial, transverse and shear, none of them have a higher capacity than eigenvalue which means that there is not any reserve strength in the system. Reserve strength linked with the thickness of the plate and will only appear for relatively thin plates, as mentioned in Section 2.1.1.

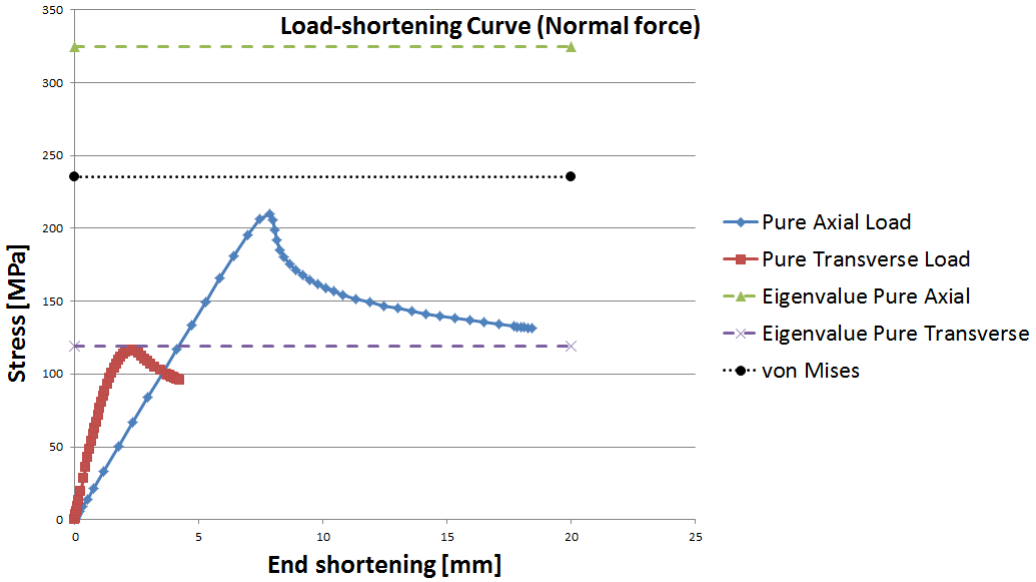

Figure 6.5: Load-shortening curve for a single plate.

It arise difficulties when plotting a load-shortening curve for shear loads, which is a result from the plate deformation when shear loads are applied. We get twisting/torsion in the buckling shape and not a clear shortening of the edges.

We now have a good compliance system for investigating the impact of a doubler and this single plated system will act as the reference to possible strengthening characteristics when applying a double plate.

6.2 CASE A: Thickness ratio 15-15

The first double plate example we are going to look at is an issue where the doubler is having the same dimensions as the original plate with stiffeners. Here the ratio of the thickness is selected to 15-15 $[mm]$. From Section 1.2 the repair with doubler plates is explained, after current standards. Here the thickness of a doubler plate was given as no more than the original plate and this is then a good starting point. In the same section it was also said that the corner of a doubler should have a radius of approximately 3 inches to avoid stress concentrations. As seen in the model we are working with, this has not been specified. This gives the system we shall examine more conservative results. But if we instead use the more strict constraints mentioned in Section 4.3.3, and 4.3.5 the stress concentration can be avoided by only having the inner plate as our main subject. By analysing this problem we, like stated in Section 4.3.3, apply more load than for a single plated system. Since the load is given as 1 MPa through the thickness we apply almost double load, $15 + 15$, only the axial loading of the flange and web is additional. We can say that we have added approximately $1.9 \approx 2$ times the load in the doubler. First we do a check for stable response, Fig. 6.6.

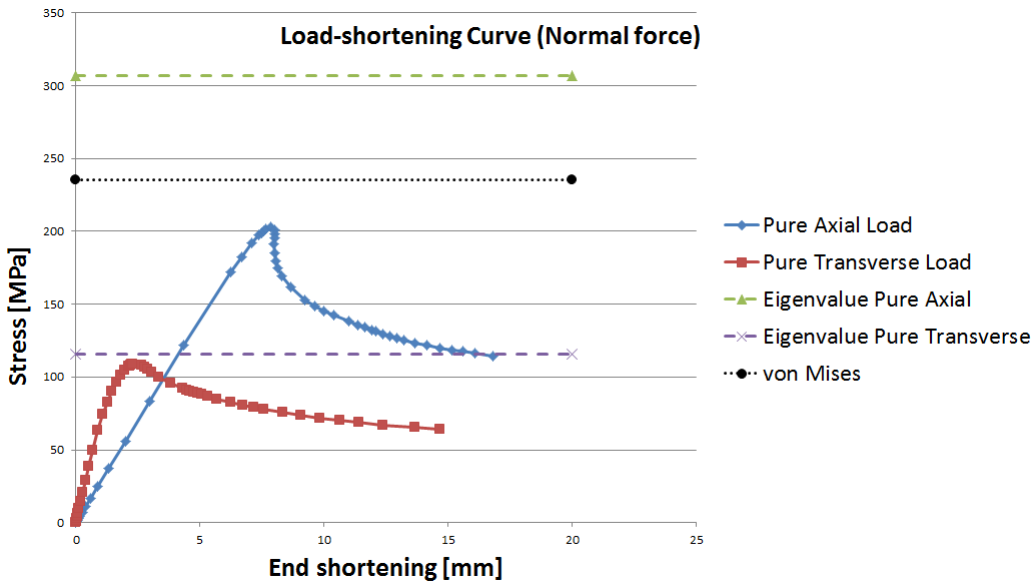

Figure 6.6: Load-shortening curve for a double plate with equal thickness.

Like for a single plate, Fig. 6.5, stable response is provided for both load directions and for these two load directions no reserve strength is available and for normal forces there will not encounter any possible material yielding. We consider two of the most crucial load directions to find the ultimate capacity of the system, Fig.

6.7 and 6.8. The figures show that the system can withstand approximately the same stresses as the single plate, even when more loading added. In addition the shear stress will, as for single, be limited by the von Mises yield criterion.

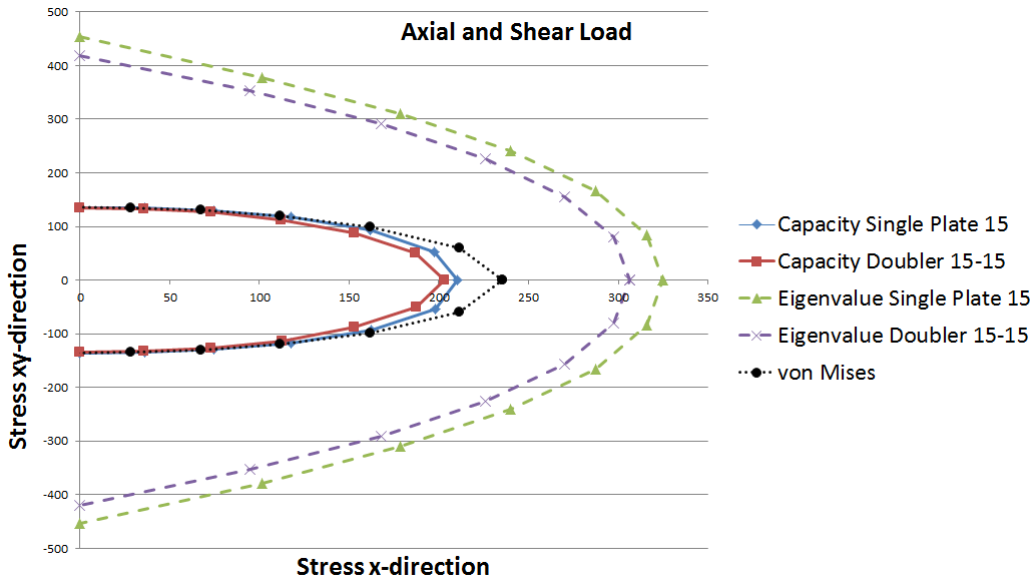

Figure 6.7: Comparison of axial and shear load between double (15-15) and single plate.

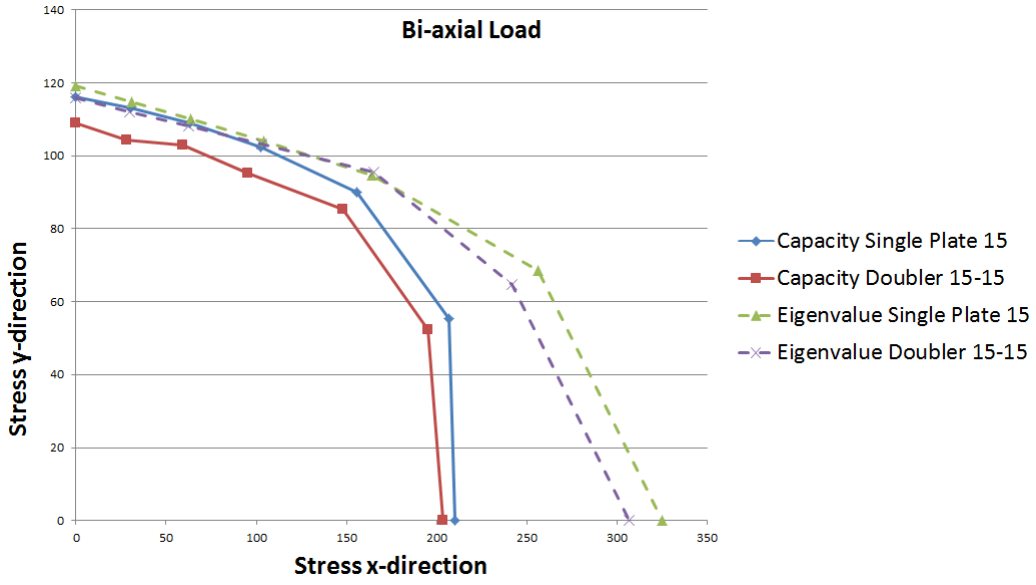

Figure 6.8: Comparison of bi-axial load between double (15-15) and single plate.

The small deviation from single, in forms of lower capacity and eigenvalue, can be addressed to loading of the plate. This deviation is also visible at the third load case, transverse and shear, Fig. 6.9. This confirms the relationship between the single plate and the equal thickness ratio for a double plate problem.

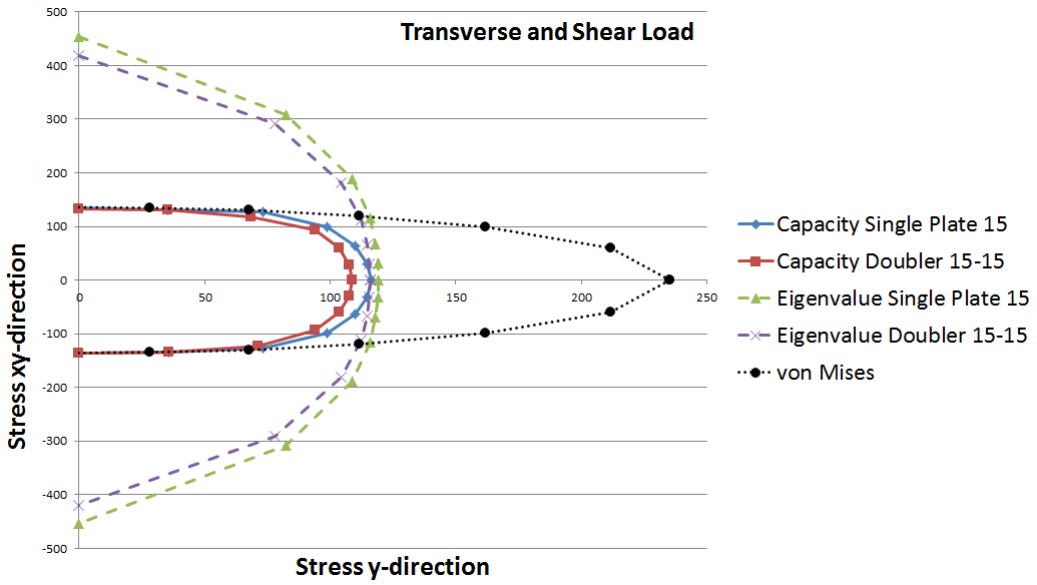

Figure 6.9: Comparison of transverse and shear load between double (15-15) and single plate.

We have in other words a much stronger system now, as expected. Both plates are intact and they have the same size, this confirms that we have added our doubler in a correct manner in the element program, and we can further compare the impact of a doubler. The eigenvalues correspond very well, as also can be seen from a plot of the buckling shape for pure transverse, Fig. 6.10.

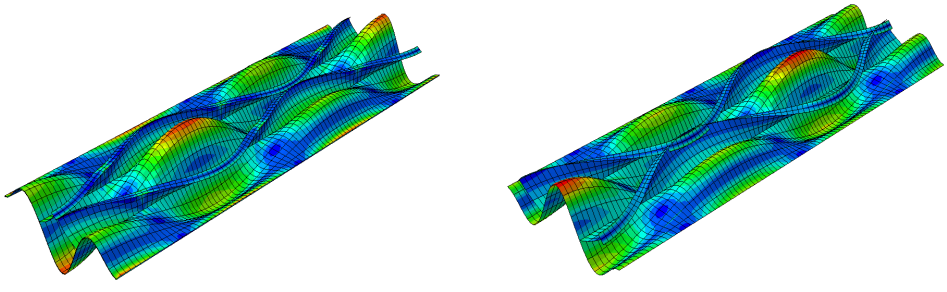

(a) (b)

Figure 6.10: Enlarged view, $\times 720$, of the buckling shape for (a) Double Plate and (b) Single Plate.

So when applying a doubler plate with equal thickness the intact structure is able to withstand approximately double force, read nearly twice area to have load applied.

6.3 CASE B: Thickness ratio 20-10

We now switch focus to see what happens when the two plates have completely different thickness. With a large ratio of 20-10 $[mm]$ the potential effect of the doubler really can be seen. The stable response for this system can be seen in Fig. 6.11.

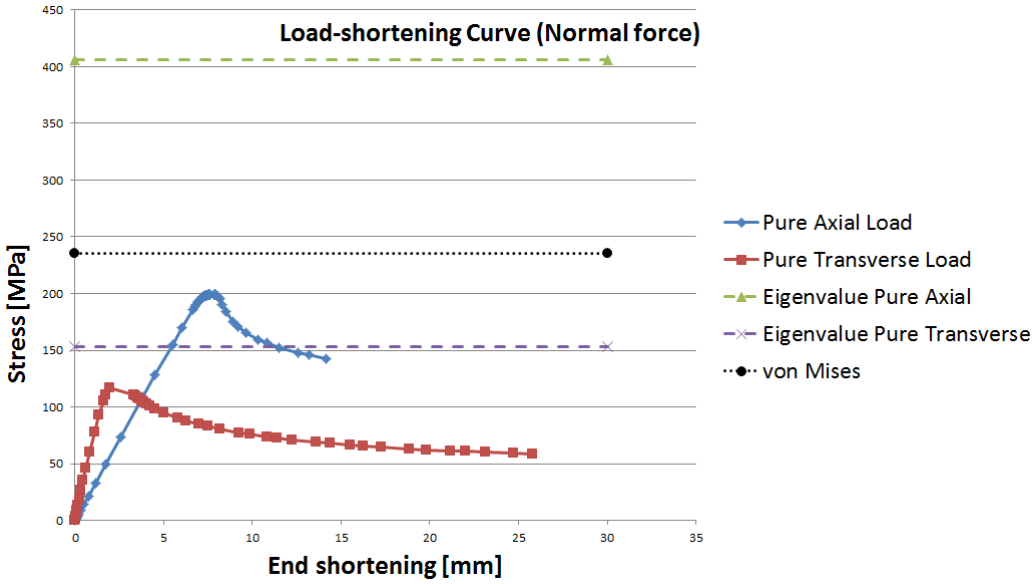

Figure 6.11: Load-shortening curve for a double plate with 20-10 thickness ratio.

When examining the results for a system with large thickness ratio, we see that the results are not as different as maybe expected in advance. The same load deviation applies here. In shear the material yield problem appears. We can see from Fig. 6.12, (and keeping in mind that the load applied is equal for these two cases, A and B), that the capacity is almost equal, but there is a large difference in the eigenvalues.

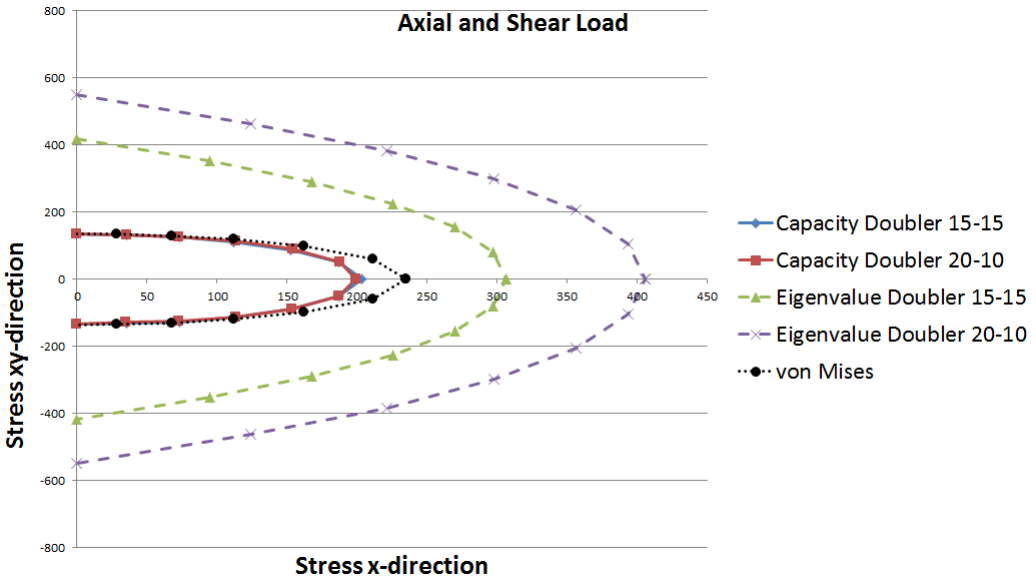

Figure 6.12: Comparison of axial and shear load between double (20-10) and double (15-15).

In Case A we had two equal plates that in bending of the plate acted equally, but when the two plates have different thickness the bending will occur different. A thin plate will be more able to have deformations, than a thicker and stockier plate. This will provoke the thick plate to be a limiter for the thin plate deformation in one direction and in the other both will have their normal deflection, which creates be a gap between them. In a cut out from the post-buckling result, Fig. 6.13, we can observe this effect.

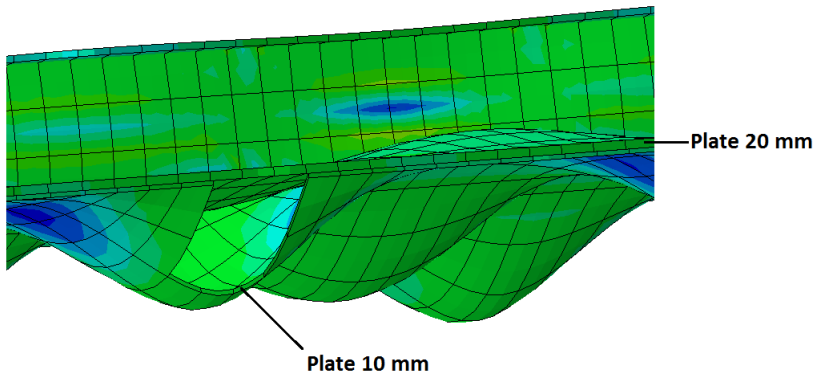

Figure 6.13: View of the difference in buckling of thick (top plate) and thin plate (bottom plate), enlarged $\times 20$.

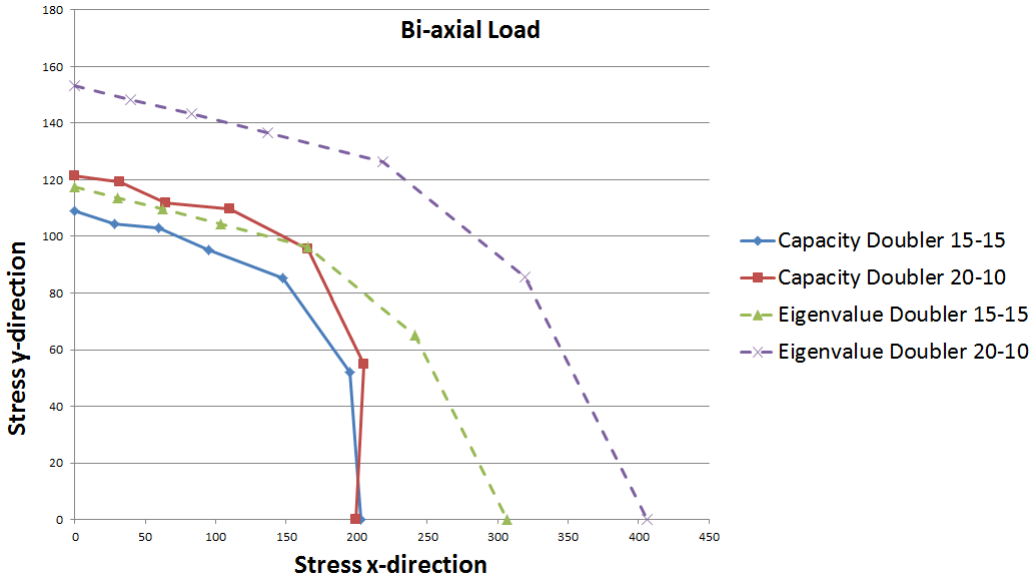

Figure 6.14: Comparison of bi-axial load between double (20-10) and double (15-15).

In another check with bi-axial loading, Fig. 6.14, we have an increase of capacity in transverse direction, that we do not have in axial. If we also plot the transverse and shear load case, Fig. 6.15, we can see the difference even better. This small enlargement in transverse direction can be linked to the way the deformations/buckling shapes are different between axial and transverse. For transverse we have larger and fewer half-waves in contrast to axial with its many and small. This affects the capacity and the rate of the change in it. With the axial buckling shape the smaller half-waves will not have as much fluctuation, smaller buckle shapes, than a larger half-waves that encounters for the transverse buckling shape. The difference in buckling attributes, described by Fig. 6.13 will have more impact for the larger half-waves, where the distance in buckling deformation between the two plates will be larger and thereby we have a large limitation of the original plate, which makes the system a bit stronger in this direction.

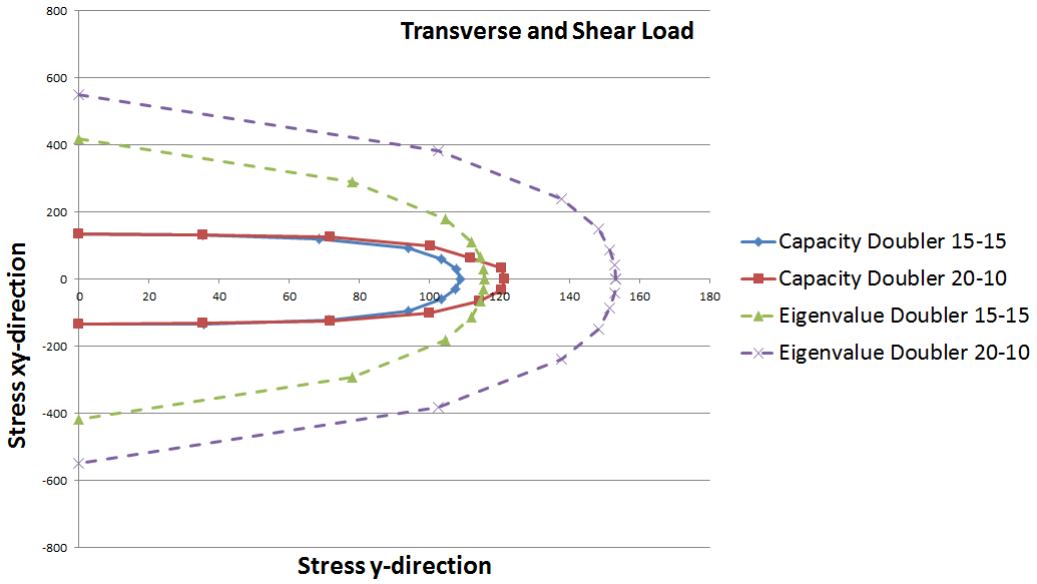

Figure 6.15: Comparison of transverse and shear load between double (20-10) and single plate.

From all three load cases reviewed for this ratio we can see that the eigenvalue for Case B is significantly higher than for an equal thickness ratio, while the capacity is quite similar for the two cases. In aspect of buckling the eigenvalue will in greater deal be a solution of the thick plate. The thin double plate reaches the limit for buckling before the thick stiffened plate and results in having a doubler which is fully buckled, but the thicker stiffened plate will still be able to withstand some more loading. Since the two plates are equal in Case A, they will reach the limit at the same time and by this having a lower eigenvalue, of the difference in the thickness between the two original plate in the two cases. The capacity on the other hand does not experience the increase of eigenvalue in a particular manner, except the slightly higher transverse capacity, discussed earlier. The approximately equal capacity is a result of the total area of loading, the decrease of doubler thickness is equalized by the increase of the thickness in the original plate.

6.4 CASE C: Thickness ratio 15-10

To get an even better understanding of the impact of the doubler we now can compare the equal thickness ratio, from Section 6.2, with a system where only the thickness of the doubler is changed, from the equal case, the ratio will then be 15-10 $[mm]$. The system gives a stable response, Fig. 6.16, and further a plot of the capacity and eigenvalue, Fig. 6.17, with the same load direction investigated in Section 6.2, the effect of the doubler still gives a clear advantage. Also here only shear will be limited by the von Mises yield criterion, Fig. 6.16 and Fig. 6.17.

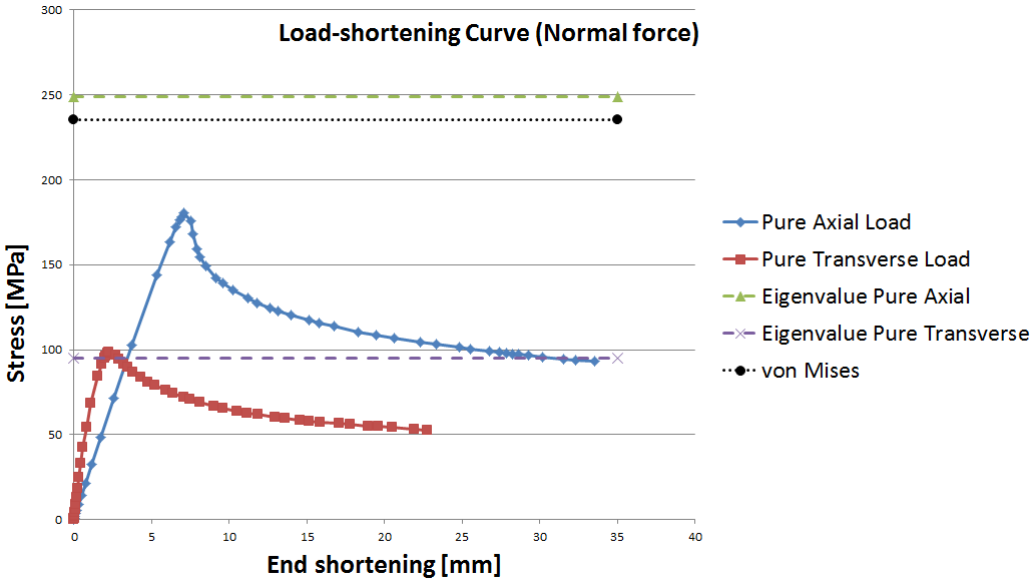

Figure 6.16: Load-shortening curve for a double plate with 15-10 thickness ratio.

As predicted, the capacity is reduced some from having an equal thickness ratio, but still the doubler is giving the system a high strengthening contribution in comparison with a single plate, still having in mind the difference in applied force. Due to the difference in the thickness of the two plates, we also here have the unequal deformations, where the thicker plate acts as the limiter for the thin plate with respect to bending, referring back to Fig. 6.13. We can also notice that the eigenvalue drops down, which is a result of the explanation of the increased eigenvalue in Case B. The thin plate will reach the limit for buckling first and by the reduced thickness of the stiffened plate, from Case B, the eigenvalue is reduced, by the properties of buckling.

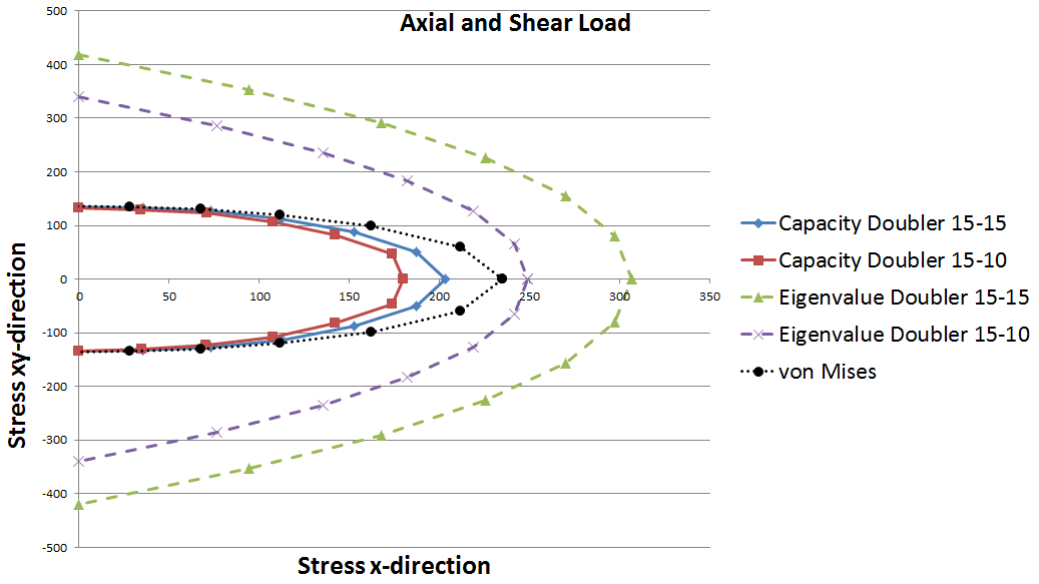

Figure 6.17: Comparison of axial and shear load between double (15-10) and double (15-15) plate.

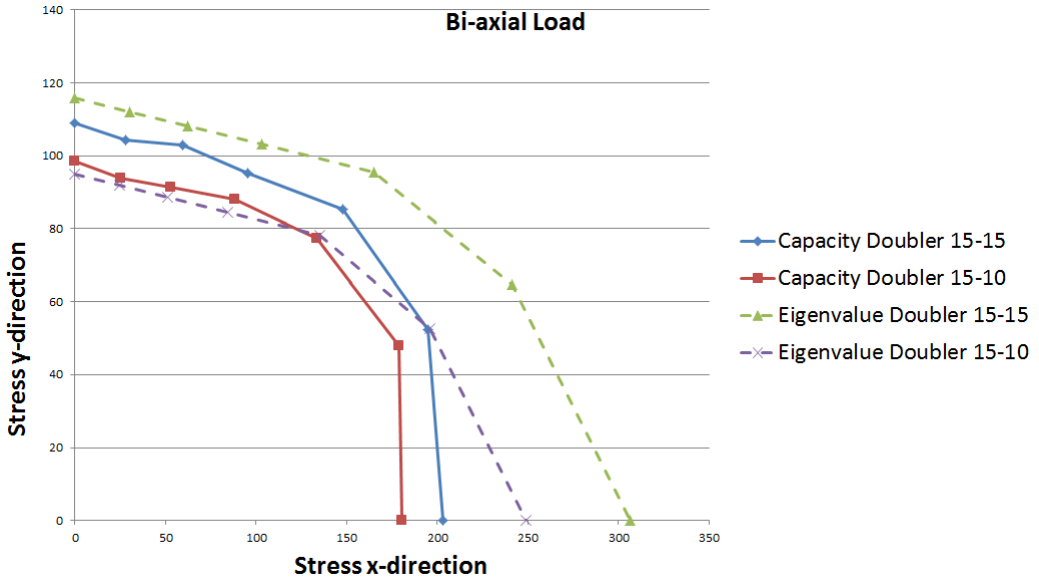

Figure 6.18: Comparison of bi-axial load between double (15-10) and single plate.

From the load-shortening curve, Fig. 6.16, pure transverse load exceeds the eigenvalue and to estimate the possibility of reserve strength here, we choose to review also the two last critical load combinations, Fig. 6.18 and 6.19.

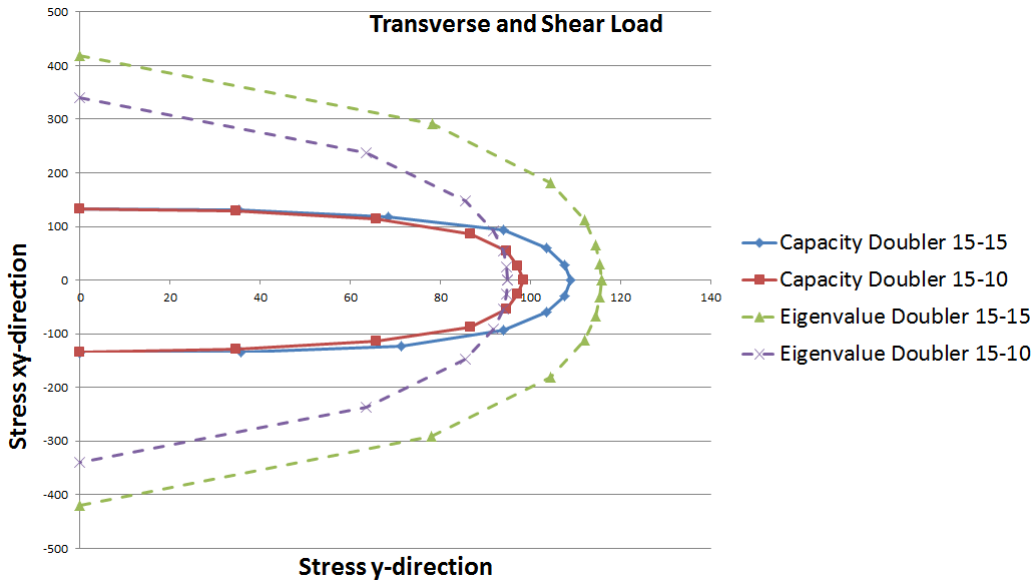

Figure 6.19: Comparison of axial and shear load between double (15-10) and single plate.

In the bi-axial loading condition, Fig. 6.18, some reserve strength will be accessible and is eligible for all load direction except when having nearly pure axial loading. This also applies for the transverse directional loading in interaction with shear. However the size of the reserve strength is small and will not have a great influence of the design of a doubler, but we notice that when the total thickness of the structure is reduced, the possibility of reserve strength is available.

6.5 Impact of other imperfections

We have up till now presented results where all the load cases have been investigated with respect to something we call real imperfection. It can be quite difficult to estimate the imperfection in such a way that it represents an actual physical problem. Imperfection, as mentioned earlier, is small deflections in the plate that erupts from the production process. We will see how the capacity of the plate problem changes when it is subjected to other then real imperfection, all load cases and imperfection is shown in Table 6.1. The contribution of the thickness ratio will act in the same manner as in the three load cases with real imperfection, investigated in the previous sections in this chapter. From this we will focus on the ratio with equal thickness, Case A.

6.5.1 Strict constraints

As discussed in Section 4.3.3 we can analyse the problem with a simplified approach to the constraints at the two short edges. The difference in buckling shapes of these can be seen in Fig. 4.5 and 4.6. First we can see what difference this makes in the capacity to the plate problem with reviewing all three crucial load directions and still having real imperfection, see Fig. 6.20, 6.21 and 6.22.

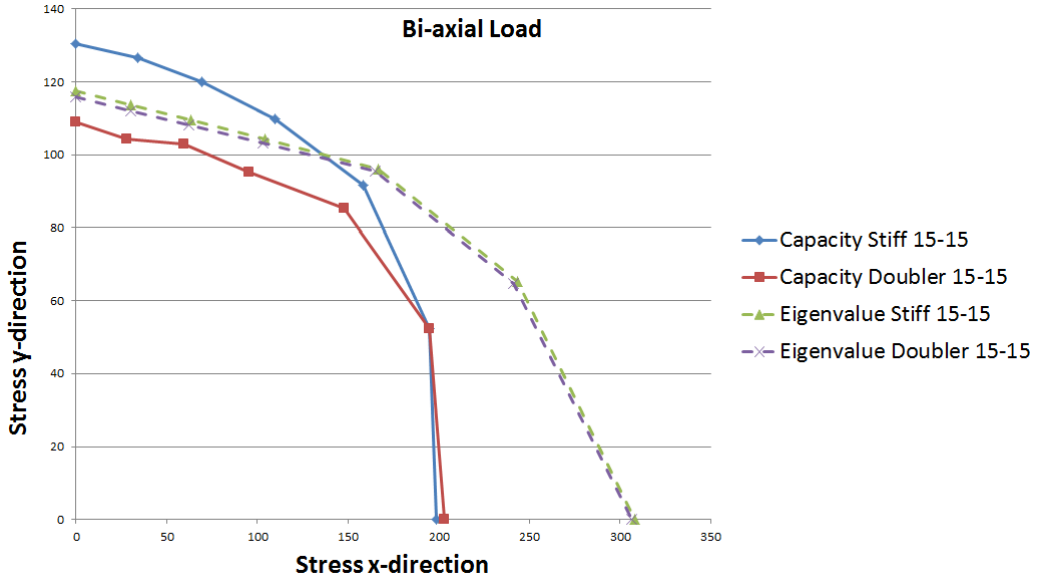

Figure 6.20: Capacity comparison between constraint definitions, bi-axial loading.

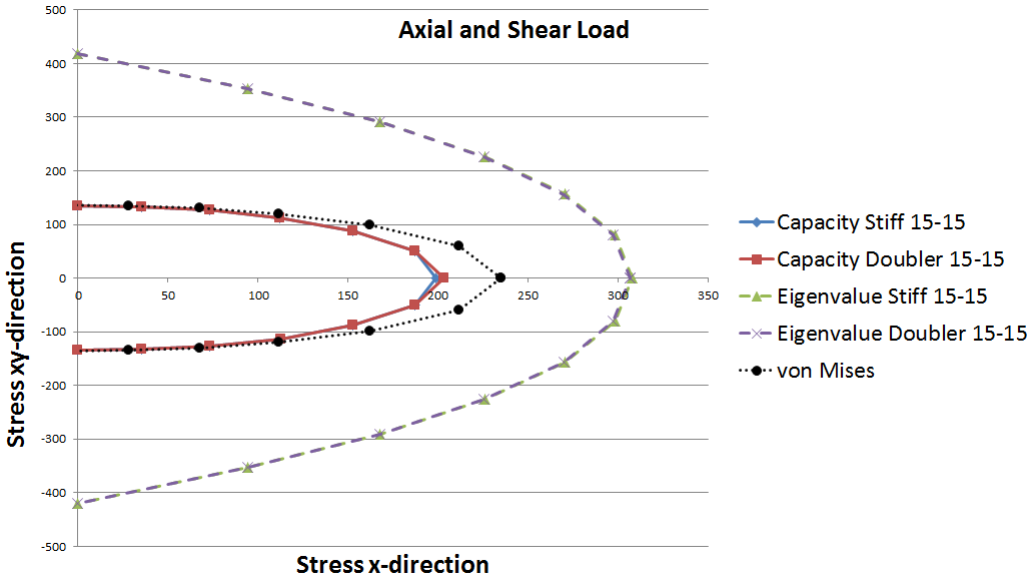

Figure 6.21: Capacity comparison between constraint definitions, axial and shear loading.

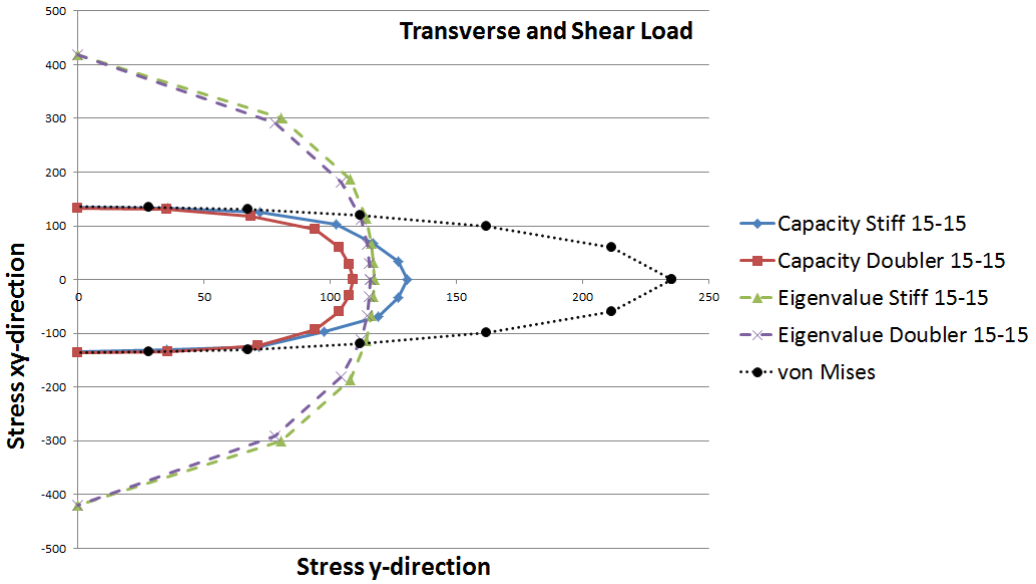

Figure 6.22: Capacity comparison between constraint definitions, transverse and shear loading.

With the strict conditions the only viewable contribution is when analysing the transverse loading. Here the capacity increases in such great extent, that we end up with a system having some reserve strength, the eigenvalue is exceeded. In the two other directions, axial and shear, the difference is almost negligible. The eigenvalue for these two conditions, also reviewed in these figures, Fig. 6.20-6.22, are also pretty much equal. Since the strict constraint is an easier and faster way to handle the problem and now shown that they, often, are comparable, we choose to use, for simplicity, this condition when we now shall investigate the impact of other imperfections.

6.5.2 Pure axial imperfection

We have here a problem where the imperfection is taken from pure axial buckling load. Illustration of the shape to the imperfection can be seen in Fig. 4.5 in contrast to fully buckled plate in Fig. 6.1.

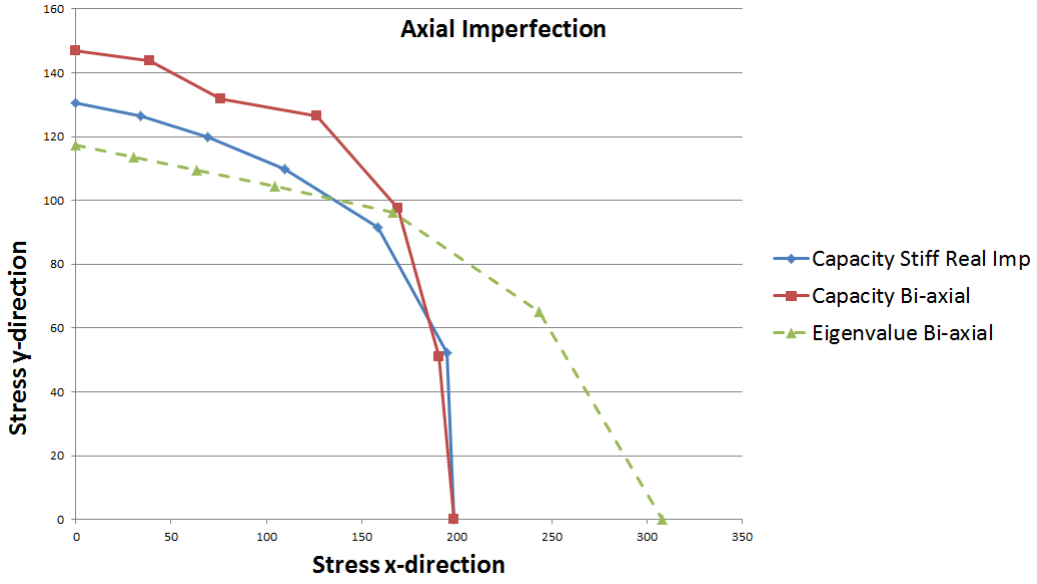

Figure 6.23: Capacity comparison of axial imperfection with bi-axial loading.

From Fig. 6.23 we can see that with pure axial imperfection the capacity of the plate increases when we reach more and more pure transverse loading. Of course when we have pure or nearly pure axial loading, the capacity will occur just in the same way as when having real imperfection. By increasing the capacity in transverse direction, we get even more ability for a system to withstand additional load after fully buckled, reserve strength. Do we look at another load case where

transverse and shear force are loaded an axial buckled imperfection model, the same increasing capacity of the transverse loading will occur, but by looking at the shear loading also here, like in all the three previous cases, the shear load will be limited by von Mises yield criterion, see Fig. 6.24.

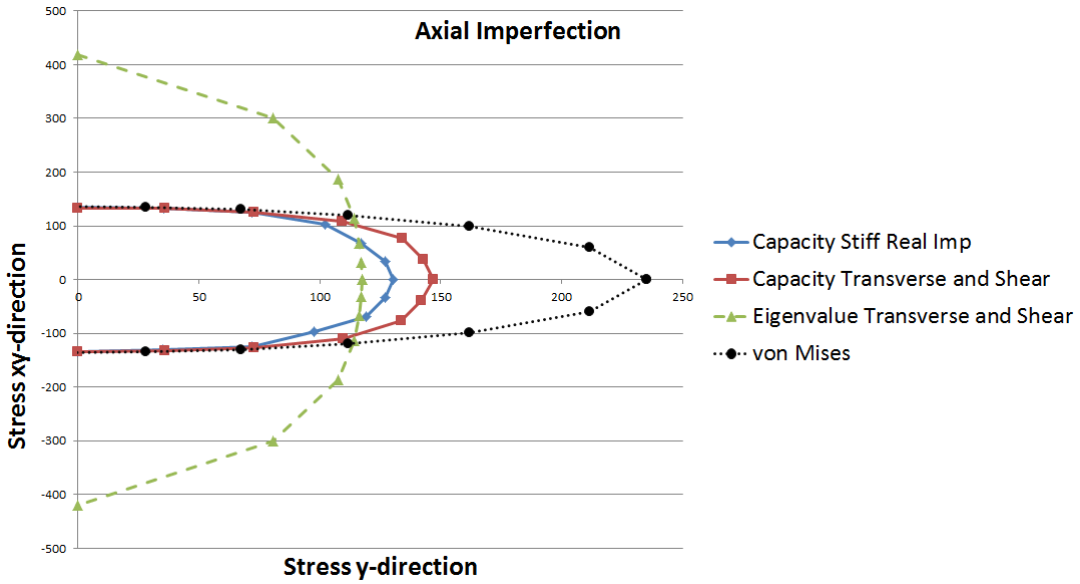

Figure 6.24: Capacity comparison of axial imperfection with transverse and shear loading.

6.5.3 Pure transverse imperfection

By switching the imperfection to pure transverse buckling load, the result of the capacity also changes its properties. We now have increasing capacity in the axial loading area, but this is not creating any capability of reserve strength as transverse loading in axial imperfection gave, Fig. 6.25 and 6.26. With shear involvement the von Mises yield criterion yet again act as a limiter.

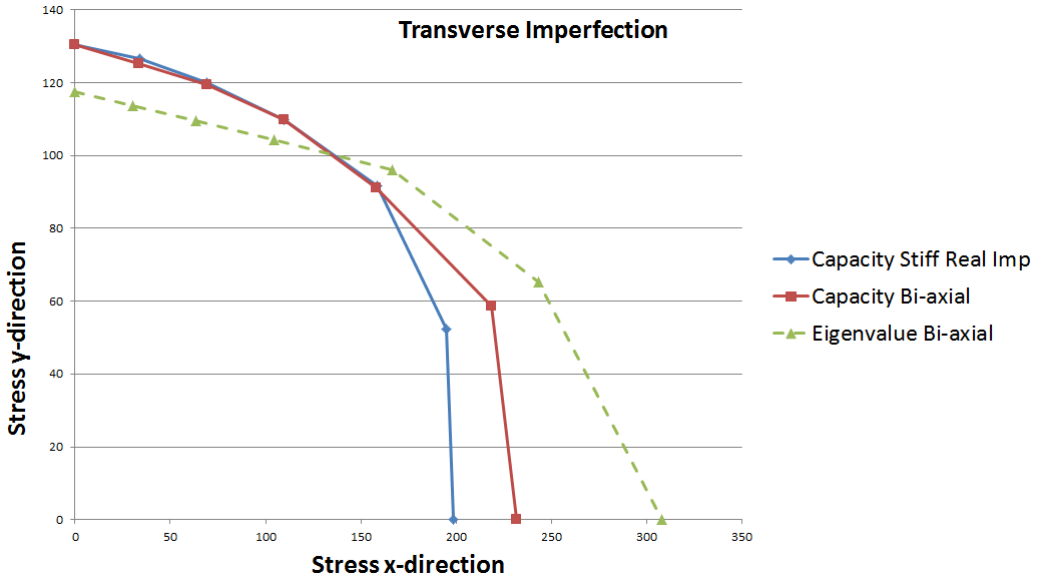

Figure 6.25: Capacity comparison of transverse imperfection with bi-axial loading.

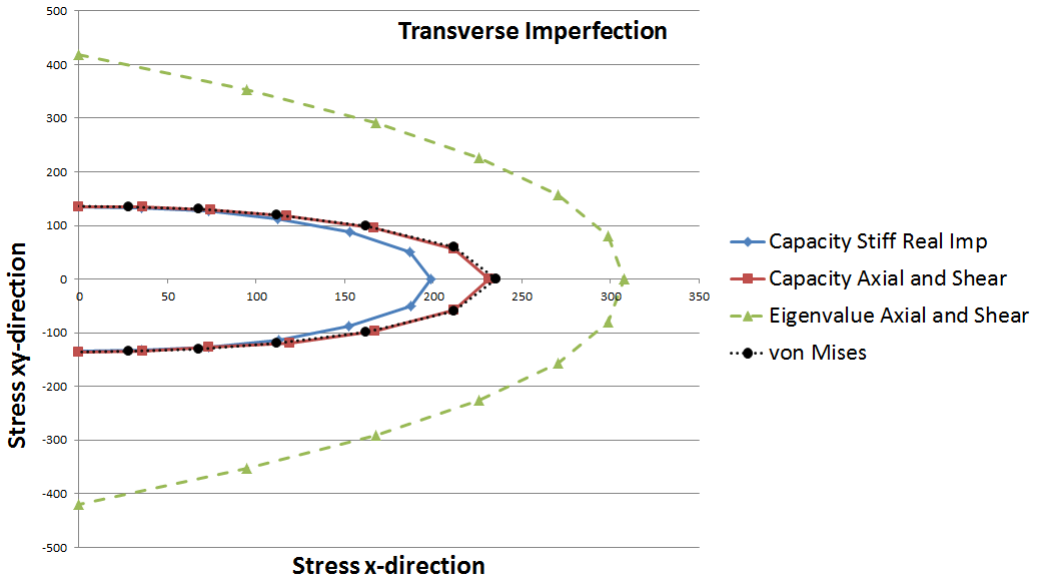

Figure 6.26: Capacity comparison of transverse imperfection with axial and shear loading.

By having other imperfections we can see that the capacity of the system with doubler will increase and it is then more applicable to use real imperfection, because the capacity is then the lowest at all load directions.

6.6 Remarks

We will finally in this chapter present the different cases reviewed earlier combined. We first look at the combinations of the two normal loads, Fig. 6.27.

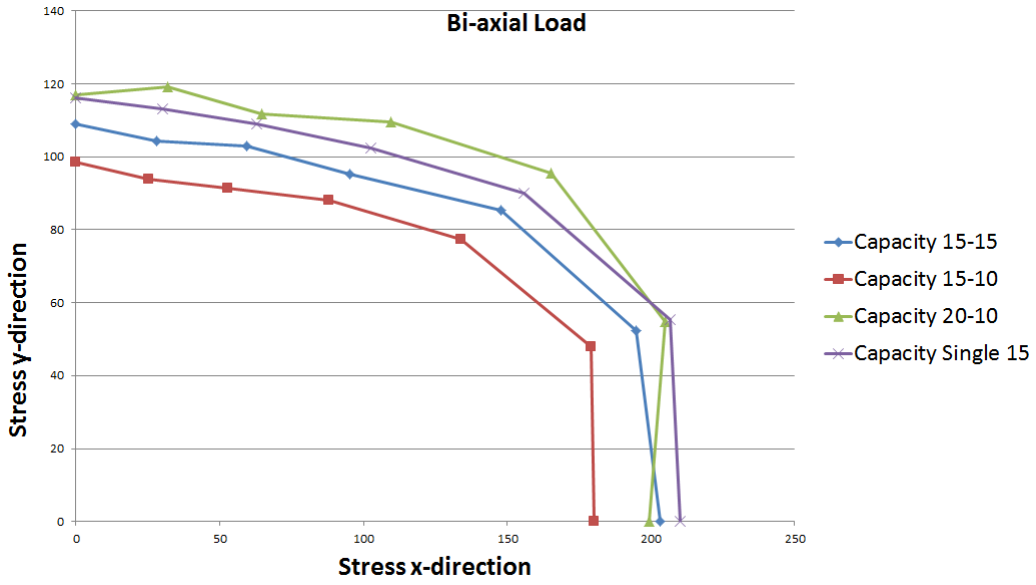

Figure 6.27: Capacity comparison of all cases in bi-axial loading, with real imperfection.

The capacity for all three cases reviewed in comparison with a single plate, although a great increase of the load, resulting in having good compliance and just some minor deviation of the stress. As we maybe could predict in advance, the capacity increases with increasing thickness. If we compare directly Case A and B, since they both have the same magnitude of load added, we can see that the plate with thinner doubler have higher capacity, but this comes from the properties of the thicker stiffened panel acting as a bigger buckling limitation of doubler in transverse direction.

However one thing worth noticing is that in this case with equal magnitude of outer load, the thinner double plate is not a disadvantage. And when only comparing with the single plate, the doubler are able to withstand almost twice the load and still have nearly the same or in transverse direction even higher capacity, Fig. 6.28, the doubler shows its full capability. For the eigenvalues the rate of strength, between the thickness ratios, is even greater, Fig. 6.29 and 6.30. Here the values are more dependent on the stiffened panel, since the doubler will reach the buckling limit first.

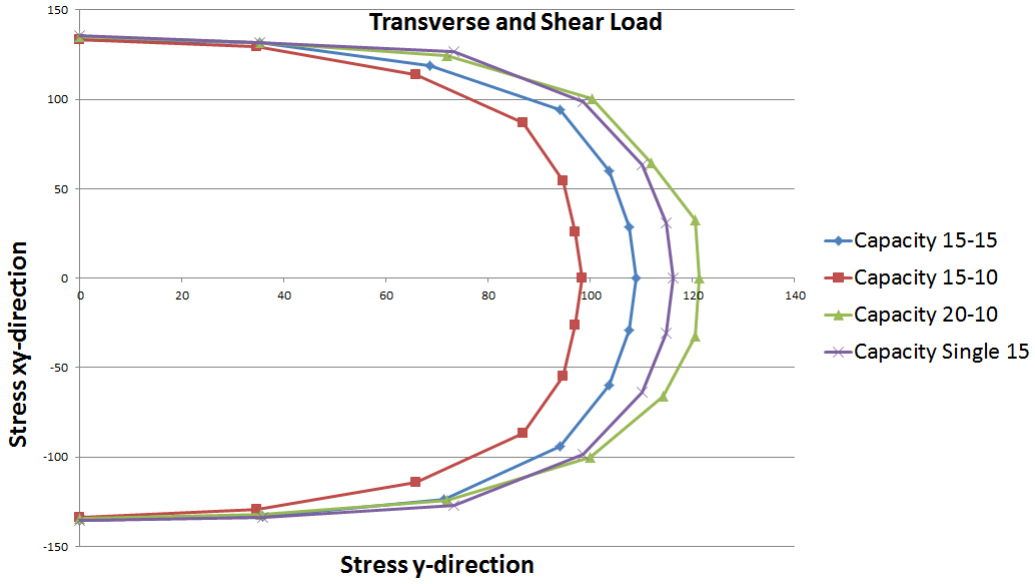

Figure 6.28: Capacity comparison of all cases in transverse and shear loading, with real imperfection.

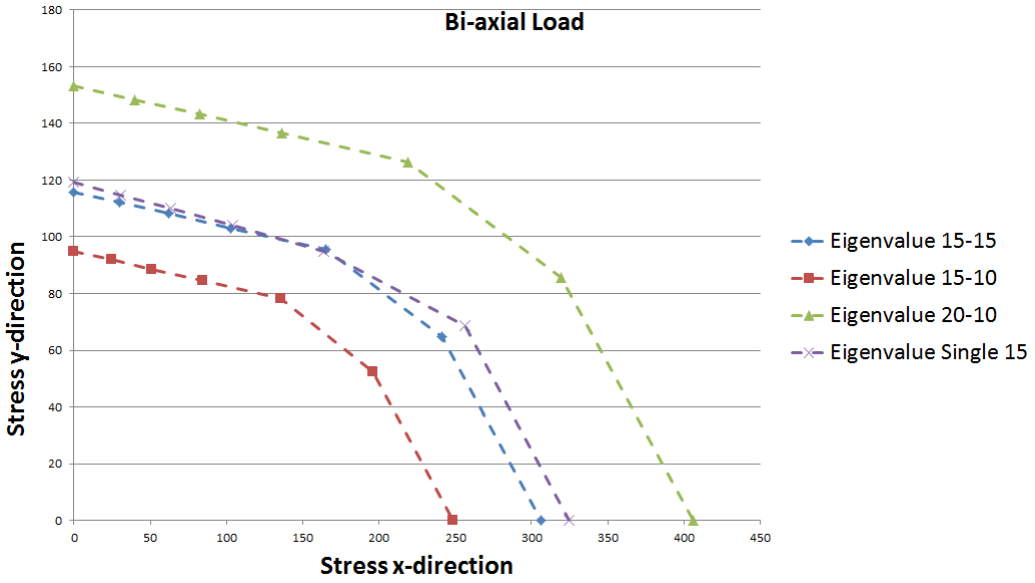

Figure 6.29: Eigenvalue comparison of all cases in bi-axial loading.

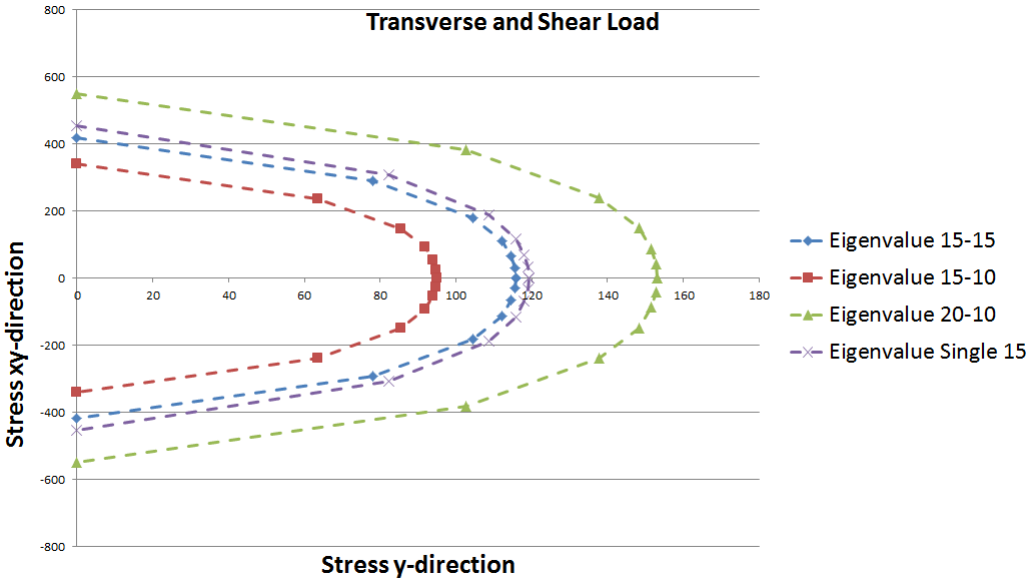

Figure 6.30: Eigenvalue comparison of all cases in transverse and shear loading.

We have now completed the analysis of the intact/undamaged problem. The doubler will in practise not be of any interest for an undamaged structure, since they are, in most cases, been used to repair for ship hulls and we can see that the thickness of the original plate have strong contribution to the capacity. But with this review we have a greater understanding of double plate behaviour. We will use this knowledge to conduct the investigation of the effect of the doubler in repair of a structure with a particular damage, which we will present in the next chapter, Chapter 7.

Chapter 7

Damaged stiffened plate

In the previous chapter we looked at a plate model without any vital deformations or damages and how the doubler affected the buckling load and capacity to an intact system. The same will be done next, but now we will look at how a doubler can strengthen a damage plate section, we will in other words do a repair on the damaged section. The damage we will look into is a problem which in marine technique language is called "Hungry Horse". This can be illustrated by Fig. 7.1, where the damage clearly can be seen on the hull of the ship.

Figure 7.1: An example of "hungry horse" damage on HMS Manchester. Courtesy of The British Royal Navy.

7.1 Single plate

To model a damage like "hungry horse" we must have imperfection that comes from lateral pressure. A damage model of this can in Abaqus look like Fig. 7.2. For this type of damage problem the strict conditions we have used earlier to reduce the running time of the analysis cannot be used. This is on the bases of the symmetrical conditions at the two short edges. If we had used this strict condition the whole section would be consisting of four separate plates, where the two end plates would have half the length of the two mid-plates and this is a closed problem of no interest. The imperfection is scaled up in such way that the deflection of the plate is much larger than the normal imperfection we used in Chapter 6, $\frac{s}{200}$. The damage lateral imperfection has a scale normal between 80 and 100. This is a big enlargement from the approximately 4 we used earlier and gives therefore a good damage approximation.

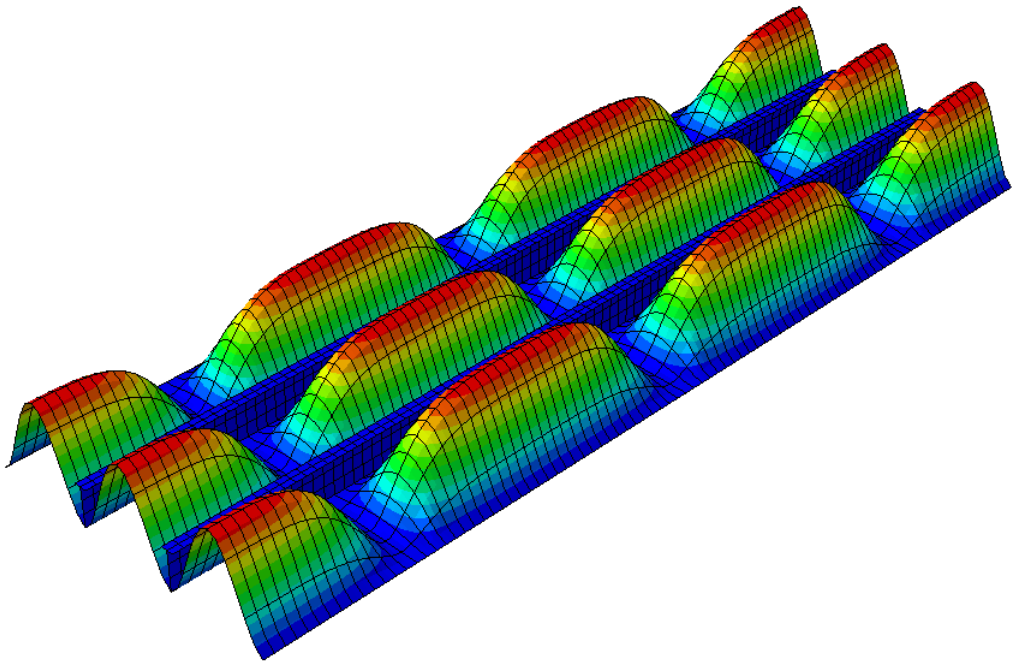

Figure 7.2: Hungry horse damage on a single plate, enlarged view $\times 3$.

We follow the same routine as in Chapter 6, with ensuring of stable response, Fig. 7.3 and to have a complete collapsed model at the end of every analyse, as can be seen in Fig. 7.5 where axial load direction have been examined for a complete buckled model. In the damage analysis we use the same eigenvalues we found for an intact problem, eigenvalues stay the same regardless of the imperfection.

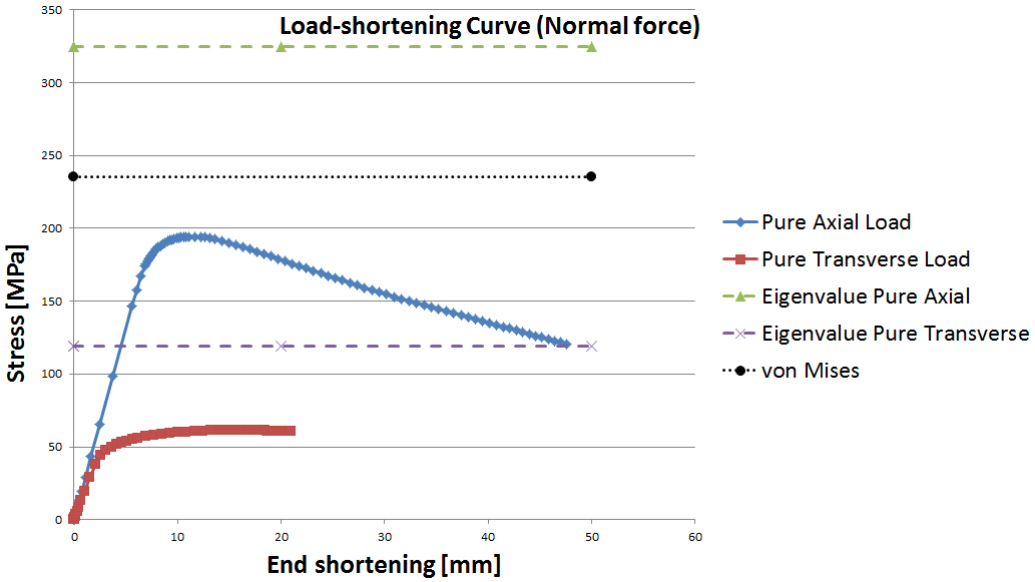

Figure 7.3: Load-shortening curve for a damaged single plate.

It may be a bit difficult to see, in Fig. 7.3, if the pure transverse loading condition is giving a stable response, but by examining only this condition alone the response is more viewable, Fig 7.4.

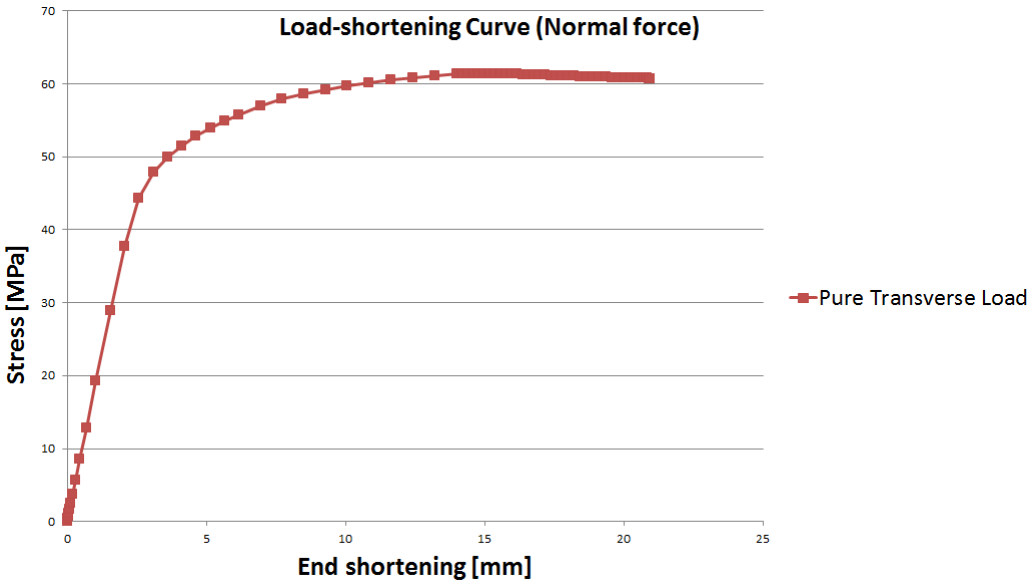

Figure 7.4: Load-shortening curve for pure transverse loading.

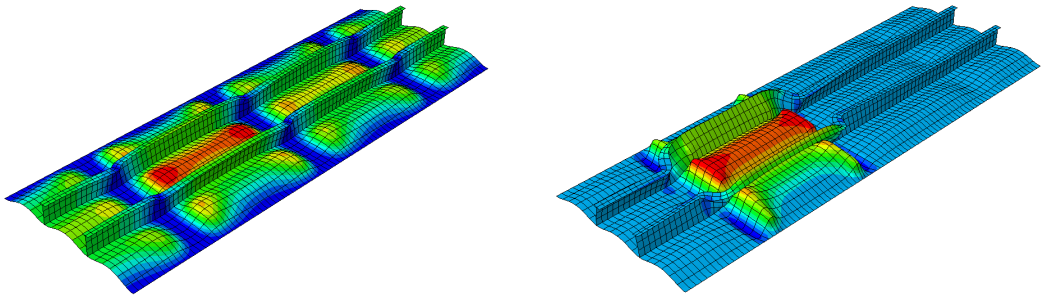

(a) (b)

Figure 7.5: Up-scaled deformation plot, ×5, with axial loading for (a) Increment of collapse and (b) Last increment in the analyse.

In comparison with the intact single plate, the capacity of this damaged system reduces, in general, massively, as predicted, Fig. 7.6. The same reduction applies for the two other crucial loading directions, where normal and shear force acts together, Fig. 7.7.

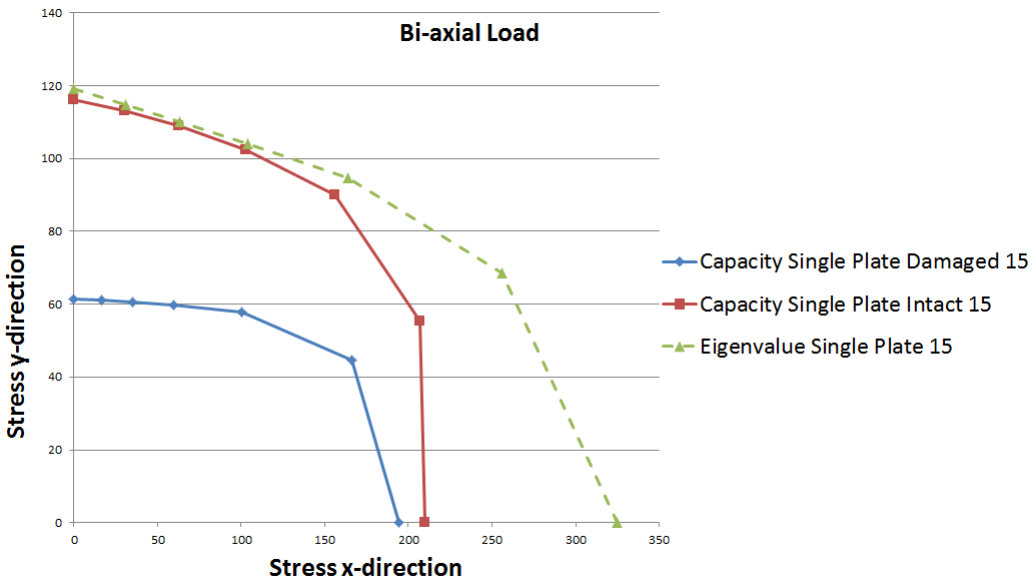

Figure 7.6: Comparison between intact and damage structure in bi-axial loading.

We notice that the reduction of capacity with axial loading is small, especially in contrast to the large reduction in transverse direction. The reason has bases in the imperfection. A hungry horse imperfection is in many ways a larger transverse imperfection, by comparing the deformation/buckling shapes in Fig. 7.2 with Fig.

6.10 we see that both have few and quite large shapes. By then, with large out-of-plane deflection in the imperfection of a damage, we have a drastic fall of the capacity in transverse direction. If we look at the Section 6.5, the capacity in axial loading direction would increase when having transverse rather than real imperfection. From this the smaller deviation for axial loading in the damaged model can be linked to the large displacement in the imperfection, in contrast to Section 6.5.3. If we further investigate the impact of shear force on the damaged plate, Fig. 7.7, we see that the curve does not reach the material yielding limit, like the intact single plate did, and by this the shear problem for a single damaged plate is controlled by buckling alone.

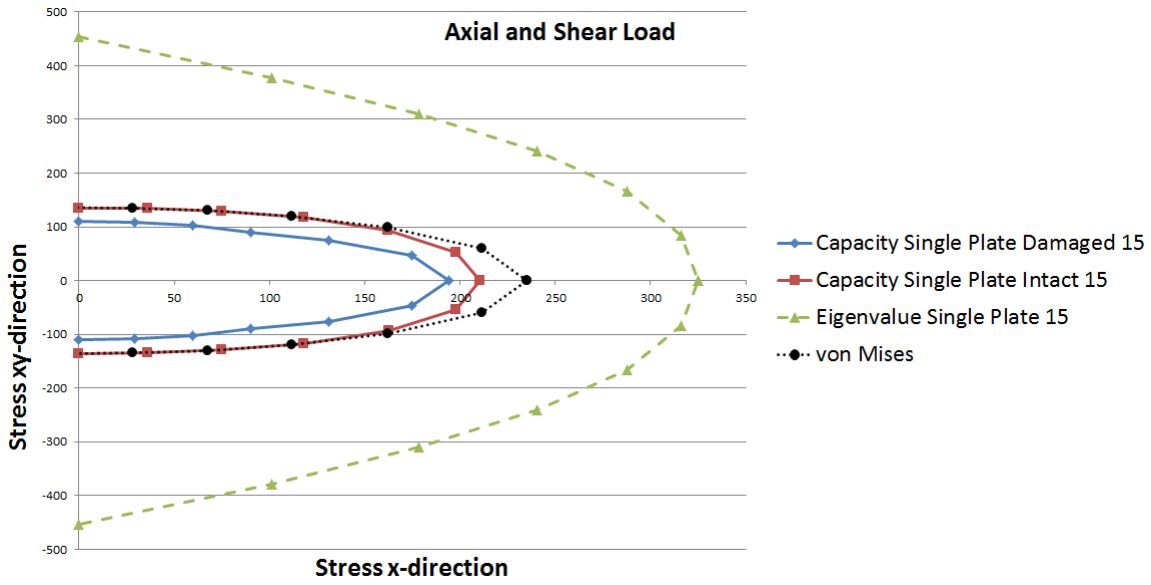

Figure 7.7: Comparison between intact and damage structure in axial and shear loading.

7.2 Double plate

In modelling a "hungry horse" damage with a doubler attached. The model must be arranged in the way that the original plate with stiffeners attached has the damage imperfection, like in the previous Section 7.1, while the doubler only has the normal production imperfection, equal to the doubler in Chapter 6. An example of this is shown in Fig. 7.8. Here the view is enlarged to give a better view of each imperfection.

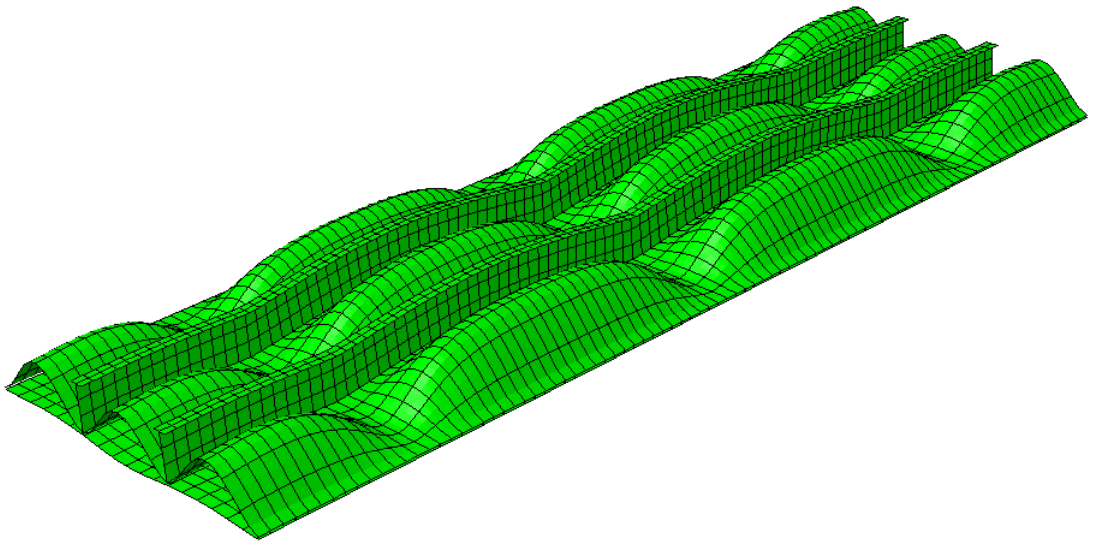

Figure 7.8: View of the damage model in Abaqus.

We will examine the same three cases like in Chapter 6, for an intact plate section, with the same control and verification methods used in Section 6.2, 6.3 and 6.4.

7.2.1 CASE A: Thickness ratio 15-15

In the problem where the ratio of the thickness is equal, 15-15 $[mm]$, we can see that the problem is giving stable response for the two pure normal load directions, Fig. 7.9, and they both have clearance to any potential reserve strength and material yielding. From examining the potential reserve strength in the intact problem, it can be seen that the most likely place for any reserve strength to occur were when having pure loading for normal forces. So with only looking at the load-shortening curve for these, the possibility of any reserve strength can be seen. In addition we can see that the peak for both curves has no influence of the limit for material yielding or von Mises stress limit as it is often called.

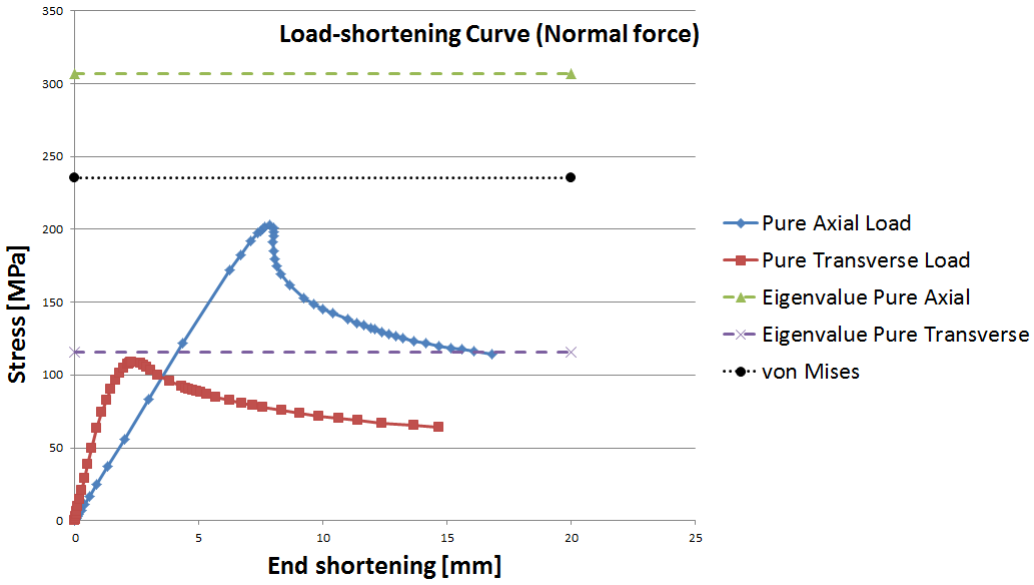

Figure 7.9: Load-shortening curve for equal thickness ratio.

When investigating the capacity some interesting characteristics are found, see Fig. 7.10. Like in Section 7.1, for a single plate, the axial capacity reduces in the same small amount from the intact problem, of the large imperfection of the stiffened plate, and reduces slightly more in forms of stress from the damaged single plate, because of the increased load deviation. While in transverse direction we have a considerable increase and the doubler is really showing its capabilities. Even so, the most obvious feature here is the decreasing capacity and the fall of the curve when reaching the transverse load. If we have in mind the imperfection we use in the double plate we are repairing the damage model with, this has a varying imperfection, real imperfection. This means that for pure axial loading we have pure axial imperfection, many and small half-waves as in Fig. 6.1, while

for pure transverse loading we have pure transverse imperfection, few and long half-waves as seen in Fig. 6.2a. With this we then have in combination with the lateral damage imperfection a more solid structure for applying axial rather than transverse loading. From Section 7.1 we concluded, with the impact of the other than real imperfection shapes, that for a single damaged plate the capacity is quite high in axial direction. But for our model with doubler, we have both real and lateral/hungry horse imperfection in the total system. Do we look at the imperfection shapes in the doubler for all the load directions, the more long and fewer half-waves are taking over at the place the curve starts to fall. But either way the system with the doubler is able to carry the same or even higher stresses, even with more loads added.

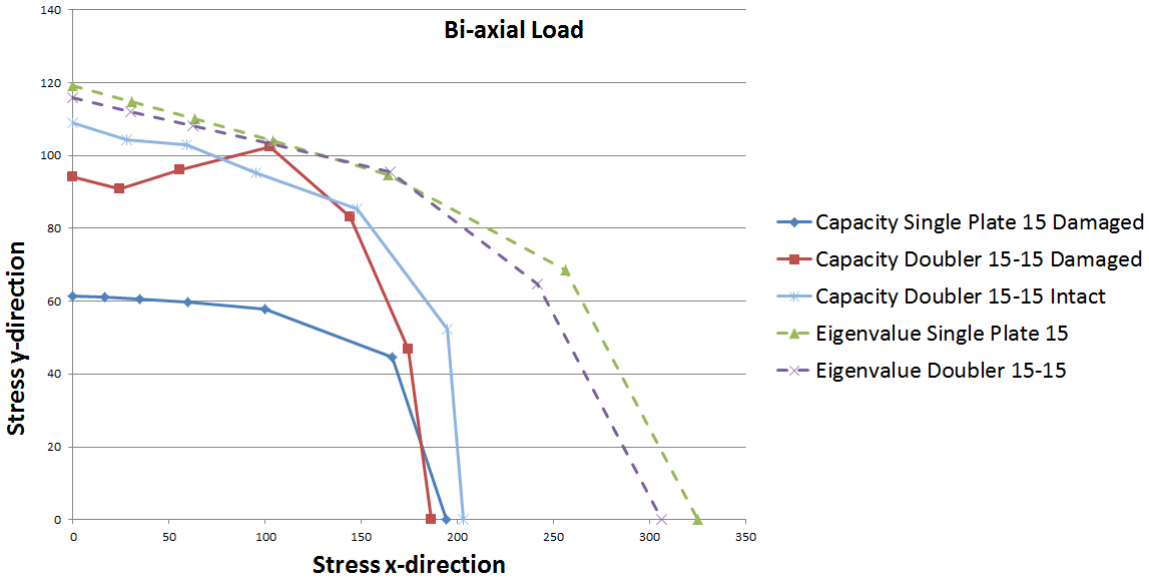

Figure 7.10: Capacity of a repaired damage model, equal thickness ratio.

We have also plotted the double plate problem for an intact model. Here the loads added are equal and we can see that the capacity of the repaired damaged model is quite similar to having an intact one. This shows the great advantage the doubler has on a system. The reduction of capacity from the intact model can be subscribed to now having a system that does not have the same buckling limit for the two plates, much in the same way as we had with different thickness ratios in Section 6.3 and 6.4. In other words the plates will have different buckling properties. The greater and unidirectional imperfection of the stiffened plate makes the system more dependent on the doubler. By comparing the capacity when shear force contributes to the system, we can see great similarities with what we saw for normal forces, Fig. 7.10. The only difference is when having a

damage on a single plate the material yielding does not encounter as a limiter for the capacity of the plate. Here buckling will be the limiter, but with attaching the doubler the material yielding once again appears, see Fig. 7.11 and 7.12.

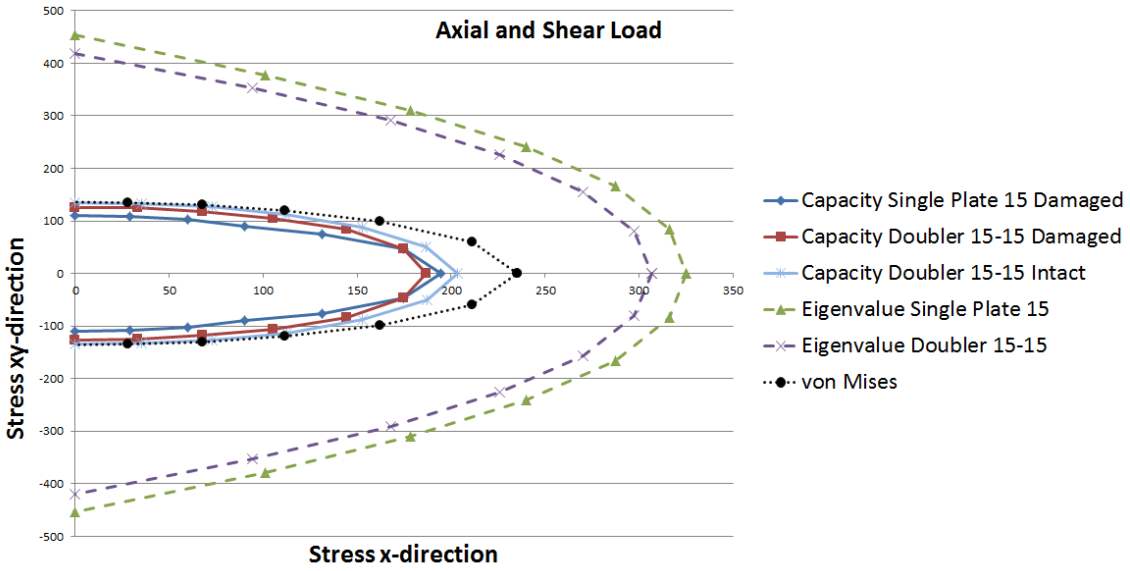

Figure 7.11: Capacity of a repaired damage model with axial and shear loading, equal thickness ratio.

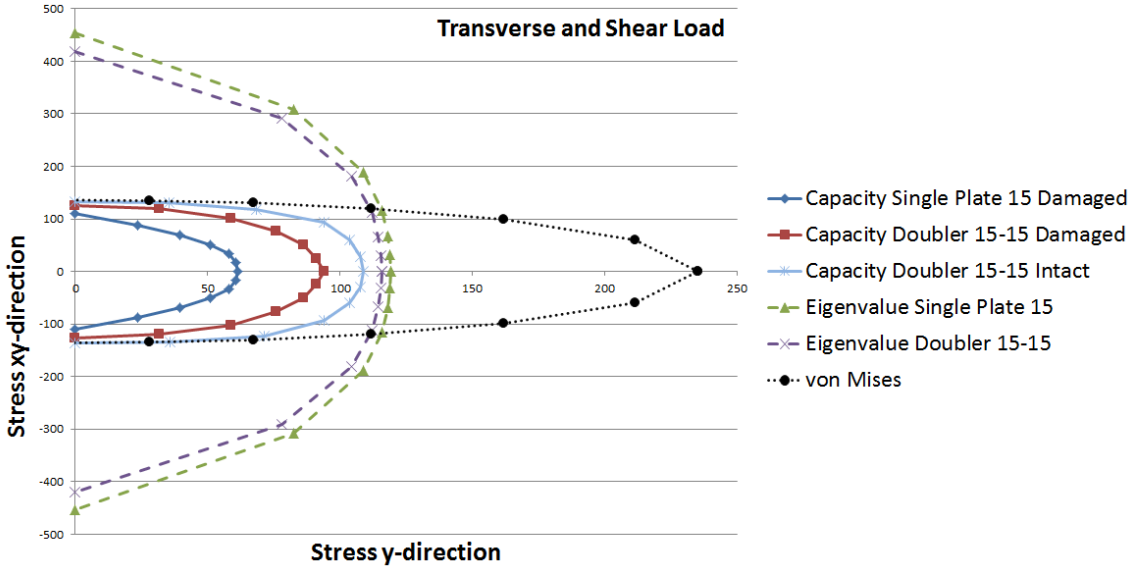

Figure 7.12: Capacity of a repaired damage model with transverse and shear loading, equal thickness ratio.

With the perspective of reaching the material limit when shear forces are applied, this also includes that the system is able to withstand even more stress than the single plate that has buckling as the limiter. This applies for both combinations of normal and shear force, Fig. 7.11 and 7.12.

As we described will the buckling behaviour for a damaged plate with equal thickness ratio have other buckling limits, which erupts from the large out-of-plane displacement, than in intact. This can be shown of Fig. 7.13 where we can see the normal axial imperfection of the doubler has larger deflection in one direction and have some restrain in the direction of the stiffened plate, but not as much as shown in Fig. 6.13. In addition we can see the difference in displacement at the starting point, Fig. 7.8, that is the basic reason to for the minor limiter in damage.

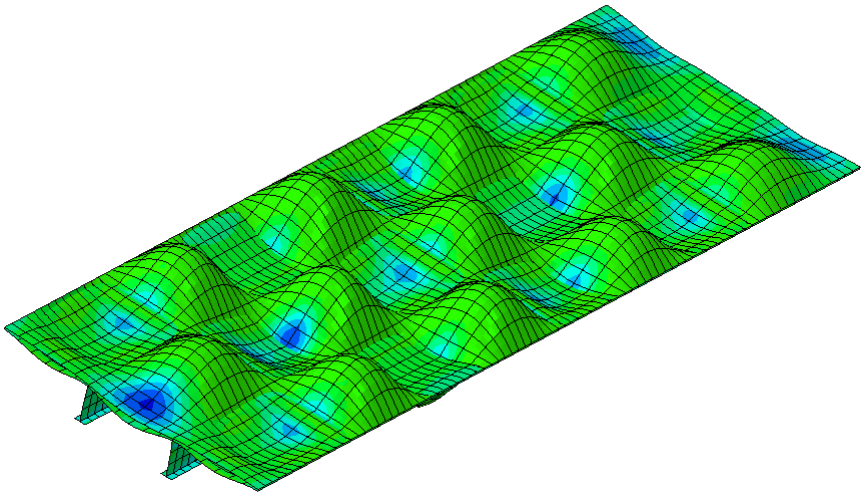

Figure 7.13: Different deformation shapes in the two plates, double plate side.

7.2.2 CASE B: Thickness ratio 20-10

From this thickness ratio in an intact plate problem we found that the eigenvalue increases a great deal, while the capacity has almost equal values as the equal thickness ratio. But what will happen when the thick and stocky plate has a significant damage? We first have to verify a stable response in our analysis, Fig. 7.14.

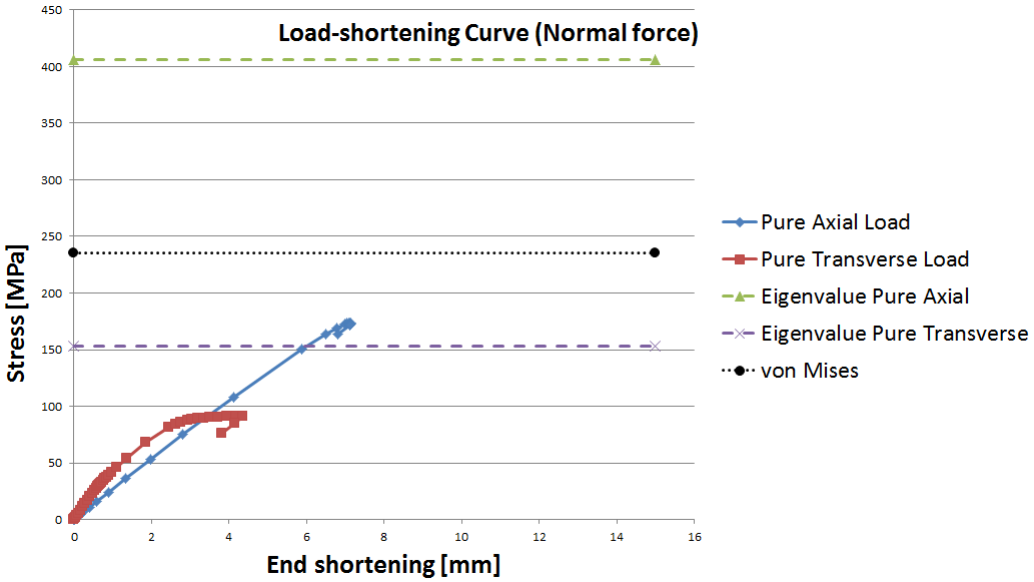

Figure 7.14: Load-shortening cure for thickness ratio of 20-10.

As for intact problem with this thickness ratio we have a large distance for both pure normal force directions to any reserve strength and the possibility of material yielding, but both are stable.

The most interesting though are the changes in capacity. From looking at equal ratio, we now have a system that, even when having a higher eigenvalue, can seem to have in total a lower ultimate capacity, Fig. 7.15 and 7.16. In shear direction it has approximately the same value since the material yielding encounters, but particularly in axial direction the capacity has dropped. The total load is, as in intact, the same in respect to the equal thickness ratio due to the total area the load is added.

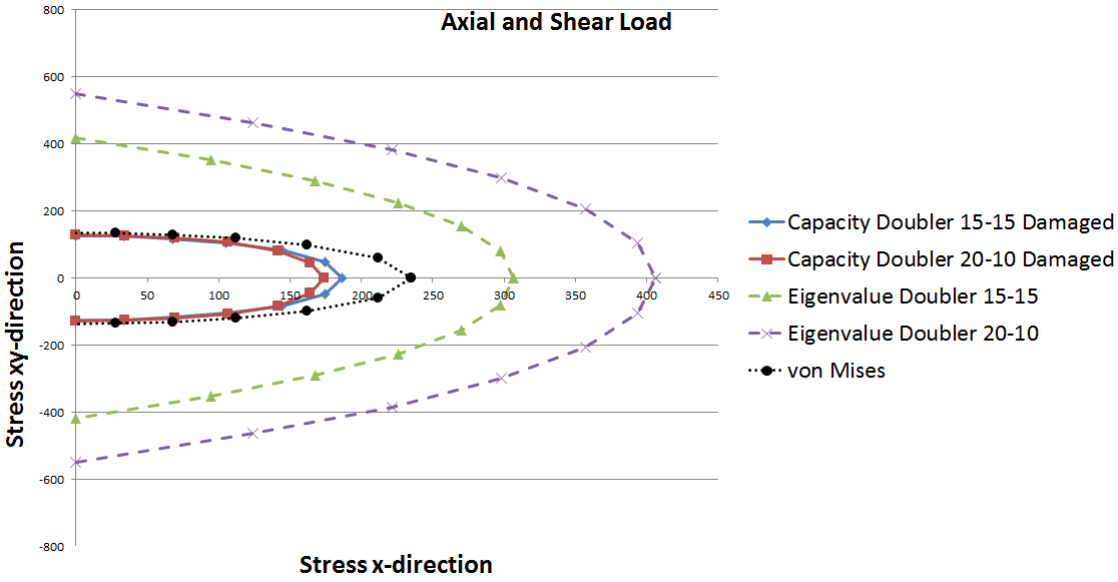

Figure 7.15: Ultimate capacity for a damaged plate with 20-10 thickness ratio, axial and shear loading.

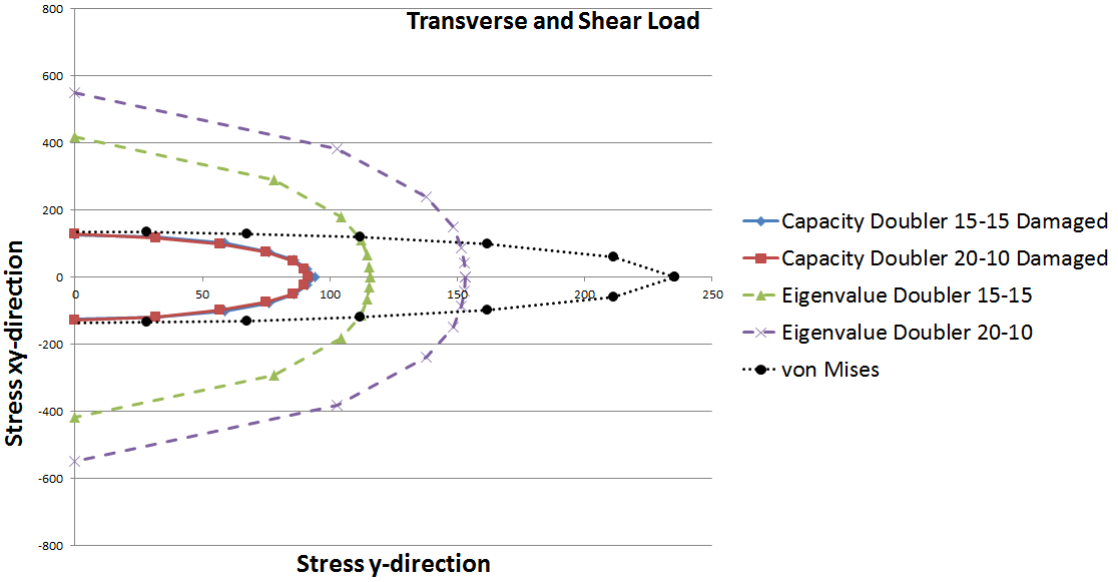

Figure 7.16: Ultimate capacity for a damaged plate with 20-10 thickness ratio, transverse and shear loading.

To get a better comparison, we plot the bi-axial loading condition, Fig. 7.17. Here we see that in total aspect of normal forces the capacity is approximately equal, even if the two plots above, Fig. 7.15 and 7.16, could tell us differently. Only the two pure loading directions give a drop of capacity. In comparison of the intact problem with the same ratio the capacity has decreased to some extent, but this is obviously reasonable as we also saw in Section 7.2.1.

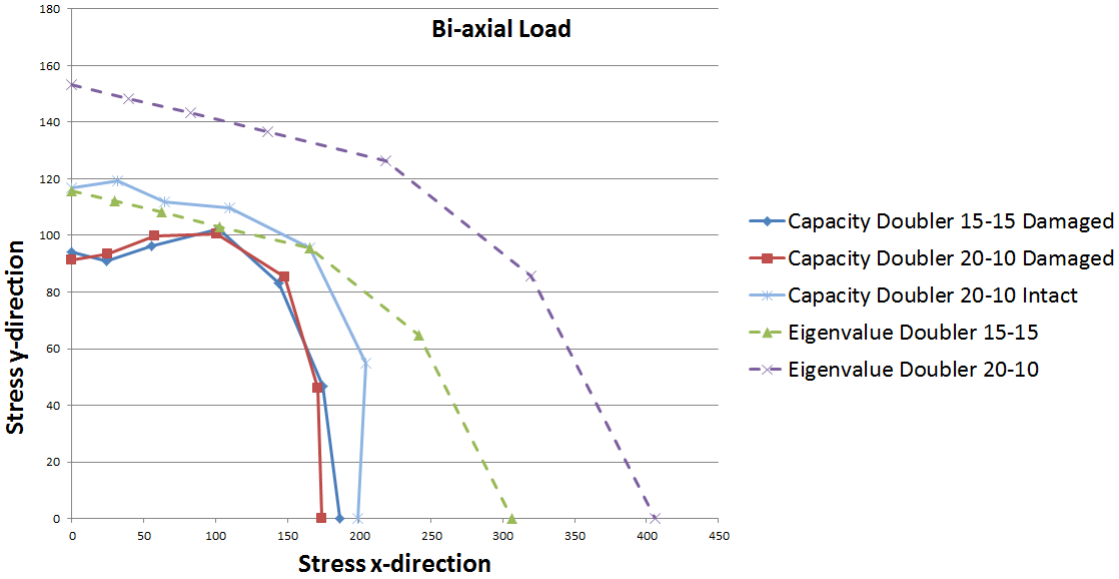

Figure 7.17: Ultimate capacity for a damaged plate with 20-10 thickness ratio, bi-axial loading.

As in Case B for an intact problem, Section 6.3, we can define the difference between the two thickness ratios by the way a thin plate will buckle/deform more than a thicker one. Since the thick plate already has a quite large deflection shape, this will not be as great boundary or limiter as it was for the two equal imperfection shapes in Section 6.3, and hence the capacity drops some. An intact problem the ratio of 20-10 gave a slightly higher capacity than the equal ratio, while here in the damaged model, the capacity is nearly equal or even a bit smaller. We see a reduction of the contribution to the stiffened plate.

In addition the imperfection shapes in the two plates are unequal, as described in Section 7.2.1. In general the large long waved shapes in the damaged imperfection will create a stronger system in axial direction and the opposite in transverse, as explained in a greater context at the end of Section 6.5, but this will by the axial imperfection of the thinner doubler in some degree be revoked. This creates the small decreasing of the capacity in pure x- and y-direction. We have already

stated that the doubler is the weakest link when looking at plates with different thickness ratio, but when the thick plate has a larger imperfection the doublers contribution is more important.

7.2.3 CASE C: Thickness ratio 15-10

The last investigation we will perform is when the damaged plate has the same thickness as original in Section 7.2.1, 15 mm, and the doubler has the same reduced thickness as in Section 7.2.2, 10 mm. With this ratio the capability of the doubler really will be shown. First we can see that the pure normal forces are preforming a stable response, Fig. 7.18.

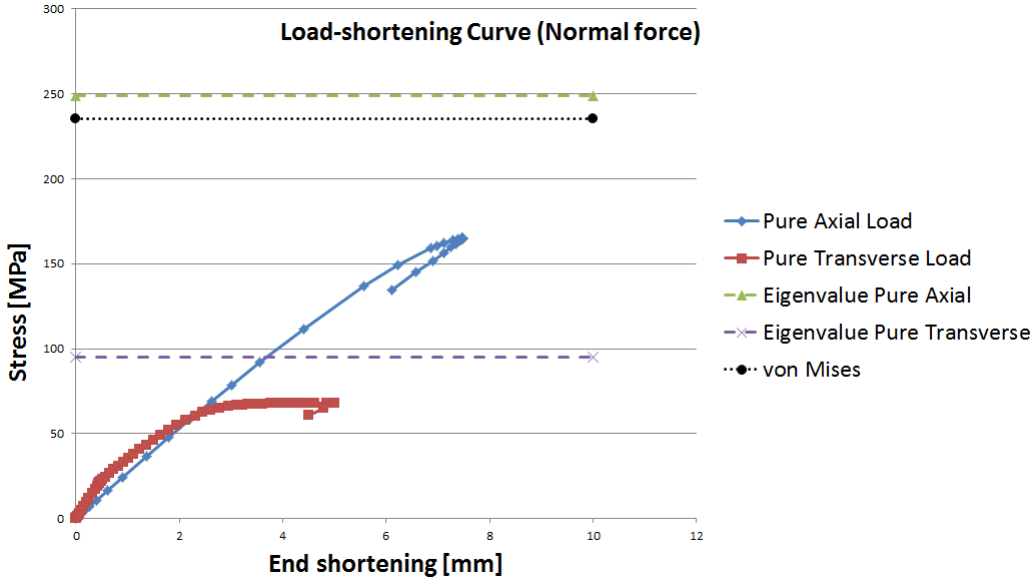

Figure 7.18: Load-shortening curve for thickness ratio of 15-10 mm.

None of these two forces seem to have any possible reserve strength and this has been the case for almost all of our investigations. This stems from the actual problem formulation where we do not have thin enough plates for this to appear. By looking into the capacity of this ratio, we can see that the same properties, as for Case B in Section 7.2.2, will appear also here, Fig. 7.19. The capacity decreases significantly when we approach more and more transverse loading by having transverse imperfection and the smaller reduction in axial loading that encounters from the higher load level than a single plate and a small reduction from an intact plate, by the large damage imperfection.

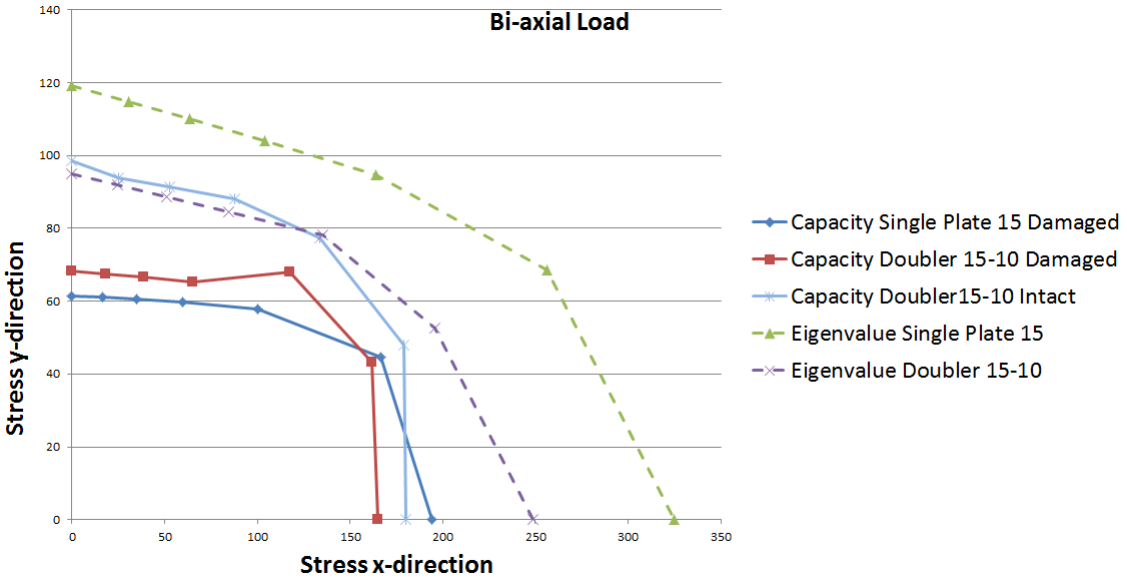

Figure 7.19: Capacity of a repaired damage model, thickness ratio of 15-10.

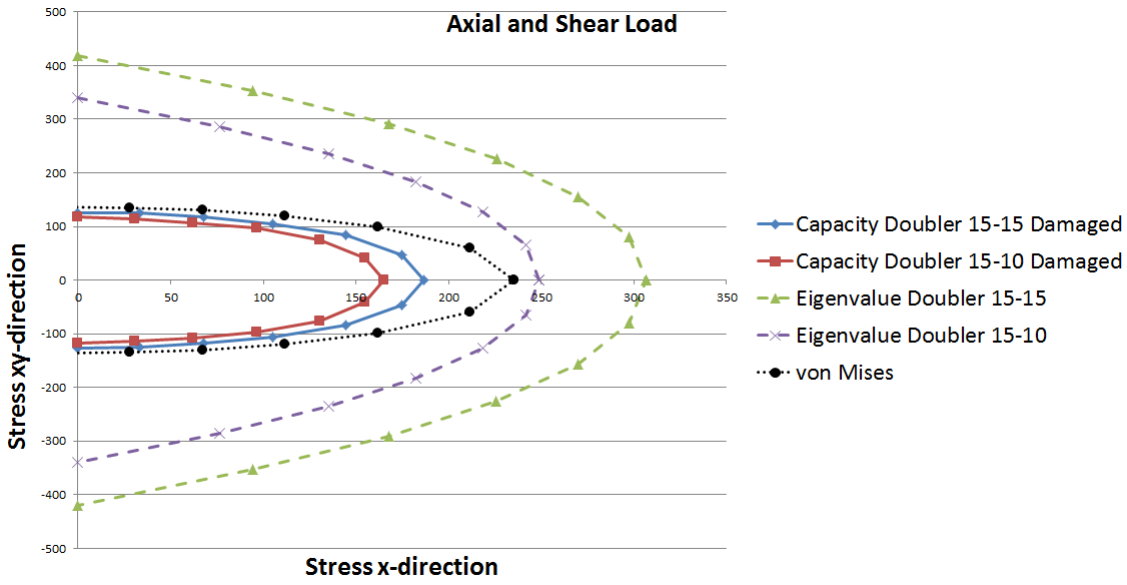

Figure 7.20: Capacity of a repaired damage model with axial and shear loading, thickness ratio of 15-10.

If we compare the axial and shear loading with the damaged model with equal thickness ratio, Fig. 7.20 we can see that the capacity in pure shear direction is not limited by the material yielding, but has a value that is just underneath. This will then as for the damaged single plate be limited only by buckling. If we compare with the last case, Section 7.2.2, the capacity is in great deal dependent on the doubler, but the capacity also drops from Case B, Fig. 7.21, where we had the same thickness in the doubler as we now have. Of this we must notice that the doubler is not alone in the design of capacity, but still we have for this ratio good contribution in making the construction stronger, with reference back to a single plate Fig. 7.19.

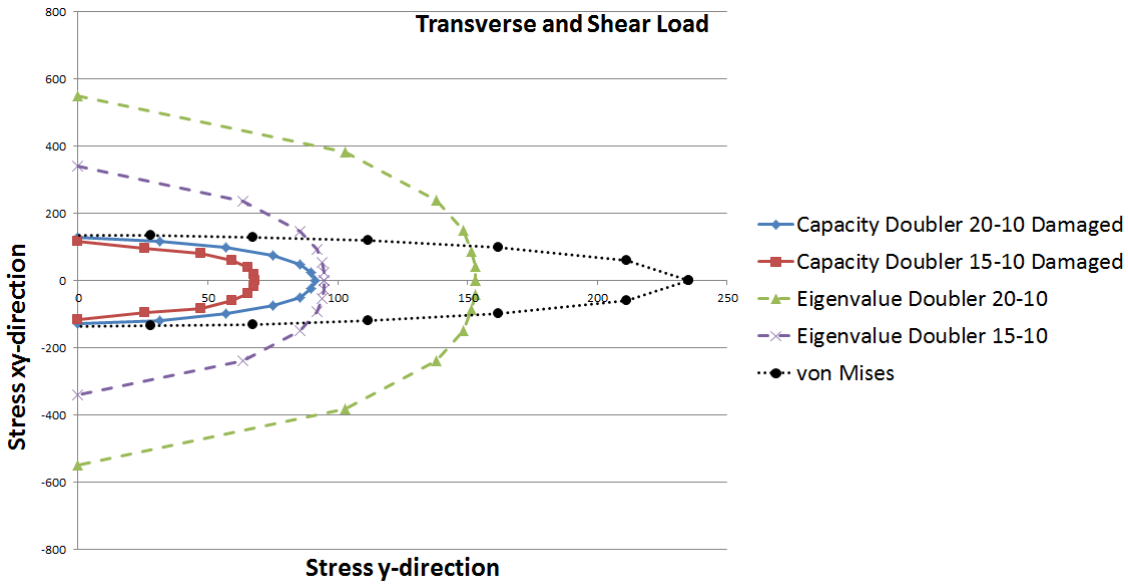

Figure 7.21: Capacity of a repaired damage model with transverse and shear loading, thickness ratio of 15-10.

7.3 Remarks

As in Chapter 6 we will compare all the different cases we have examined for a damaged plate, starting with the bi-axial loading, Fig. 7.22.

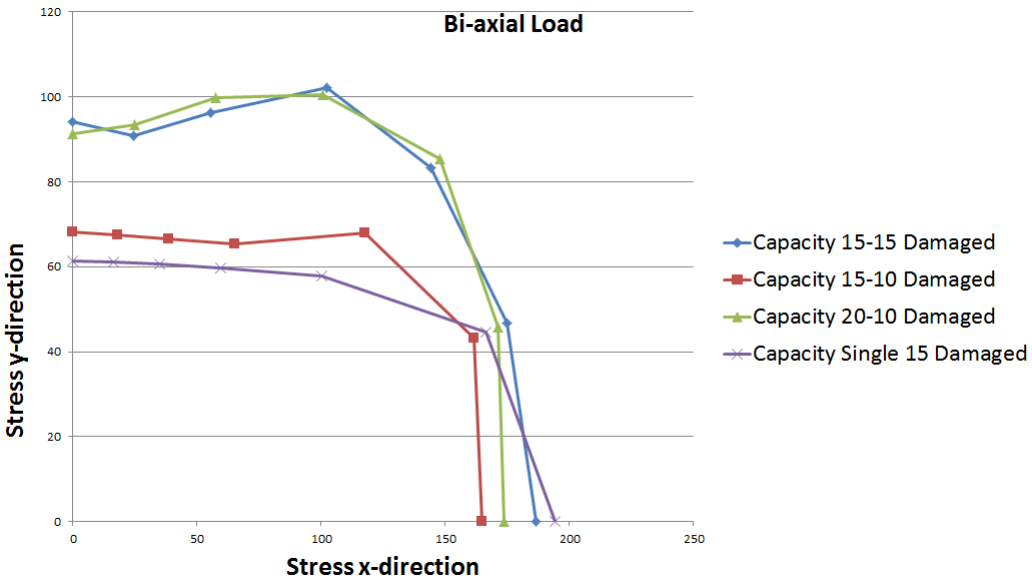

Figure 7.22: Capacity comparison of all cases in bi-axial loading.

As we also saw in the intact problem, Section 6.6, the capacity is depending on the thickness of both doubler and the damaged plate. In contrast to Chapter 6 we now, with the damage, have a system that is more depending on the doubler, naturally, and of the bi-axial loading we can see that the doubler contributes well and even more with shear load added, Fig. 7.23 and 7.24. For a single plate and Case C the capacity is determined only by the buckling limit and not by material yielding, but this encounters for shear loading when analysing the repair for Case A and B, Fig. 7.23 and 7.24.

We have mentioned the load deviation often during this thesis, but this is an important factor to have in mind when analysing these different thickness ratios. When adding a doubler to the system we also increase the area where the external loads act and we apply the load in the way of having 1 N/mm^2 over the length. This means that the load also is dependent on the thickness of the plates, when applying a magnitude. So if we then analyse once again the bi-axial loading condition, Fig. 7.22, Case A and B are having equal load added while Case C has a little lower rate. The two first cases will then be able to withstand greater loads if they had equal stress levels, but here we see that those with the largest

load contributions also have the highest capacity. These are then the two strongest systems and they have different doubler thickness. While Case B has the thinnest doubler thickness, the increase of the damaged plate thickness also plays a part in the total capacity assignment.

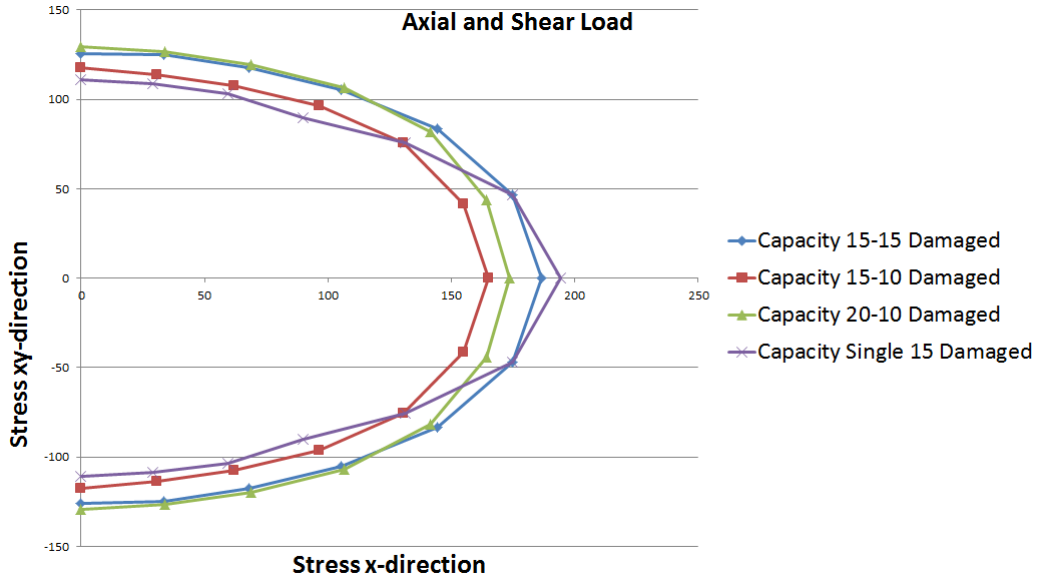

Figure 7.23: Capacity comparison of all cases in axial and shear loading.

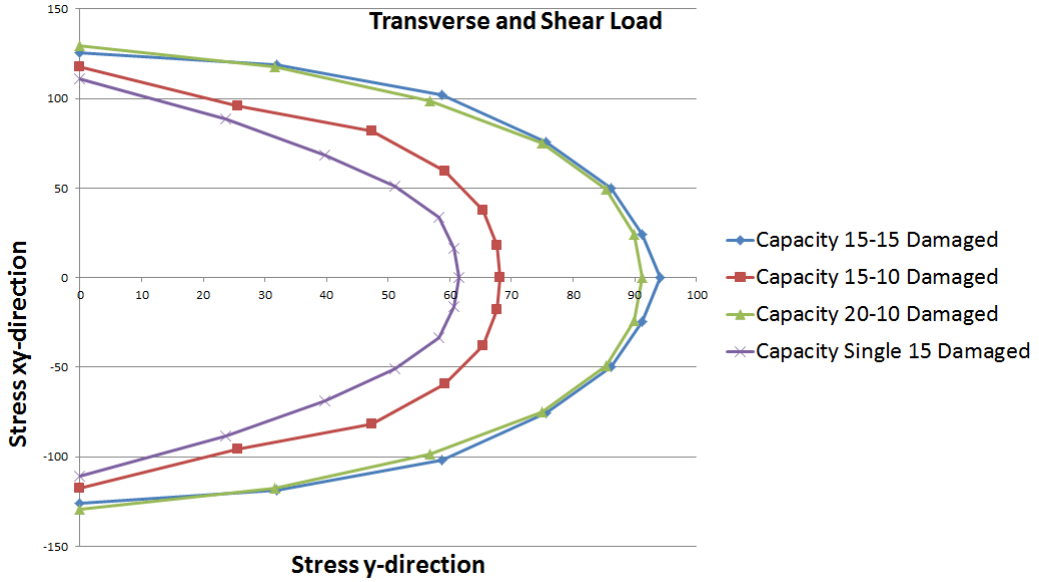

Figure 7.24: Capacity comparison of all cases in transverse and shear loading.

Chapter 8

Discussion and Conclusion

8.1 Introduction

In this thesis we have investigated the effect of repair on a damaged ship structure with doubler plate. The plate model has been analysed by selecting different thickness ratios, to see a more complete picture on how the doubler affects the system. It was chosen to focus on a particular damaged type, hungry horse. In the derivation of the problem in this thesis we have tried to arrive with a semi-analytical model, with use of the Rayleigh Ritz method, and a full finite element analysis, numerical method, with use of Abaqus. The extent of this thesis are mainly concerning the element method, by the difficulties of retrieving good approximations for two separate plates that act together in the analytical segment.

The repair of a ship hull is currently looked upon as a temporary solution, since there does not exist enough experimental material data in this field. This thesis will contribute to this, of the large computerized analysis performed during this period. The current standards of double plating repair have been used as ground rules in modelling the problem. The main results from the element analysis are the capacity of the different cases with double plate repair.

In derivation of the semi-analytical method we have chosen to use an energy approach, with use of the variational method of Rayleigh-Ritz, but also the classical thin plate theory has been reviewed. The Rayleigh-Ritz method has bases in using assumed displacement fields, variation of the principle potential energy expression and Fourier series to approximate the problem variables. These calculations and the intention of the semi-analytical method are to have a quick solution procedure of the eigenvalues/critical loads, which are often used as design

criteria of the conservative type. The result of the semi-analytical method has been implemented in a Matlab code, but can rather easily be reprogrammed into FORTRAN.

8.2 Semi-analytical method

When using the Rayleigh-Ritz method to determine the critical loads for a system we must assume a displacement field that satisfies the whole problem of interest. In our problem we have two plates that can either buckle together, in the same way, or buckle from one another. This causes trouble in selecting a displacement field. We have then instead used additional approximations and this leads to having a problem where only the double plate buckles. This is caused by the doubler to be a great deal thinner than the existing original plate with stiffeners. We then need a displacement field that only deflects in one direction.

Even if we have a displacement function that represents unidirectional deflection, the solution will have results that give deflection both ways, this is caused by the amplitude, $\mathbf{a_{ij}}$, which will both appear with positive and negative signs. This leads to "searching" for the correct results, which can be done by either make an additional Matlab script that only prints the unidirectional results or by manually find them. The method has been verified against a finite element model in Abaqus and the results are quite satisfying.

The Rayleigh-Ritz approach gives a slightly higher estimate of the eigenvalues, but this method will always overestimate the system, by underestimating the deformations and the solution converge from above, with more degrees of freedom chosen. This makes the Rayleigh-Ritz method to always be a conservative measure. Unfortunately the approximations we made earlier of the unidirectional deflection of only the doubler, is a large overestimation of the system and it makes the model act far too stiff. The eigenvalues/critical load assessments appear approximately four times higher than the real system. Even if the model itself has a quite strict application area, we have with this work a much greater understanding of the buckling properties and we have a greater theoretical background.

8.3 Capacity assessment

From having a not fully functional semi-analytical method the main focus was distributed to the capacity calculations and effects of double plate repair of a damaged ship hull. This was done by element modelling in Abaqus. The finite element method is a great tool to carry out strength and deformation calculations of all kinds of constructions. It use numerical methods and is based on approximated solutions of defined problems within advanced mathematics, which cannot be solved analytically. To be able to verify our model and calculations we started off with a stiffened single plate that could be compared to the already existing semi-analytical tool, PULS. This could further be compared to a double plate problem.

To get an understanding of the double plate contribution, we first analysed an intact/undamaged double plating problem. By reviewing different thickness of the doubler and different ratios between the two plates, we could determine the doublers strengthening capabilities. Also many different kinds of imperfections and load cases were examined. Having real imperfection and in-plane normal and shear loading interacting gave us the weakest system. These properties created a good comprehension of the effect to the doubler in a system that we used in our further work with a damaged structure. In the revision of the damaged plate repair we can see the same properties that encountered in the intact system and the doubler contribution is in much larger extent visible.

There is large increase of the capacity in the repaired damaged model from only looking at a single damaged plate. The doubler contributes especially in transverse and shear direction, on the bases of having the kind of damage we investigate, with a large out of plane deflection by few and long half-waves. From the way we analyse, with calculation of stress, capacity, it can sometimes look like we do not have any contribution of the doubler, but with adding a second plate and loading it in the same way as the original plate we increase the added load sometimes to almost the double, depending on the thickness. This makes the total problem withstanding higher pressure, even if the capacity can look equal.

In the design of the capacity we limited our analyse to only calculate for buckling problems and of this we selected the capacity to not exceed the material yielding point, which we controlled by the von Mises yield criterion. We were also eager to see if the capacity could exceed the buckling load/eigenvalue at some point. By having this property, we could decide if the system was able to have some reserve strength, be able to withstand additional load after the buckling load were reached. This is decided in the non-linear analysis, but in our problem formulation we use plates that are rather thick and reserve strength will, beside the smallest ratio, not be available.

As a final conclusion, the repair of a damaged ship hull with double plates gives a good strength contribution to the system. Important to keep in mind however is that in a repair of the damaged structure, the capacity is depending of both the thickness of the doubler as well as the damaged plate. With this large survey of the problem with major finite element analysis in hand, the experimental data of this type of repair are expanded. The results also comply with the assumptions of the shipyards, that a double plate repair of a damaged section in a ship hull have as almost as good qualities as an intact single plate and of this will be fully usable as a permanent repair.

8.4 Suggestions to further work

By reviewing the thesis it is clear that the large extent of the finite element analysis is very time consuming and a shipyard or an engineering company or even a classification society will have great benefit in having a semi-analytical tool for calculation of this problem, allowing the different users to calculate their own distinctive damaged construction part. So for suggestion of further work these items can be interesting to look at:

- Further development of the semi-analytical method for a damage plate repair calculation of both buckling load and ultimate capacity, with or without stiffeners in the original plate. By having other assumptions and a displacement field that also can handle shear forces. This can be done with use of the analytical work done here as bases and by having the large extent of finite element results as a verification tool.
- Look into ways to strengthen the stiffeners instead of the plates. By having reduced stiffeners the plate will be more able to have global buckling shapes, the stiffeners gets more out-of-plane displacement. Stiffening of these could be by improving the flanges.
- Extend both the semi-analytical and the element model to also including lateral pressures.
- Look at other boundary conditions for the doubler plate problem, free edges, like cross-ties or stringer.

Reference

[1] IACS. *No.47 Shipbuilding and Repair Quality Standard.* Technical report, IACS, Rev.6, 2012.

[2] Dinovitzer A. Traynham Y. Sensharma, P.K. *Design guidelines for doubler plate repairs of ship structures.* Final Report SCS-443, Ship Structure Committee, August 2005. Sponserd by the Ship Structure Committee. Jointly funded by its member agencies.

[3] L. Euler. *Sur la force de colonnes.* Mèm. acad. Berlin, 1759.

[4] J. Bernoulli. *Essai theorique sur les vibrations de plaques elastiques rectangularies et libers.* Nova Acta Acad Petropolit, 1789.

[5] S. Germain. *Remarques sur la nature, les bornes et l'etendue de la question des surfaces elastiques et equation general de ces surfaces.* Paris, 1826.

[6] J. L. Lagrange. *Ann Chim.* 1828.

[7] S. D. Poisson. *Memoire sur l'eequilibre et le mouvement des corps elastique.* Mem Acad Sci, 1829.

[8] C. L. M. H. Navier. *Bulletin des Sciences de la Societe Philomathique de Paris.* Paris, 1823.

[9] G. Kirchhoff. *Über das geleichgewicht und die bewegung einer elastichen scheibe.* J. Reine und Angewandte Matematic, 1850.

[10] B. G. Galerkin. *Thin Elastic Plates.* Gostrojisdat, Leningrad, 1933.

[11] Gere J. Timoshenko, S. *Theory of Plates and Shells.* New York: McGraw-Hill Book Company, 1959.

[12] Gere J. Timoshenko, S. *Theory of Elastic Stability.* New York: McGraw-Hill Book Company, 1961.

[13] I. G. Bubnov. *Theory of Structures of Ships.* St. Petersburg, 1914.

[14] H. Hencky. *Der spanngszustand in rechteckigen platten.* Z Andew Math und Mech, 1921.

[15] T. von Karman. *Festigkeitsprobleme im maschinenbau.* Encycl. der math. Wiss, 1910.

[16] K. Marguerre. *Die mittragende breite der gedruckten platte.* Luftfharts-forschung, 1937.

[17] W. Ritz. *Theorie der transversalschwingungen, einer quadratischen platte mit frein rändern.* Ann Physic, 1909.

[18] Clough R. Martin G. Topp L. Turner, M. *Stiffness and deflection analysis of complex structures.* Journal of Aeron. Sci., 1956.

[19] Østvold T. Steen, E. *Basis for a new buckling model for strength assessment of stiffened panels.* Technical report, DNV, 2000.

[20] E. Byklum. *Ultimate strength analysis of stiffened steel and aluminium panels using semi-analytical methods.* Technical report, DNV, 2002.

[21] R.D. Cook. *Concepts and applications of finite element analysis.* Wiley, 2001.

[22] L. Brubak. *Knekning av plater og skall i skipskonstruksjoner.* Cand. scient. thesis, Mechanics Division, Department of Mathematics, University of Oslo, 2003.

[23] Z.P. Bažant and L. Cedolin. *Stability of Structures: Elastic, Inelastic, Fracture and Damage Theories.* World Scientific, 2010.

[24] J. Hellesland. *Todimensjonal elastisitetsteori for tynne plater.* Compendium, Mechanics Division, Department of Mathematics, University of Oslo, Rev. nov. 2009.

[25] P.G. Bergan and T.G Syvertsen. *Knekning av søyler og rammer.* Tapir forlag, 1989.

[26] O. J. Hareide. *Analytical and semi-analytical methods for buckling and bending of steel elastomer sandwich plates.* Master thesis, Mechanics Division, Department of Mathematics, University of Oslo, 2012.

[27] Almroth B. O. Brush, D. O. *Buckling of bars, plates and shells.* McGraw-Hill, Inc., 1975.

[28] John C. Bruch Jr. *Plane stress and plane strain.* preprint (2006), available at `http://www.engineering.ucsb.edu/~hpscicom/projects/stress/introge.pdf`.

[29] T. E. Hals. *Konstruksjonsmekanikk.* Tapir forlag, 1999.

[30] J.N. Reddy. *Theory And Analysis of Elastic Plates And Shells.* Series in Systems and Control Series. CRC Press, 2007.

[31] MathWorks. *R2012b Documentation.* Technical report, 2012.

[32] Jon Kippenes. *Non-linear finite element collapse analyses of stiffened panels, Procedure description.* Technical report, Det Norske Veritas, 2009.

[33] Simulia. *Abaqus 6.11 Analysis User's Manual.* Technical report, Dassault Systemes, 2011.

Appendix A

Rayleigh-Ritz method

A.1 Integrals for developing of potential energy

$$\int_0^L sin\left(\frac{i\pi x}{L}\right) sin\left(\frac{k\pi x}{L}\right) dx = \begin{cases} \frac{L}{2} & , i = k \\ 0 & , else \end{cases} \tag{A.1.1}$$

$$\int_0^L cos\left(\frac{i\pi x}{L}\right) cos\left(\frac{k\pi x}{L}\right) dx = \begin{cases} \frac{L}{2} & , i = k \\ 0 & , else \end{cases} \tag{A.1.2}$$

$$\int_0^L sin\left(\frac{i\pi x}{L}\right) cos\left(\frac{k\pi x}{L}\right) dx = \begin{cases} 0 & , i = k \\ -\frac{Li\left(-1+(-1)^{i+k}\right)}{\pi(i^2-k^2)} & , else \end{cases} \tag{A.1.3}$$

$$\int_0^L \left(1 - cos\left(\frac{i\pi x}{L}\right)\right)\left(1 - cos\left(\frac{k\pi x}{L}\right)\right) dx = \begin{cases} \frac{3}{2}L & , i = k \\ L & , else \end{cases} \tag{A.1.4}$$

$$\int_0^L sin\left(\frac{i\pi x}{L}\right)\left(1 - cos\left(\frac{k\pi x}{L}\right)\right) dx = \begin{cases} -\frac{L\left(-1+(-1)^i\right)}{i\pi} & , i = k \\ -\frac{L\left(-k^2-(-1)^i i^2+(-1)^i k^2+(-1)^{i+k} i^2\right)}{i\pi(-i^2+k^2)} & , else \end{cases} \tag{A.1.5}$$

$$\int_0^L cos\left(\frac{i\pi x}{L}\right)\left(1 - cos\left(\frac{k\pi x}{L}\right)\right) dx = \begin{cases} -\frac{L}{2} & , i = k \\ 0 & , else \end{cases} \tag{A.1.6}$$

A.2 Calculation of strain energy

The expression for strain energy:

$$\begin{aligned} U =& \frac{D}{2}\int_0^L\int_0^s \left[\left(w_{,xx}+w_{,yy}\right)^2 - 2\left(1-\nu\right)\left(w_{,xx}w_{,yy}-w_{,xy}^2\right)\right] dydx \\ =& \frac{D}{2}\int_0^L\int_0^s \left[w_{,xx}^2 + w_{,yy}^2 + 2\nu w_{,xx}w_{,yy} + 2\left(1-\nu\right)w_{,xy}^2\right] dydx \end{aligned} \tag{A.2.1}$$

Displacement field, which will be inserted in the expression above.

$$w = \sum_{i=1}^{m}\sum_{j=1}^{n} a_{ij}\left(1-cos\left(2\frac{i\pi x}{L}\right)\right)\left(1-cos\left(2\frac{j\pi y}{s}\right)\right) \tag{A.2.2}$$

Calculation divided into separate parts:

$$w_{,xx} = \frac{\partial^2 w}{\partial x^2} = \sum_{i=1}^{m}\sum_{j=1}^{n} a_{ij}\left(2\frac{i\pi}{L}\right)^2 cos\left(2\frac{i\pi x}{L}\right)\left(1-cos\left(2\frac{j\pi y}{s}\right)\right) \tag{A.2.3}$$

$$w_{,yy} = \frac{\partial^2 w}{\partial y^2} = \sum_{i=1}^{m}\sum_{j=1}^{n} a_{ij}\left(2\frac{j\pi}{s}\right)^2 \left(1-cos\left(2\frac{i\pi x}{L}\right)\right) cos\left(2\frac{j\pi y}{s}\right) \tag{A.2.4}$$

$$w_{,xy} = \frac{\partial w}{\partial x}\frac{\partial w}{\partial y} = \sum_{i=1}^{m}\sum_{j=1}^{n} a_{ij}\left(2\frac{i\pi}{L}\right)\left(2\frac{j\pi}{s}\right) sin\left(2\frac{i\pi x}{L}\right) sin\left(2\frac{j\pi y}{s}\right) \tag{A.2.5}$$

The first part of the energy expression can be rewritten into:

$$\left(w_{,xx}+w_{,yy}\right)^2 = w_{,xx}^2 + 2w_{,xx}w_{,yy} + w_{,yy}^2 \tag{A.2.6}$$

where each parts can be calculated separately:

$$\begin{aligned} w_{,xx}^2 = \left(\frac{\partial^2 w}{\partial x^2}\right)^2 =& \sum_{i=1}^{m}\sum_{j=1}^{n} a_{ij}\left(2\frac{i\pi}{L}\right)^2 cos\left(2\frac{i\pi x}{L}\right)\left(1-cos\left(2\frac{j\pi y}{s}\right)\right) \\ & \cdot \sum_{k=1}^{p}\sum_{l=1}^{q} a_{kl}\left(2\frac{k\pi}{L}\right)^2 cos\left(2\frac{k\pi x}{L}\right)\left(1-cos\left(2\frac{l\pi y}{s}\right)\right) \end{aligned} \tag{A.2.7}$$

$$\begin{aligned} =& \sum_{i=1}^{m}\sum_{j=1}^{n}\sum_{k=1}^{p}\sum_{l=1}^{q} a_{ij}a_{kl}\left(2\frac{i\pi}{L}\right)^2\left(2\frac{k\pi}{L}\right)^2 cos\left(2\frac{i\pi x}{L}\right) cos\left(2\frac{k\pi x}{L}\right) \\ & \cdot \left(1-cos\left(2\frac{j\pi y}{s}\right)\right)\left(1-cos\left(2\frac{l\pi y}{s}\right)\right) \end{aligned} \tag{A.2.8}$$

$$w_{,yy}^2 = \left(\frac{\partial^2 w}{\partial y^2}\right)^2 = \sum_{i=1}^{m}\sum_{j=1}^{n} a_{ij}\left(2\frac{j\pi}{s}\right)^2\left(1-cos\left(2\frac{i\pi x}{L}\right)\right)cos\left(2\frac{j\pi y}{s}\right) \quad \text{(A.2.9)}$$

$$\cdot \sum_{k=1}^{p}\sum_{l=1}^{q} a_{kl}\left(2\frac{l\pi}{s}\right)^2\left(1-cos\left(2\frac{k\pi x}{L}\right)\right)cos\left(2\frac{l\pi y}{s}\right)$$

$$= \sum_{i=1}^{m}\sum_{j=1}^{n}\sum_{k=1}^{p}\sum_{l=1}^{q} a_{ij}a_{kl}\left(2\frac{j\pi}{s}\right)^2\left(2\frac{l\pi}{s}\right)^2\left(1-cos\left(2\frac{i\pi x}{L}\right)\right)\left(1-cos\left(2\frac{k\pi x}{L}\right)\right) \quad \text{(A.2.10)}$$

$$\cdot cos\left(2\frac{j\pi y}{s}\right)cos\left(2\frac{l\pi y}{s}\right)$$

$$w_{,xy}^2 = \left(\frac{\partial w}{\partial x}\frac{\partial w}{\partial y}\right)^2 = \sum_{i=1}^{m}\sum_{j=1}^{n} a_{ij}\left(2\frac{i\pi}{L}\right)\left(2\frac{j\pi}{s}\right)sin\left(2\frac{i\pi x}{L}\right)sin\left(2\frac{j\pi y}{s}\right) \quad \text{(A.2.11)}$$

$$\sum_{k=1}^{p}\sum_{l=1}^{q} a_{kl}\left(2\frac{k\pi}{L}\right)\left(2\frac{l\pi}{s}\right)sin\left(2\frac{k\pi x}{L}\right)sin\left(2\frac{l\pi y}{s}\right) \quad \text{(A.2.12)}$$

$$= \sum_{i=1}^{m}\sum_{j=1}^{n}\sum_{k=1}^{p}\sum_{l=1}^{q} a_{ij}a_{kl}\left(2\frac{i\pi}{L}\right)\left(2\frac{j\pi}{s}\right)\left(2\frac{k\pi}{L}\right)\left(2\frac{l\pi}{s}\right)$$

$$\cdot sin\left(2\frac{i\pi x}{L}\right)sin\left(2\frac{j\pi y}{s}\right)sin\left(2\frac{k\pi x}{L}\right)sin\left(2\frac{l\pi y}{s}\right)$$

$$w_{,xx}w_{,yy} = \sum_{i=1}^{m}\sum_{j=1}^{n} a_{ij}\left(2\frac{i\pi}{L}\right)^2 cos\left(2\frac{i\pi x}{L}\right)\left(1-cos\left(2\frac{j\pi y}{s}\right)\right) \quad \text{(A.2.13)}$$

$$\sum_{k=1}^{p}\sum_{l=1}^{q} a_{kl}\left(2\frac{l\pi}{s}\right)^2\left(1-cos\left(2\frac{k\pi x}{L}\right)\right)cos\left(2\frac{l\pi y}{s}\right)$$

$$= \sum_{i=1}^{m}\sum_{j=1}^{n}\sum_{k=1}^{p}\sum_{l=1}^{q} a_{ij}a_{kl}\left(2\frac{i\pi}{L}\right)^2\left(2\frac{l\pi}{s}\right)^2 cos\left(2\frac{i\pi x}{L}\right)\left(1-cos\left(2\frac{k\pi x}{L}\right)\right) \quad \text{(A.2.14)}$$

$$\cdot \left(1-cos\left(2\frac{j\pi y}{s}\right)\right)cos\left(2\frac{l\pi y}{s}\right)$$

A.2.1 Integrations

$$\int_0^L \int_0^s w_{,xx}^2 dydx = \sum_{i=1}^{m}\sum_{j=1}^{n}\sum_{k=1}^{p}\sum_{l=1}^{q} \int_0^L \int_0^s w_{,xx}^2 dydx \tag{A.2.15}$$

$$= \sum_{i=1}^{m}\sum_{j=1}^{n}\sum_{k=1}^{p}\sum_{l=1}^{q} \int_0^L \int_0^s a_{ij}a_{kl} \left(2\frac{i\pi}{L}\right)^2 \left(2\frac{k\pi}{L}\right)^2 cos\left(2\frac{i\pi x}{L}\right) cos\left(2\frac{k\pi x}{L}\right) \left(1 - cos\left(2\frac{j\pi y}{s}\right)\right)\left(1 - cos\left(2\frac{l\pi y}{s}\right)\right) dydx$$

If $i = k$ and $j = l$

$$\sum_{i=1}^{m}\sum_{j=1}^{n}\sum_{k=1}^{p}\sum_{l=1}^{q} a_{ij}a_{kl} \left(2\frac{i\pi}{L}\right)^2 \left(2\frac{k\pi}{L}\right)^2 \cdot \frac{L}{2} \cdot \frac{3\cdot s}{2}\delta_{ik}\delta_{jl} \tag{A.2.16}$$

If $i = k$ and $j \neq l$

$$\sum_{i=1}^{m}\sum_{j=1}^{n}\sum_{k=1}^{p}\sum_{l=1}^{q} a_{ij}a_{kl} \left(2\frac{i\pi}{L}\right)^2 \left(2\frac{k\pi}{L}\right)^2 \cdot \frac{L\cdot s}{2}\delta_{ik}I_{jl} \tag{A.2.17}$$

If $i \neq k$ and $j = l$

$$\sum_{i=1}^{m}\sum_{j=1}^{n}\sum_{k=1}^{p}\sum_{l=1}^{q} a_{ij}a_{kl} \left(2\frac{i\pi}{L}\right)^2 \left(2\frac{k\pi}{L}\right)^2 \cdot 0 \cdot \frac{3\cdot s}{2}I_{ik}\delta_{jl} = 0 \tag{A.2.18}$$

If $i \neq k$ and $j \neq l$

$$\sum_{i=1}^{m}\sum_{j=1}^{n}\sum_{k=1}^{p}\sum_{l=1}^{q} a_{ij}a_{kl} \left(2\frac{i\pi}{L}\right)^2 \left(2\frac{k\pi}{L}\right)^2 \cdot 0 \cdot sI_{ik}I_{jl} = 0 \tag{A.2.19}$$

This gives the total expression for this integration as:

$$\Rightarrow \sum_{i=1}^{m}\sum_{j=1}^{n}\sum_{k=1}^{p}\sum_{l=1}^{q} a_{ij}a_{kl} \left(2\frac{i\pi}{L}\right)^2 \left(2\frac{k\pi}{L}\right)^2 \frac{3}{4}L\cdot s\delta_{ik}\delta_{jl} + \sum_{i=1}^{m}\sum_{j=1}^{n}\sum_{k=1}^{p}\sum_{l=1}^{q} a_{ij}a_{kl} \left(2\frac{i\pi}{L}\right)^2 \left(2\frac{k\pi}{L}\right)^2 \cdot \frac{Ls}{2}\delta_{ik}I_{jl} \tag{A.2.20}$$

$$\int_0^L \int_0^s w_{,yy}^2 dydx = \sum_{i=1}^{m}\sum_{j=1}^{n}\sum_{k=1}^{p}\sum_{l=1}^{q} \int_0^L \int_0^s w_{,yy}^2 dydx \tag{A.2.21}$$

$$= \sum_{i=1}^{m}\sum_{j=1}^{n}\sum_{k=1}^{p}\sum_{l=1}^{q} \int_0^L \int_0^s a_{ij}a_{kl} \left(2\frac{j\pi}{s}\right)^2 \left(2\frac{l\pi}{s}\right)^2 \left(1 - cos\left(2\frac{i\pi x}{L}\right)\right)\left(1 - cos\left(2\frac{k\pi x}{L}\right)\right) cos\left(2\frac{j\pi y}{s}\right) cos\left(2\frac{l\pi y}{s}\right) dydx$$

If $i = k$ and $j = l$

$$\sum_{i=1}^{m}\sum_{j=1}^{n}\sum_{k=1}^{p}\sum_{l=1}^{q} a_{ij}a_{kl}\left(2\frac{j\pi}{s}\right)^2\left(2\frac{l\pi}{s}\right)^2\cdot\frac{3L}{2}\cdot\frac{s}{2}\delta_{ik}\delta_{jl} \tag{A.2.22}$$

If $i = k$ and $j \neq l$

$$\sum_{i=1}^{m}\sum_{j=1}^{n}\sum_{k=1}^{p}\sum_{l=1}^{q} a_{ij}a_{kl}\left(2\frac{j\pi}{s}\right)^2\left(2\frac{l\pi}{s}\right)^2\cdot\frac{3L}{2}\cdot 0\delta_{ik}I_{jl} = 0 \tag{A.2.23}$$

If $i \neq k$ and $j = l$

$$\sum_{i=1}^{m}\sum_{j=1}^{n}\sum_{k=1}^{p}\sum_{l=1}^{q} a_{ij}a_{kl}\left(2\frac{j\pi}{s}\right)^2\left(2\frac{l\pi}{s}\right)^2\cdot L\cdot\frac{s}{2}I_{ik}\delta_{jl} \tag{A.2.24}$$

If $i \neq k$ and $j \neq l$

$$\sum_{i=1}^{m}\sum_{j=1}^{n}\sum_{k=1}^{p}\sum_{l=1}^{q} a_{ij}a_{kl}\left(2\frac{j\pi}{s}\right)^2\left(2\frac{l\pi}{s}\right)^2\cdot L\cdot 0 I_{ik}I_{jl} = 0 \tag{A.2.25}$$

This gives the total expression for this integration as:

$$\begin{aligned}\Rightarrow&\sum_{i=1}^{m}\sum_{j=1}^{n}\sum_{k=1}^{p}\sum_{l=1}^{q} a_{ij}a_{kl}\left(2\frac{j\pi}{s}\right)^2\left(2\frac{l\pi}{s}\right)^2\cdot\frac{3}{2}L\cdot\frac{s}{2}\delta_{ik}\delta_{jl}\\ &+\sum_{i=1}^{m}\sum_{j=1}^{n}\sum_{k=1}^{p}\sum_{l=1}^{q} a_{ij}a_{kl}\left(2\frac{j\pi}{s}\right)^2\left(2\frac{l\pi}{s}\right)^2\cdot L\cdot\frac{s}{2}I_{ik}\delta_{jl}\end{aligned} \tag{A.2.26}$$

$$\begin{aligned}&\int_0^L\int_0^s w_{,xx}w_{,yy}dydx\\ =&\sum_{i=1}^{m}\sum_{j=1}^{n}\sum_{k=1}^{p}\sum_{l=1}^{q}\int_0^L\int_0^s a_{ij}a_{kl}\left(2\frac{i\pi}{L}\right)^2\left(2\frac{l\pi}{s}\right)^2\\ &cos\left(2\frac{i\pi x}{L}\right)\left(1-cos\left(2\frac{k\pi x}{L}\right)\right)\left(1-cos\left(2\frac{j\pi y}{s}\right)\right)cos\left(2\frac{l\pi y}{s}\right)dydx\end{aligned} \tag{A.2.27}$$

If $i = k$ and $j = l$

$$\sum_{i=1}^{m}\sum_{j=1}^{n}\sum_{k=1}^{p}\sum_{l=1}^{q} a_{ij}a_{kl}\left(2\frac{i\pi}{L}\right)^2\left(2\frac{l\pi}{s}\right)^2\cdot\left(-\frac{L}{2}\right)\cdot\left(-\frac{s}{2}\right)\delta_{ik}\delta_{jl} \tag{A.2.28}$$

If $i = k$ and $j \neq l$

$$\sum_{i=1}^{m}\sum_{j=1}^{n}\sum_{k=1}^{p}\sum_{l=1}^{q} a_{ij}a_{kl}\left(2\frac{i\pi}{L}\right)^2\left(2\frac{l\pi}{s}\right)^2\cdot\left(-\frac{L}{2}\right)\cdot 0\delta_{ik}I_{jl} = 0 \tag{A.2.29}$$

If $i \neq k$ and $j = l$

$$\sum_{i=1}^{m}\sum_{j=1}^{n}\sum_{k=1}^{p}\sum_{l=1}^{q} a_{ij}a_{kl}\left(2\frac{i\pi}{L}\right)^2\left(2\frac{l\pi}{s}\right)^2\cdot 0\cdot\left(-\frac{s}{2}\right)I_{ik}\delta_{jl} = 0 \tag{A.2.30}$$

If $i \neq k$ and $j \neq l$

$$\sum_{i=1}^{m}\sum_{j=1}^{n}\sum_{k=1}^{p}\sum_{l=1}^{q} a_{ij}a_{kl}\left(2\frac{i\pi}{L}\right)^2\left(2\frac{l\pi}{s}\right)^2\cdot 0\cdot 0 I_{ik}I_{jl} = 0 \tag{A.2.31}$$

This gives the total expression for this integration as:

$$\Rightarrow \sum_{i=1}^{m}\sum_{j=1}^{n}\sum_{k=1}^{p}\sum_{l=1}^{q} a_{ij}a_{kl}\left(2\frac{i\pi}{L}\right)^2\left(2\frac{l\pi}{s}\right)^2\cdot\frac{L}{2}\cdot\frac{s}{2}\delta_{ik}\delta_{jl} \tag{A.2.32}$$

$$\int_0^L\int_0^s w_{,xy}^2 dydx \tag{A.2.33}$$
$$= \sum_{i=1}^{m}\sum_{j=1}^{n}\sum_{k=1}^{p}\sum_{l=1}^{q}\int_0^L\int_0^s a_{ij}a_{kl}\left(2\frac{i\pi}{L}\right)\left(2\frac{j\pi}{s}\right)\left(2\frac{k\pi}{L}\right)\left(2\frac{l\pi}{s}\right)$$
$$sin\left(2\frac{i\pi x}{L}\right)sin\left(2\frac{j\pi y}{s}\right)sin\left(2\frac{k\pi x}{L}\right)sin\left(2\frac{l\pi y}{s}\right)dydx$$

If $i = k$ and $j = l$

$$\sum_{i=1}^{m}\sum_{j=1}^{n}\sum_{k=1}^{p}\sum_{l=1}^{q} a_{ij}a_{kl}\left(2\frac{i\pi}{L}\right)\left(2\frac{j\pi}{s}\right)\left(2\frac{k\pi}{L}\right)\left(2\frac{l\pi}{s}\right)\cdot\left(\frac{L}{2}\right)\cdot\left(\frac{s}{2}\right)\delta_{ik}\delta_{jl} \tag{A.2.34}$$

If $i = k$ and $j \neq l$

$$\sum_{i=1}^{m}\sum_{j=1}^{n}\sum_{k=1}^{p}\sum_{l=1}^{q} a_{ij}a_{kl}\left(2\frac{i\pi}{L}\right)\left(2\frac{j\pi}{s}\right)\left(2\frac{k\pi}{L}\right)\left(2\frac{l\pi}{s}\right)\cdot\left(\frac{L}{2}\right)\cdot 0\delta_{ik}I_{jl} = 0 \tag{A.2.35}$$

If $i \neq k$ and $j = l$

$$\sum_{i=1}^{m}\sum_{j=1}^{n}\sum_{k=1}^{p}\sum_{l=1}^{q} a_{ij}a_{kl}\left(2\frac{i\pi}{L}\right)\left(2\frac{k\pi}{L}\right)\left(2\frac{j\pi}{s}\right)\left(2\frac{l\pi}{s}\right)\cdot 0\cdot\left(\frac{s}{2}\right)I_{ik}\delta_{jl} = 0 \tag{A.2.36}$$

If $i \neq k$ and $j \neq l$

$$\sum_{i=1}^{m}\sum_{j=1}^{n}\sum_{k=1}^{p}\sum_{l=1}^{q} a_{ij}a_{kl}\left(2\frac{i\pi}{L}\right)\left(2\frac{k\pi}{L}\right)\left(2\frac{j\pi}{s}\right)\left(2\frac{l\pi}{s}\right)\cdot 0\cdot 0 I_{ik}I_{jl} = 0 \tag{A.2.37}$$

This gives the total expression for this integration as:

$$\Rightarrow \sum_{i=1}^{m}\sum_{j=1}^{n}\sum_{k=1}^{p}\sum_{l=1}^{q} a_{ij}a_{kl}\left(2\frac{i\pi}{L}\right)\left(2\frac{k\pi}{L}\right)\left(2\frac{j\pi}{s}\right)\left(2\frac{l\pi}{s}\right)\cdot\left(\frac{L}{2}\right)\cdot\left(\frac{s}{2}\right)\delta_{ik}\delta_{jl} \tag{A.2.38}$$

All of these expressions is then inserted into the strain energy equation at the top of this appendix.

$$\begin{aligned}
U = \frac{D}{2}\Bigg[& \sum_{i=1}^{m}\sum_{j=1}^{n}\sum_{k=1}^{p}\sum_{l=1}^{q} a_{ij}a_{kl}\left(2\frac{i\pi}{L}\right)^2\left(2\frac{k\pi}{L}\right)^2\cdot\frac{3}{4}\cdot L\cdot s\delta_{ik}\delta_{jl} \\
& + \sum_{i=1}^{m}\sum_{j=1}^{n}\sum_{k=1}^{p}\sum_{l=1}^{q} a_{ij}a_{kl}\left(2\frac{i\pi}{L}\right)^2\left(2\frac{k\pi}{L}\right)^2\cdot\frac{L\cdot s}{2}\delta_{ik}I_{jl} \\
& + \sum_{i=1}^{m}\sum_{j=1}^{n}\sum_{k=1}^{p}\sum_{l=1}^{q} a_{ij}a_{kl}\left(2\frac{j\pi}{s}\right)^2\left(2\frac{l\pi}{s}\right)^2\cdot\frac{3L}{2}\cdot\frac{s}{2}\delta_{ik}\delta_{jl} \\
& + \sum_{i=1}^{m}\sum_{j=1}^{n}\sum_{k=1}^{p}\sum_{l=1}^{q} a_{ij}a_{kl}\left(2\frac{j\pi}{s}\right)^2\left(2\frac{l\pi}{s}\right)^2\cdot L\cdot\frac{s}{2}I_{ik}\delta_{jl} \\
& + 2\nu\sum_{i=1}^{m}\sum_{j=1}^{n}\sum_{k=1}^{p}\sum_{l=1}^{q} a_{ij}a_{kl}\left(2\frac{i\pi}{L}\right)^2\left(2\frac{l\pi}{s}\right)^2\cdot\frac{L\cdot s}{4}\delta_{ik}\delta_{jl} \\
& + 2(1-\nu)\sum_{i=1}^{m}\sum_{j=1}^{n}\sum_{k=1}^{p}\sum_{l=1}^{q} a_{ij}a_{kl}\left(2\frac{i\pi}{L}\right)\left(2\frac{k\pi}{L}\right)\left(2\frac{j\pi}{s}\right)\left(2\frac{l\pi}{s}\right)\cdot\frac{L\cdot s}{4}\delta_{ik}\delta_{jl}\Bigg]
\end{aligned} \tag{A.2.39}$$

A.3 Calculation of load potential

The expression for load potential is written as:

$$H = -\frac{t}{2}\int_0^L \int_0^s \left(S_x w_{,x}^2 + 2S_{xy} w_{,x} w_{,y} + S_y w_{,y}^2\right) dydx \tag{A.3.1}$$

However can we neglect the shear contribution since a displacement field consisting of only cosine terms not will give a asymmetrical pattern shear forces will create.

Displacement field are still

$$w = \sum_{i=1}^{m}\sum_{j=1}^{n} a_{ij}\left(1 - cos\left(2\frac{i\pi x}{L}\right)\right)\left(1 - cos\left(2\frac{j\pi y}{s}\right)\right) \tag{A.3.2}$$

Calculation divided into separate parts:

$$w_{,x} = \frac{\partial w}{\partial x}\sum_{i=1}^{m}\sum_{j=1}^{n} a_{ij}\left(2\frac{i\pi}{L}\right) sin\left(2\frac{i\pi x}{L}\right)\left(1 - cos\left(2\frac{j\pi y}{s}\right)\right) \tag{A.3.3}$$

$$w_{,y} = \frac{\partial w}{\partial y}\sum_{i=1}^{m}\sum_{j=1}^{n} a_{ij}\left(2\frac{j\pi}{s}\right)\left(1 - cos\left(2\frac{i\pi x}{L}\right)\right) sin\left(2\frac{j\pi y}{s}\right) \tag{A.3.4}$$

Displacement field inserted in each part of the equation:

$$\begin{aligned} w_{,x}^2 = \left(\frac{\partial w}{\partial x}^2\right) =& \sum_{i=1}^{m}\sum_{j=1}^{n} a_{ij}\left(2\frac{i\pi}{L}\right) sin\left(2\frac{i\pi x}{L}\right)\left(1 - cos\left(2\frac{j\pi y}{s}\right)\right) \\ & \sum_{k=1}^{p}\sum_{l=1}^{q} a_{kl}\left(2\frac{k\pi}{L}\right) sin\left(2\frac{k\pi x}{L}\right)\left(1 - cos\left(2\frac{l\pi y}{s}\right)\right) \\ =& \sum_{i=1}^{m}\sum_{j=1}^{n}\sum_{k=1}^{p}\sum_{l=1}^{q} a_{ij}a_{kl}\left(2\frac{i\pi}{L}\right)\left(2\frac{k\pi}{L}\right) sin\left(2\frac{i\pi x}{L}\right) sin\left(2\frac{k\pi x}{L}\right) \\ & \left(1 - cos\left(2\frac{j\pi y}{s}\right)\right)\left(1 - cos\left(2\frac{l\pi y}{s}\right)\right) \end{aligned} \tag{A.3.5}$$

$$w_{,y}^2 = \left(\frac{\partial w}{\partial y}^2\right) = \sum_{i=1}^{m}\sum_{j=1}^{n} a_{ij}\left(2\frac{j\pi}{s}\right)\left(1-cos\left(2\frac{i\pi x}{L}\right)\right) sin\left(2\frac{j\pi y}{s}\right) \quad (A.3.6)$$
$$\sum_{k=1}^{p}\sum_{l=1}^{q} a_{kl}\left(2\frac{l\pi}{s}\right)\left(1-cos\left(2\frac{k\pi x}{L}\right)\right) sin\left(2\frac{l\pi y}{s}\right)$$
$$= \sum_{i=1}^{m}\sum_{j=1}^{n}\sum_{k=1}^{p}\sum_{l=1}^{q} a_{ij}a_{kl}\left(2\frac{j\pi}{s}\right)\left(2\frac{l\pi}{s}\right)\left(1-cos\left(2\frac{i\pi x}{L}\right)\right)$$
$$\left(1-cos\left(2\frac{k\pi x}{L}\right)\right) sin\left(2\frac{j\pi y}{s}\right) sin\left(2\frac{l\pi y}{s}\right)$$

A.3.1 Integration

$$\int_0^L\int_0^s w_{,x}^2 dydx = \sum_{i=1}^{m}\sum_{j=1}^{n}\sum_{k=1}^{p}\sum_{l=1}^{q}\int_0^L\int_0^s w_{,x}^2 dydx \quad (A.3.7)$$
$$= \sum_{i=1}^{m}\sum_{j=1}^{n}\sum_{k=1}^{p}\sum_{l=1}^{q}\int_0^L\int_0^s a_{ij}a_{kl}\left(2\frac{i\pi}{L}\right)\left(2\frac{k\pi}{L}\right) sin\left(2\frac{i\pi x}{L}\right) sin\left(2\frac{k\pi x}{L}\right)$$
$$\left(1-cos\left(2\frac{j\pi y}{s}\right)\right)\left(1-cos\left(2\frac{l\pi y}{s}\right)\right) dydx$$

If $i = k$ and $j = l$

$$\sum_{i=1}^{m}\sum_{j=1}^{n}\sum_{k=1}^{p}\sum_{l=1}^{q} a_{ij}a_{kl}\left(2\frac{i\pi}{L}\right)\left(2\frac{k\pi}{L}\right)\cdot\frac{L}{2}\cdot\frac{3s}{2}\delta_{ik}\delta_{jl} \quad (A.3.8)$$

If $i = k$ and $j \neq l$

$$\sum_{i=1}^{m}\sum_{j=1}^{n}\sum_{k=1}^{p}\sum_{l=1}^{q} a_{ij}a_{kl}\left(2\frac{i\pi}{L}\right)\left(2\frac{k\pi}{L}\right)\cdot\frac{L}{2}\cdot s\delta_{ik}I_{jl} \quad (A.3.9)$$

If $i \neq k$ and $j = l$

$$\sum_{i=1}^{m}\sum_{j=1}^{n}\sum_{k=1}^{p}\sum_{l=1}^{q} a_{ij}a_{kl}\left(2\frac{i\pi}{L}\right)\left(2\frac{k\pi}{L}\right)\cdot 0\cdot\frac{3s}{2}I_{ik}\delta_{jl} = 0 \quad (A.3.10)$$

If $i \neq k$ and $j \neq l$

$$\sum_{i=1}^{m}\sum_{j=1}^{n}\sum_{k=1}^{p}\sum_{l=1}^{q} a_{ij}a_{kl}\left(2\frac{i\pi}{L}\right)\left(2\frac{k\pi}{L}\right)\cdot 0\cdot s)I_{ik}I_{jl} = 0 \quad (A.3.11)$$

This gives the total expression for this integration as:

$$\Rightarrow \sum_{i=1}^{m}\sum_{j=1}^{n}\sum_{k=1}^{p}\sum_{l=1}^{q} a_{ij}a_{kl}\left(2\frac{i\pi}{L}\right)\left(2\frac{k\pi}{L}\right)\cdot\frac{L}{2}\cdot\frac{3s}{2}\delta_{ik}\delta_{jl}+ \tag{A.3.12}$$
$$\sum_{i=1}^{m}\sum_{j=1}^{n}\sum_{k=1}^{p}\sum_{l=1}^{q} a_{ij}a_{kl}\left(2\frac{i\pi}{L}\right)\left(2\frac{k\pi}{L}\right)\cdot\frac{L}{2}\cdot s\delta_{ik}I_{jl}$$

$$\int_0^L\int_0^s w_{,y}^2 dydx = \sum_{i=1}^{m}\sum_{j=1}^{n}\sum_{k=1}^{p}\sum_{l=1}^{q}\int_0^L\int_0^s w_{,y}^2 dydx \tag{A.3.13}$$
$$= \sum_{i=1}^{m}\sum_{j=1}^{n}\sum_{k=1}^{p}\sum_{l=1}^{q}\int_0^L\int_0^s a_{ij}a_{kl}\left(2\frac{j\pi}{s}\right)\left(2\frac{l\pi}{s}\right)$$
$$\left(1-cos\left(2\frac{i\pi x}{L}\right)\right)\left(1-cos\left(2\frac{k\pi x}{L}\right)\right)sin\left(2\frac{j\pi y}{s}\right)sin\left(2\frac{l\pi y}{s}\right)dydx$$

If $i = k$ and $j = l$

$$\sum_{i=1}^{m}\sum_{j=1}^{n}\sum_{k=1}^{p}\sum_{l=1}^{q} a_{ij}a_{kl}\left(2\frac{j\pi}{s}\right)\left(2\frac{l\pi}{s}\right)\cdot\frac{3L}{2}\cdot\frac{s}{2}\delta_{ik}\delta_{jl} \tag{A.3.14}$$

If $i = k$ and $j \neq l$

$$\sum_{i=1}^{m}\sum_{j=1}^{n}\sum_{k=1}^{p}\sum_{l=1}^{q} a_{ij}a_{kl}\left(2\frac{j\pi}{s}\right)\left(2\frac{l\pi}{s}\right)\cdot\frac{3L}{2}\cdot 0\delta_{ik}I_{jl} = 0 \tag{A.3.15}$$

If $i \neq k$ and $j = l$

$$\sum_{i=1}^{m}\sum_{j=1}^{n}\sum_{k=1}^{p}\sum_{l=1}^{q} a_{ij}a_{kl}\left(2\frac{j\pi}{s}\right)\left(2\frac{l\pi}{s}\right)\cdot L\cdot\frac{s}{2}I_{ik}\delta_{jl} \tag{A.3.16}$$

If $i \neq k$ and $j \neq l$

$$\sum_{i=1}^{m}\sum_{j=1}^{n}\sum_{k=1}^{p}\sum_{l=1}^{q} a_{ij}a_{kl}\left(2\frac{j\pi}{s}\right)\left(2\frac{l\pi}{s}\right)\cdot L\cdot 0 I_{ik}I_{jl} = 0 \tag{A.3.17}$$

$$\Rightarrow \sum_{i=1}^{m}\sum_{j=1}^{n}\sum_{k=1}^{p}\sum_{l=1}^{q} a_{ij}a_{kl}\left(2\frac{j\pi}{s}\right)\left(2\frac{l\pi}{s}\right)\cdot\frac{3L}{2}\cdot\frac{s}{2}\delta_{ik}\delta_{jl} \tag{A.3.18}$$
$$+\sum_{i=1}^{m}\sum_{j=1}^{n}\sum_{k=1}^{p}\sum_{l=1}^{q} a_{ij}a_{kl}\left(2\frac{j\pi}{s}\right)\left(2\frac{l\pi}{s}\right)\cdot L\cdot\frac{s}{2}I_{ik}\delta_{jl}$$

All of these expressions is then inserted into the load potential equation at the top of this appendix.

$$
\begin{aligned}
H = -\frac{t}{2}\Bigg[& S_x \left(\sum_{i=1}^{m}\sum_{j=1}^{n}\sum_{k=1}^{p}\sum_{l=1}^{q} a_{ij}a_{kl} \left(2\frac{i\pi}{L}\right)\left(2\frac{k\pi}{L}\right)\cdot\frac{L}{2}\cdot\frac{3s}{2}\delta_{ik}\delta_{jl} \right. \\
& \left. + \sum_{i=1}^{m}\sum_{j=1}^{n}\sum_{k=1}^{p}\sum_{l=1}^{q} a_{ij}a_{kl} \left(2\frac{i\pi}{L}\right)\left(2\frac{k\pi}{L}\right)\cdot\frac{L}{2}\cdot s\delta_{ik}I_{jl} \right) \\
& + S_y \left(\sum_{i=1}^{m}\sum_{j=1}^{n}\sum_{k=1}^{p}\sum_{l=1}^{q} a_{ij}a_{kl} \left(2\frac{j\pi}{s}\right)\left(2\frac{l\pi}{s}\right)\cdot\frac{3L}{2}\cdot\frac{s}{2}\delta_{ik}\delta_{jl} \right. \\
& \left. + \sum_{i=1}^{m}\sum_{j=1}^{n}\sum_{k=1}^{p}\sum_{l=1}^{q} a_{ij}a_{kl} \left(2\frac{j\pi}{s}\right)\left(2\frac{l\pi}{s}\right)\cdot L\cdot\frac{s}{2}I_{ik}\delta_{jl} \right) \Bigg]
\end{aligned}
\tag{A.3.19}
$$

A.4 Differentiating the strain energy

$$
\mathbf{K}^{M}_{pqrt} = \begin{bmatrix} \frac{\partial^2 U}{\partial a_{11}\partial a_{11}} & \cdots & \frac{\partial^2 U}{\partial a_{11}\partial a_{mn}} \\ \vdots & & \vdots \\ \frac{\partial^2 U}{\partial a_{mn}\partial a_{11}} & \cdots & \frac{\partial^2 U}{\partial a_{mn}\partial a_{mn}} \end{bmatrix}
\tag{A.4.1}
$$

We divide the total expression, form Appendix A2, for U into six separate parts and calculate them one by one.

$$
\begin{aligned}
& \frac{\partial^2}{\partial a_{pq}\partial a_{rt}} \left[\frac{D}{2} \sum_{i=1}^{m}\sum_{j=1}^{n}\sum_{k=1}^{p}\sum_{l=1}^{q} a_{ij}a_{kl} \left(2\frac{i\pi}{L}\right)^2 \left(2\frac{k\pi}{L}\right)^2 \cdot\frac{3}{4}\cdot L\cdot s\delta_{ik}\delta_{jl} \right] \\
= & \frac{\partial}{\partial a_{pq}} \frac{D}{2} \left[\sum_{k=1}^{p}\sum_{l=1}^{q} a_{kl} \left(2\frac{r\pi}{L}\right)^2 \left(2\frac{k\pi}{L}\right)^2 \cdot\frac{3}{4}\cdot L\cdot s\delta_{rk}\delta_{tl} \right. \\
& \left. + \sum_{i=1}^{m}\sum_{j=1}^{n} a_{ij} \left(2\frac{i\pi}{L}\right)^2 \left(2\frac{r\pi}{L}\right)^2 \cdot\frac{3}{4}\cdot L\cdot s\delta_{ir}\delta_{jt} \right] \\
= & \frac{D}{2} \left[\left(2\frac{r\pi}{L}\right)^2 \left(2\frac{p\pi}{L}\right)^2 \cdot\frac{3}{4}\cdot L\cdot s\delta_{rp}\delta_{tq} + \left(2\frac{p\pi}{L}\right)^2 \left(2\frac{r\pi}{L}\right)^2 \cdot\frac{3}{4}\cdot L\cdot s\delta_{pr}\delta_{qt} \right]
\end{aligned}
\tag{A.4.2}
$$

$$\frac{\partial^2}{\partial a_{pq}\partial a_{rt}}\left[\frac{D}{2}\sum_{i=1}^{m}\sum_{j=1}^{n}\sum_{k=1}^{p}\sum_{l=1}^{q}a_{ij}a_{kl}\left(2\frac{i\pi}{L}\right)^2\left(2\frac{k\pi}{L}\right)^2\cdot\frac{L\cdot s}{2}\delta_{ik}I_{jl}\right] \tag{A.4.3}$$

$$\begin{aligned}
=&\frac{\partial}{\partial a_{pq}}\frac{D}{2}\left[\sum_{k=1}^{p}\sum_{l=1}^{q}a_{kl}\left(2\frac{r\pi}{L}\right)^2\left(2\frac{k\pi}{L}\right)^2\cdot\frac{L\cdot s}{2}\delta_{rk}I_{tl}\right.\\
&\left.+\sum_{i=1}^{m}\sum_{j=1}^{n}a_{ij}\left(2\frac{i\pi}{L}\right)^2\left(2\frac{r\pi}{L}\right)^2\cdot\frac{L\cdot s}{2}\delta_{ir}I_{jt}\right]\\
=&\frac{D}{2}\left[\left(2\frac{r\pi}{L}\right)^2\left(2\frac{p\pi}{L}\right)^2\cdot\frac{L\cdot s}{2}\delta_{rp}I_{tq}+\left(2\frac{p\pi}{L}\right)^2\left(2\frac{r\pi}{L}\right)^2\cdot\frac{L\cdot s}{2}\delta_{pr}I_{qt}\right]
\end{aligned}$$

$$\frac{\partial^2}{\partial a_{pq}\partial a_{rt}}\left[\frac{D}{2}\sum_{i=1}^{m}\sum_{j=1}^{n}\sum_{k=1}^{p}\sum_{l=1}^{q}a_{ij}a_{kl}\left(2\frac{j\pi}{s}\right)^2\left(2\frac{l\pi}{s}\right)^2\cdot\frac{3L}{2}\cdot\frac{s}{2}\delta_{ik}\delta_{jl}\right] \tag{A.4.4}$$

$$\begin{aligned}
=&\frac{\partial}{\partial a_{pq}}\frac{D}{2}\left[\sum_{k=1}^{p}\sum_{l=1}^{q}a_{kl}\left(2\frac{t\pi}{s}\right)^2\left(2\frac{l\pi}{s}\right)^2\cdot\frac{3L}{2}\cdot\frac{s}{2}\delta_{rk}\delta_{tl}\right.\\
&\left.+\sum_{i=1}^{m}\sum_{j=1}^{n}a_{ij}\left(2\frac{j\pi}{s}\right)^2\left(2\frac{t\pi}{s}\right)^2\cdot\frac{3L}{2}\cdot\frac{s}{2}\delta_{ir}\delta_{jt}\right]\\
=&\frac{D}{2}\left[\left(2\frac{t\pi}{s}\right)^2\left(2\frac{q\pi}{s}\right)^2\cdot\frac{3L}{2}\cdot\frac{s}{2}\delta_{rp}\delta_{tq}+\left(2\frac{q\pi}{s}\right)^2\left(2\frac{t\pi}{s}\right)^2\cdot\frac{3L}{2}\cdot\frac{s}{2}\delta_{pr}\delta_{qt}\right]
\end{aligned}$$

$$\frac{\partial^2}{\partial a_{pq}\partial a_{rt}}\left[\frac{D}{2}\sum_{i=1}^{m}\sum_{j=1}^{n}\sum_{k=1}^{p}\sum_{l=1}^{q}a_{ij}a_{kl}\left(2\frac{j\pi}{s}\right)^2\left(2\frac{l\pi}{s}\right)^2\cdot L\cdot\frac{s}{2}I_{ik}\delta_{jl}\right] \tag{A.4.5}$$

$$\begin{aligned}
=&\frac{\partial}{\partial a_{pq}}\frac{D}{2}\left[\sum_{k=1}^{p}\sum_{l=1}^{q}a_{kl}\left(2\frac{t\pi}{s}\right)^2\left(2\frac{l\pi}{s}\right)^2\cdot L\cdot\frac{s}{2}I_{rk}\delta_{tl}\right.\\
&\left.+\sum_{i=1}^{m}\sum_{j=1}^{n}a_{ij}\left(2\frac{j\pi}{s}\right)^2\left(2\frac{t\pi}{s}\right)^2\cdot L\cdot\frac{s}{2}I_{ir}\delta_{jt}\right]\\
=&\frac{D}{2}\left[\left(2\frac{t\pi}{s}\right)^2\left(2\frac{q\pi}{s}\right)^2\cdot L\cdot\frac{s}{2}I_{rp}\delta_{tq}+\left(2\frac{q\pi}{s}\right)^2\left(2\frac{t\pi}{s}\right)^2\cdot L\cdot\frac{s}{2}I_{pr}\delta_{qt}\right]
\end{aligned}$$

$$\frac{\partial^2}{\partial a_{pq}\partial a_{rt}}\left[\frac{D}{2}\cdot 2\nu\cdot\sum_{i=1}^{m}\sum_{j=1}^{n}\sum_{k=1}^{p}\sum_{l=1}^{q}a_{ij}a_{kl}\left(2\frac{i\pi}{L}\right)^2\left(2\frac{j\pi}{s}\right)^2\cdot\frac{L\cdot s}{4}\delta_{ik}\delta_{jl}\right] \tag{A.4.6}$$

$$\begin{aligned}
=&\frac{\partial}{\partial a_{pq}}D\nu\left[\sum_{k=1}^{p}\sum_{l=1}^{q}a_{kl}\left(2\frac{r\pi}{L}\right)^2\left(2\frac{t\pi}{s}\right)^2\cdot\frac{L\cdot s}{4}\delta_{rk}\delta_{tl}\right.\\
&\left.+\sum_{i=1}^{m}\sum_{j=1}^{n}a_{ij}\left(2\frac{i\pi}{L}\right)^2\left(2\frac{j\pi}{s}\right)^2\cdot\frac{L\cdot s}{4}\delta_{ir}\delta_{jt}\right]\\
=&D\nu\left[\left(2\frac{r\pi}{L}\right)^2\left(2\frac{t\pi}{s}\right)^2\cdot\frac{L\cdot s}{4}\delta_{rp}\delta_{tq}+\left(2\frac{p\pi}{L}\right)^2\left(2\frac{q\pi}{s}\right)^2\cdot\frac{L\cdot s}{4}\delta_{pr}\delta_{qt}\right]
\end{aligned}$$

$$\begin{aligned}
&\frac{\partial^2}{\partial a_{pq}\partial a_{rt}}\left[\frac{D}{2}\cdot 2\left(1-\nu\right)\cdot\sum_{i=1}^{m}\sum_{j=1}^{n}\sum_{k=1}^{p}\sum_{l=1}^{q}a_{ij}a_{kl}\right.\\
&\left.\left(2\frac{i\pi}{L}\right)\left(2\frac{k\pi}{L}\right)\left(2\frac{j\pi}{s}\right)\left(2\frac{l\pi}{s}\right)\cdot\frac{L\cdot s}{4}\delta_{ik}\delta_{jl}\right] \qquad \text{(A.4.7)}\\
=&\frac{\partial}{\partial a_{pq}}\frac{D}{2}\cdot 2\left(1-\nu\right)\left[\sum_{k=1}^{p}\sum_{l=1}^{q}a_{kl}\left(2\frac{r\pi}{L}\right)\left(2\frac{k\pi}{L}\right)\left(2\frac{t\pi}{s}\right)\left(2\frac{l\pi}{s}\right)\cdot\frac{L\cdot s}{4}\delta_{rk}\delta_{tl}\right.\\
&\left.+\sum_{i=1}^{m}\sum_{j=1}^{n}a_{ij}\left(2\frac{i\pi}{L}\right)\left(2\frac{r\pi}{L}\right)\left(2\frac{j\pi}{s}\right)\left(2\frac{t\pi}{s}\right)\cdot\frac{L\cdot s}{4}\delta_{ir}\delta_{jt}\right]\\
=&\frac{D}{2}\cdot 2\left(1-\nu\right)\left[\left(2\frac{r\pi}{L}\right)\left(2\frac{p\pi}{L}\right)\left(2\frac{t\pi}{s}\right)\left(2\frac{q\pi}{s}\right)\cdot\frac{L\cdot s}{4}\delta_{rp}\delta_{tq}\right.\\
&\left.+\left(2\frac{p\pi}{L}\right)\left(2\frac{r\pi}{L}\right)\left(2\frac{q\pi}{s}\right)\left(2\frac{t\pi}{s}\right)\cdot\frac{L\cdot s}{4}\delta_{pr}\delta_{qt}\right]
\end{aligned}$$

A.5 Differentiating the load potential

$$\mathbf{K}^{G}_{pqrt} = \begin{bmatrix} \frac{\partial^2 H}{\partial a_{11}\partial a_{11}} & \cdots & \frac{\partial^2 H}{\partial a_{11}\partial a_{mn}} \\ \vdots & & \vdots \\ \frac{\partial^2 H}{\partial a_{mn}\partial a_{11}} & \cdots & \frac{\partial^2 H}{\partial a_{mn}\partial a_{mn}} \end{bmatrix} \tag{A.5.1}$$

We divide the total expression, form Appendix A3, for H into eight separate parts and calculate them one by one.

$$\frac{\partial^2}{\partial a_{pq}\partial a_{rt}}\left[\left(-\frac{t}{2}\right) S_x \sum_{i=1}^{m}\sum_{j=1}^{n}\sum_{k=1}^{p}\sum_{l=1}^{q} a_{ij}a_{kl}\left(2\frac{i\pi}{L}\right)\left(2\frac{k\pi}{L}\right)\cdot\frac{L}{2}\cdot\frac{3s}{2}\delta_{ik}\delta_{jl}\right] \tag{A.5.2}$$

$$\begin{aligned}
=&\frac{\partial}{\partial a_{pq}}\left(-\frac{t}{2}\right) S_x \left[\sum_{k=1}^{p}\sum_{l=1}^{q} a_{kl}\left(2\frac{r\pi}{L}\right)\left(2\frac{k\pi}{L}\right)\cdot\frac{L}{2}\cdot\frac{3s}{2}\delta_{rk}\delta_{tl}\right.\\
&\left.+\sum_{i=1}^{m}\sum_{j=1}^{n} a_{ij}\left(2\frac{i\pi}{L}\right)\left(2\frac{r\pi}{L}\right)\cdot\frac{L}{2}\cdot\frac{3s}{2}\delta_{ir}\delta_{jt}\right]\\
=&\left(-\frac{t}{2}\right) S_x \left[\left(2\frac{r\pi}{L}\right)\left(2\frac{p\pi}{L}\right)\cdot\frac{L}{2}\cdot\frac{3s}{2}\delta_{rp}\delta_{tq}+\left(2\frac{p\pi}{L}\right)\left(2\frac{r\pi}{L}\right)\cdot\frac{L}{2}\cdot\frac{3s}{2}\delta_{pr}\delta_{qt}\right]
\end{aligned}$$

$$\frac{\partial^2}{\partial a_{pq}\partial a_{rt}}\left[\left(-\frac{t}{2}\right) S_x \sum_{i=1}^{m}\sum_{j=1}^{n}\sum_{k=1}^{p}\sum_{l=1}^{q} a_{ij}a_{kl}\left(2\frac{i\pi}{L}\right)\left(2\frac{k\pi}{L}\right)\cdot\frac{L}{2}\cdot s\delta_{ik}I_{jl}\right] \tag{A.5.3}$$

$$\begin{aligned}
=&\frac{\partial}{\partial a_{pq}}\left(-\frac{t}{2}\right) S_x \left[\sum_{k=1}^{p}\sum_{l=1}^{q} a_{kl}\left(2\frac{r\pi}{L}\right)\left(2\frac{k\pi}{L}\right)\cdot\frac{L}{2}\cdot s\delta_{rk}I_{tl}\right.\\
&\left.+\sum_{i=1}^{m}\sum_{j=1}^{n} a_{ij}\left(2\frac{i\pi}{L}\right)\left(2\frac{r\pi}{L}\right)\cdot\frac{L}{2}\cdot s\delta_{ir}I_{jt}\right]\\
=&\left(-\frac{t}{2}\right) S_x \left[\left(2\frac{r\pi}{L}\right)\left(2\frac{p\pi}{L}\right)\cdot\frac{L}{2}\cdot s\delta_{rp}I_{tq}+\left(2\frac{p\pi}{L}\right)\left(2\frac{r\pi}{L}\right)\cdot\frac{L}{2}\cdot s\delta_{pr}I_{qt}\right]
\end{aligned}$$

$$\frac{\partial^2}{\partial a_{pq}\partial a_{rt}}\left[\left(-\frac{t}{2}\right)S_y\sum_{i=1}^{m}\sum_{j=1}^{n}\sum_{k=1}^{p}\sum_{l=1}^{q}a_{ij}a_{kl}\left(2\frac{j\pi}{s}\right)\left(2\frac{l\pi}{s}\right)\cdot\frac{3L}{2}\cdot\frac{s}{2}\delta_{ik}\delta_{jl}\right] \tag{A.5.4}$$

$$\begin{aligned}
=&\frac{\partial}{\partial a_{pq}}\left(-\frac{t}{2}\right)S_y\left[\sum_{k=1}^{p}\sum_{l=1}^{q}a_{kl}\left(2\frac{t\pi}{s}\right)\left(2\frac{l\pi}{s}\right)\cdot\frac{3L}{2}\cdot\frac{s}{2}\delta_{rk}\delta_{tl}\right.\\
&\left.+\sum_{i=1}^{m}\sum_{j=1}^{n}a_{ij}\left(2\frac{j\pi}{s}\right)\left(2\frac{t\pi}{s}\right)\cdot\frac{3L}{2}\cdot\frac{s}{2}\delta_{ir}\delta_{jt}\right]\\
=&\left(-\frac{t}{2}\right)S_y\left[\left(2\frac{t\pi}{s}\right)\left(2\frac{q\pi}{s}\right)\cdot\frac{3L}{2}\cdot\frac{s}{2}\delta_{rp}\delta_{tq}+\left(2\frac{q\pi}{s}\right)\left(2\frac{t\pi}{s}\right)\cdot\frac{3L}{2}\cdot\frac{s}{2}\delta_{pr}\delta_{qt}\right]
\end{aligned}$$

$$\frac{\partial^2}{\partial a_{pq}\partial a_{rt}}\left[\left(-\frac{t}{2}\right)S_y\sum_{i=1}^{m}\sum_{j=1}^{n}\sum_{k=1}^{p}\sum_{l=1}^{q}a_{ij}a_{kl}\left(2\frac{j\pi}{s}\right)\left(2\frac{l\pi}{s}\right)\cdot L\cdot\frac{s}{2}I_{ik}\delta_{jl}\right] \tag{A.5.5}$$

$$\begin{aligned}
=&\frac{\partial}{\partial a_{pq}}\left(-\frac{t}{2}\right)S_y\left[\sum_{k=1}^{p}\sum_{l=1}^{q}a_{kl}\left(2\frac{t\pi}{s}\right)\left(2\frac{l\pi}{s}\right)\cdot L\cdot\frac{s}{2}I_{rk}\delta_{tl}\right.\\
&\left.+\sum_{i=1}^{m}\sum_{j=1}^{n}a_{ij}\left(2\frac{j\pi}{s}\right)\left(2\frac{t\pi}{s}\right)\cdot L\cdot\frac{s}{2}I_{ir}\delta_{jt}\right]\\
=&\left(-\frac{t}{2}\right)S_y\left[\left(2\frac{t\pi}{s}\right)\left(2\frac{q\pi}{s}\right)\cdot L\cdot\frac{s}{2}I_{rp}\delta_{tq}+\left(2\frac{q\pi}{s}\right)\left(2\frac{t\pi}{s}\right)\cdot L\cdot\frac{s}{2}I_{pr}\delta_{qt}\right]
\end{aligned}$$

Appendix B

Rayleigh-Ritz Matlab scripts

```
% Plate properties
E=208000;
L=2400;
s=830;
nu=0.3;
t=20;
D=(E*t^3)/(12*(1-nu^2));
Sx=1;
Sy=0;
Sxy=0;

%Degrees of freedom
maxMM=100;
maxMN=1;

%Initial matrix
KKU=zeros(maxMM*maxMN,maxMM*maxMN);
KKH=zeros(maxMM*maxMN,maxMM*maxMN);

%Stiffness matrix(U)
for intP=1:maxMM
    for intQ=1:maxMN
        for intR=1:maxMM
            for intT=1:maxMN
                PQ=maxMN*intP-maxMN+intQ;
                RT=maxMN*intR-maxMN+intT;
                if intP==intR;
                    if intQ==intT;
                        KKU(PQ,RT)=KKU(PQ,RT)+((6)*D*L*s)*(((intR*pi)/L)^2*((
                            intP*pi)/L)^2+((intP*pi)/L)^2*((intR*pi)/L)^2)+((6)*
                            D*L*s)*(((intT*pi)/s)^2*((intQ*pi)/s)^2+((intQ*pi)/s
                            )^2*((intT*pi)/s)^2)+(4*D*nu*((L*s)))*(((intR*pi)/L)
                            ^2*((intQ*pi)/s)^2+((intP*pi)/L)^2*((intT*pi)/s)^2)
                            +(4*D*(1-nu)*(L*s))*(((intR*pi)/L)*((intP*pi)/L)*((
                            intT*pi)/s)*((intQ*pi)/s)+((intP*pi)/L)*((intR*pi)/L
                            )*((intQ*pi)/s)*((intT*pi)/s));

                        KKH(PQ,RT)=KKH(PQ,RT)+Sx*((3/2)*t*L*s)*(((intR*pi)/L)*((
                            intP*pi)/L)+((intP*pi)/L)*((intR*pi)/L))+Sy*((3/2)*t
                            *L*s)*(((intT*pi)/s)*((intQ*pi)/s)+((intQ*pi)/s)*((
                            intT*pi)/s))+2*Sxy*(t/2)*4*(((intR*pi)/L)*((intT*pi)
                            /s)*(-(L*(-1+(-1)^intR))/(intR*pi))*(-(s*(-1+(-1)^
                            intT))/(intT*pi))+((intP*pi)/L)*((intQ*pi)/s)*(-(L
```

```
                        *(-1+(-1)^intP))/(intP*pi))*(-(s*(-1+(-1)^intQ))/(
                        intQ*pi)));
                end
            end
            if intP==intR;
                if intQ~=intT;
                    KKU(PQ,RT)=KKU(PQ,RT)+((D*L*s)*4)*(((intR*pi)/L)^2*((
                        intP*pi)/L)^2+((intP*pi)/L)^2*((intR*pi)/L)^2);

                    KKH(PQ,RT)=KKH(PQ,RT)+Sx*((t*L*s))*(((intR*pi)/L)*((intP
                        *pi)/L)+((intP*pi)/L)*((intR*pi)/L))+2*Sxy*(t/2)
                        *4*(((intR*pi)/L)*((intT*pi)/s)*(-(L*(-1+(-1)^intR))
                        /(intR*pi))*(-(s*(-intQ^2-(-1)^intT*intT^2+(-1)^intT
                        *intQ^2+(-1)^(intT+intQ)*intT^2))/(intT*pi*(-intT^2+
                        intQ^2)))+((intP*pi)/L)*((intQ*pi)/s)*(-(L*(-1+(-1)^
                        intP))/(intP*pi))*(-(s*(-intT^2-(-1)^intQ*intQ
                        ^2+(-1)^intQ*intT^2+(-1)^(intQ+intT)*intQ^2))/(intQ*
                        pi*(-intQ^2+intT^2))));
                end
            end
            if intP~=intR;
                if intQ==intT
                    KKU(PQ,RT)=KKU(PQ,RT)+((D*L*s)*4)*(((intT*pi)/s)^2*((
                        intQ*pi)/s)^2+((intQ*pi)/s)^2*((intT*pi)/s)^2);

                    KKH(PQ,RT)=KKH(PQ,RT)+Sy*((t*L*s))*(((intT*pi)/s)*((intQ
                        *pi)/s)+((intQ*pi)/s)*((intT*pi)/s))+2*Sxy*(t/2)
                        *4*(((intR*pi)/L)*((intT*pi)/s)*(-(L*(-intP^2-(-1)^
                        intR*intR^2+(-1)^intR*intP^2+(-1)^(intR+intP)*intR
                        ^2))/(intR*pi*(-intR^2+intP^2)))*(-(s*(-1+(-1)^intT)
                        )/(intT*pi))+((intP*pi)/L)*((intQ*pi)/s)*(-(L*(-intR
                        ^2-(-1)^intP*intP^2+(-1)^intP*intR^2+(-1)^(intP+intR
                        )*intP^2))/(intP*pi*(-intP^2+intR^2)))*(-(s*(-1+(-1)
                        ^intQ))/(intQ*pi)));
                end
            end
            if intP~=intR;
                if intQ~=intT
                    KKH(PQ,RT)=KKH(PQ,RT)+2*Sxy*(t/2)*4*(((intR*pi)/L)*((
                        intT*pi)/s)*(-(L*(-intP^2-(-1)^intR*intR^2+(-1)^intR
                        *intP^2+(-1)^(intR+intP)*intR^2))/(intR*pi*(-intR^2+
                        intP^2)))*(-(s*(-intQ^2-(-1)^intT*intT^2+(-1)^intT*
                        intQ^2+(-1)^(intT+intQ)*intT^2))/(intT*pi*(-intT^2+
                        intQ^2)))+((intP*pi)/L)*((intQ*pi)/s)*(-(L*(-intR
                        ^2-(-1)^intP*intP^2+(-1)^intP*intR^2+(-1)^(intP+intR
                        )*intP^2))/(intP*pi*(-intP^2+intR^2)))*(-(s*(-intT
                        ^2-(-1)^intQ*intQ^2+(-1)^intQ*intT^2+(-1)^(intQ+intT
                        )*intQ^2))/(intQ*pi*(-intQ^2+intT^2))));
                end
            end
        end
    end
end
KKU;
KKH;

lambda1=eig(KKU,KKH);
lambda2=min(real(eig(KKU,KKH)));
[v,d]=eig(KKU,KKH);

%Displacement Shape
w_r=zeros(50,50);
for intM=1:50
    for intN=1:50
```

```
        xValue=(intN-1)*L/49;
        yValue=(intM-1)*s/49;
        intJ=0;
        for intK=1:maxMM
            for intL=1:maxMN
                xArgument=2*pi*intK*xValue/L;
                yArgument=2*pi*intL*yValue/s;
                intJ=intJ+1;
                w_r(intN,intM)=w_r(intN,intM)+v(intJ,9)*(1-cos(xArgument))*(1-
                    cos(yArgument));
            end
        end
    end
end
w_r;
plot(w_r)
```